

RS-04-070

May 12, 2004

U. S. Nuclear Regulatory Commission
ATTN: Document Control Desk
Washington, DC 20555-0001

Dresden Nuclear Power Station, Units 2 and 3
Facility Operating License Nos. DPR-19 and DPR-25
NRC Docket Nos. 50-237 and 50-249

Quad Cities Nuclear Power Station, Units 1 and 2
Facility Operating License Nos. DPR-29 and DPR-30
NRC Docket Nos. 50-254 and 50-265

Subject: Commitments and Plans Related to Extended Power Uprate Operation

- References:
1. Letter from J. A. Benjamin (Exelon Generation Company, LLC) to U. S. NRC, "Commitments and Information Related to Extended Power Uprate," dated April 2, 2004
 2. Letter from U. S. NRC to C. M. Crane (Exelon Generation Company, LLC), "Commitments and Information Related to the Extended Power Uprate at Dresden and Quad Cities Nuclear Power Stations," dated April 20, 2004

In Reference 1, Exelon Generation Company, LLC (EGC) made several regulatory commitments regarding operation of Quad Cities Nuclear Power Station (QCNPS), Units 1 and 2, at extended power uprate (EPU) conditions. The commitments included receiving NRC approval prior to continuous operation of QCNPS, Units 1 and 2, above pre-EPU power levels. Additionally, one of the commitments stated that during the week of May 3, 2004, EGC would provide the NRC specific commitments regarding EPU operation. An extension to provide the commitments by May 12, 2004, was agreed to in a May 5, 2004, telephone discussion between Mr. A. Mendiola (NRC) and Mr. P. Simpson (EGC).

Attachment 1 of Reference 1 provided EGC's Plan for Evaluation of Flow Effects, which is being used to evaluate flow effects on the steam dryers, main steam and feedwater system components. Based on evaluations performed to date, EGC has determined that additional time is necessary to complete the associated technical evaluations prior to making specific commitments related to the steam dryers. Therefore, this letter provides specific commitments related to the EPU vulnerability review, and commitments related to the steam dryers will be provided to the NRC in the future.

A001

The specific commitments related to the EPU vulnerability review and the steam dryer evaluations will describe the actions EGC will take to collectively form the basis for long-term operation of the QCNPS units at EPU conditions. In the interim, EGC intends to continue to limit operation on both QCNPS units to pre-EPU power levels, except for brief periods to allow collection of data as described in Attachment 2. EGC's plans for continuing the steam dryer evaluations are described below.

As stated in Reference 1, EGC has initiated planning to replace the steam dryers at QCNPS at the earliest practical opportunity. EGC currently plans to replace the steam dryers at QCNPS Units 1 and 2 during upcoming scheduled refueling outages for each unit beginning with QCNPS Unit 1 in March 2005. The new steam dryer design for QCNPS Unit 1 will be developed based on insights gained through the Plan for Evaluation of Flow Effects provided in Attachment 1 of Reference 1, and EGC intends to refine the new steam dryer design through scale model testing. During the first refueling outage after installation of the new steam dryer at QCNPS Unit 1, EGC plans to conduct inspections in accordance with accepted industry standards to verify that only service-related non-consequential cracking has occurred.

For QCNPS Unit 2, EGC plans to continue the analyses described in the Plan for Evaluation of Flow Effects, submitted to the NRC as Attachment 1 to Reference 1. The results of these analyses may demonstrate that the modified QCNPS Unit 2 steam dryer is capable of maintaining its structural integrity during operation above the pre-EPU level, with an adequate safety factor. Therefore, the results of these analyses, combined with the actions committed to in Attachment 2 to this letter, could collectively form the basis for resumed operation of QCNPS Unit 2 at EPU conditions prior to dryer replacement. If EGC determines that the Plan for Evaluation of Flow Effects is successful in demonstrating that the modified steam dryer is adequate for operation above the pre-EPU level, EGC will meet with the NRC technical staff to discuss the details regarding the justification for operation at EPU conditions for QCNPS Unit 2. Afterwards, EGC will submit the justification for operation at EPU conditions, and meet with NRC management to present and request approval of the justification for operation for QCNPS Unit 2 at EPU conditions. For QCNPS Unit 1, EGC expects that a similar approach will be followed to gain NRC approval.

If EGC determines that the results of the Plan for Evaluation of Flow Effects are inconclusive for demonstrating that the modified steam dryer at QCNPS Unit 2 is adequate for operation above the pre-EPU level, EGC will continue to limit operation on QCNPS Unit 2 to the pre-EPU level until the steam dryer is replaced and NRC approval is obtained for operation above pre-EPU levels.

EGC is also considering instrumenting the new QCNPS Unit 1 steam dryer to collect data during the startup following installation of the new steam dryer. EGC will communicate the decision to instrument the new steam dryer to the NRC when finalized.

In Attachment 2 of Reference 1, EGC submitted a summary of the basis for continued operation of the Dresden Nuclear Power Station (DNPS) Units 2 and 3 at EPU levels. The NRC noted in Reference 2 that the summary basis did not provide a quantitative technical assessment of the potential loadings and resulting stresses that could cause failure of the DNPS steam dryers or other plant components. To address this concern, EGC is providing the quantitative input to the technical assessment of the loadings of the DNPS steam dryers in Attachment 1 to this letter.

The reports provided in Attachment 1 are used to support the basis for continuous operation of the DNPS units at EPU conditions. The reports are the result of evaluations done in December 2003 by Continuum Dynamics Incorporated (CDI). The models used for these evaluations have been revised as part of the Plan for Evaluation of Flow Effects. Steam line pressure data is being gathered at both DNPS units and will be evaluated using the improved model. The results of these evaluations will be used to update the DNPS operability evaluations, as appropriate. However, based on evaluations completed to date, EGC has concluded that the structural integrity of the DNPS steam dryers will not be compromised as a result of operation at EPU conditions.

Additionally, in Reference 2, the NRC identified concerns with EGC's plans to justify long-term EPU operation of the QCNPS units and the summary basis for continued long-term EPU operation of the DNPS units. As stated above, EGC is providing the quantitative input to the technical assessment of the potential loadings that could cause failure of the steam dryers at DNPS in Attachment 1. The remaining concerns will be addressed as part of the steam dryer evaluations and the justification for operation of the QCNPS units at EPU conditions.

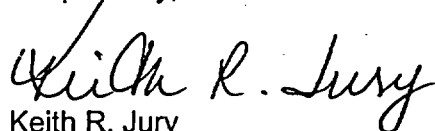
EGC requested MPR Associates, Incorporated (MPR) to provide an independent review of the report contained in Attachment 1. In addition, Dr. Fred Moody, an independent consultant, also performed an independent review of our evaluation. Both reviews concluded that the analytical methods and associated results are reasonable for the purpose of supporting the DNPS operability evaluations.

As described above, evaluations of operation at EPU are ongoing. As new insights are gained, EGC will promptly apply the lessons learned to DNPS and QCNPS. Where lessons learned from these evaluations indicate significant potential degradation of the steam dryer, or the reactor pressure vessel internals, steam or feedwater systems and components, EGC will take appropriate actions up to and including shutting down the applicable DNPS or QCNPS unit to conduct inspections or modifications on an expedited basis.

Attachment 2 provides regulatory commitments that EGC is making related to EPU operation. This letter satisfies the third commitment in Reference 1, which EGC originally agreed to provide during the week of May 3, 2004. The remaining commitments made in Reference 1 are included in Attachment 2 to this letter. Therefore, the commitments in Attachment 2 represent our commitments in their entirety.

If you have any questions concerning this submittal, please contact Mr. Patrick R. Simpson, at (630) 657-2823.

Respectfully,



Keith R. Jury
Director - Licensing and Regulatory Affairs

May 12, 2004
U. S. Nuclear Regulatory Commission
Page 4

Attachments:

1. Quantitative Technical Assessment of Potential Loading
2. Summary of Commitments

cc: Regional Administrator – NRC Region III
NRC Senior Resident Inspector – Dresden Nuclear Power Station
NRC Senior Resident Inspector – Quad Cities Nuclear Power Station

ATTACHMENT 1

Quantitative Technical Assessment of Potential Loading

Hydrodynamic Loads on Dresden Unit 2 Steam Dryer

Final Report

Revision 2

Prepared by

Continuum Dynamics, Inc.
34 Lexington Avenue
Ewing, NJ 08618

Prepared under Purchase Order No. 64992 for

Exelon Generation LLC
4300 Winfield Road
Warrenville, IL 60555

Approved by:



Alan J. Bilanin

May 2004

Object

In plant measured pressure oscillation data in main steam lines of Dresden Unit 2 (DR2) are used to force a dynamic model of the steam system. The model is then used to predict the fluctuating pressures across components of the steam dryer in the reactor vessel. This effort provides Exelon with a dryer load definition which comes directly from measured data. The hydrodynamic load data then will be used by a structural analyst to assess the structural adequacy of the "as built" steam dryer in DR2.

Physical Observations

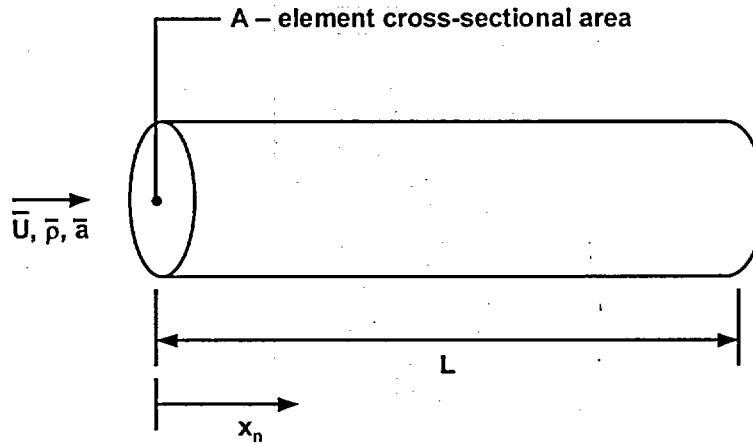
Analysis by others, of dryer failure at Quad Cities Unit 2 (QC2) during the summer of 2003, used the observed fatigue dryer damage to back calculate a structural load which was consistent with this damage. Fatigue damage, however, is dependent upon both magnitude of load and frequency of application. The analysis was not able to identify discrete frequencies and therefore recommended that a flat spectrum be used with an amplitude which was determined to be consistent with the observed damage. This flat spectrum is equivalent to the assumption that the forcing is random, in spite of the fact that the subscale tests conducted by others indicated that discrete frequencies were observed in the steam lines and the reactor steam dome. Exelon obtained unsteady pressure data in the plant (DR2) during operation, and the effort reported herein is the analysis of these data. Contrary to the assumption of a flat loading spectrum, the data show that there are discrete deterministic phenomenon at work in the steam dome and main steam lines that are responsible for the loading on the dryer. This report quantifies this load from full scale test data.

Modeling Considerations

Pulsation in a single phase compressible medium, where acoustic wavelengths are long compared to component dimensions and in particular long compared to transverse dimensions (directions perpendicular to the primary flow directions), lend themselves to an analysis methodology known as acoustic circuit analysis. If the analysis is restricted to frequencies below 50 Hz, acoustic wavelengths are approximately 30 feet in length and wavelengths are long compared to most components of interest.

Acoustic circuit analysis divides the system to be analyzed into elements which are characterized as sketched below in a length (L), cross sectional area (A), mean density ($\bar{\rho}$), mean flow velocity (\bar{U}) and mean acoustic speed (\bar{a})

nth-element



It can be shown that the fluctuating pressure P' and velocity u'_n in this nth element must satisfy

$$P'_n = (A_n e^{ik_{1n}X_n} + B_n e^{ik_{2n}X_n}) e^{i\omega t}$$

$$u'_n = \frac{1}{-\omega\rho} (A_n k_{1n} e^{ik_{1n}X_n} + B_n k_{2n} e^{ik_{2n}X_n}) e^{i\omega t}$$

where harmonic time dependence of the form $e^{i\omega t}$ has been assumed. The wave numbers k_{1n} and k_{2n} are the two complex roots of

$$k_n^2 + i4f_n \frac{|\bar{U}_n|}{D_n a} (\omega + \bar{U}_n k_n) - \frac{\omega}{a} (\omega + \bar{U}_n k_n) = 0$$

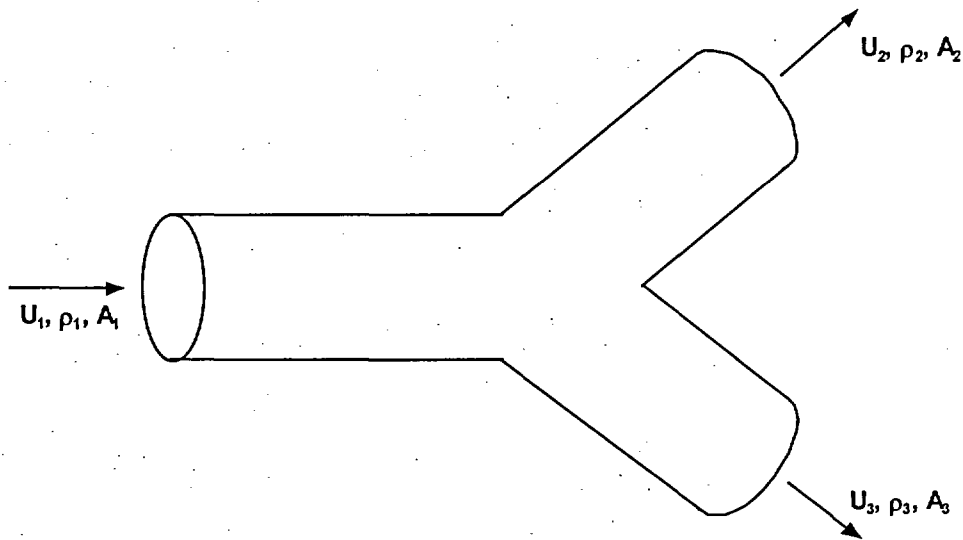
where f_n - pipe friction factor for element n
 D_n - hydrodynamic diameter for element n
 $i = \sqrt{-1}$

A_n and B_n are constants which are a function of frequency and are determined by satisfying continuity of pressure at element junctions and mass conservation at a junction.

Mass conservation at a junction requires that (see sketch below)

$$\rho_1 U_1 A_1 = \rho_2 U_2 A_2 + \rho_3 U_3 A_3$$

where $()_m$ refer to each segment.



The flow passages for the DR2 reactor and main steam lines are discretized into 78 elements and the resulting system can be driven with prescribed shear layer motions at geometric discontinuities. These discontinuities exist in the steam delivery system where convective velocities are high.

One source of energy transfer from the main steam velocity to unsteady motion results from the impingement of the shear layer in the main steam line over the 30 inch diameter D ring junction. This oscillation of the shear layer over the cavity formed by the D ring header has an empirically determined preferred frequency of oscillation (f) of

$$f = 0.44 \frac{\bar{U}}{D}$$

The preferred driving frequency with a main steam velocity at this junction of 145 ft/sec and $D = 2.5$ ft is 25.5 Hz. As will be shown, the plant data suggest that energy does indeed exist at this frequency in the main steam lines. The circuit analysis should tell whether the energy at this frequency can propagate into the reactor dome.

Model Discretization

The 78 elements which are used to model the dynamics of the steam system are sketched schematically below and physical dimensions used in defining the individual elements are shown in Figures 2 and 3. The dimensions used were the best available at the time of analysis.

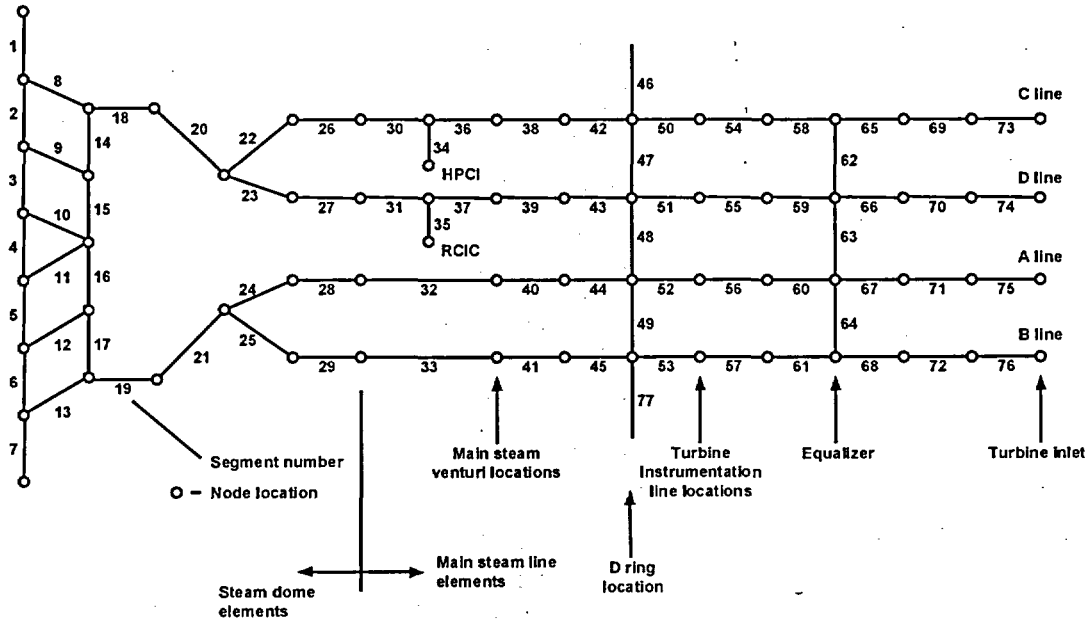


Figure 1: Schematic of the elements used in the acoustic circuit analysis.

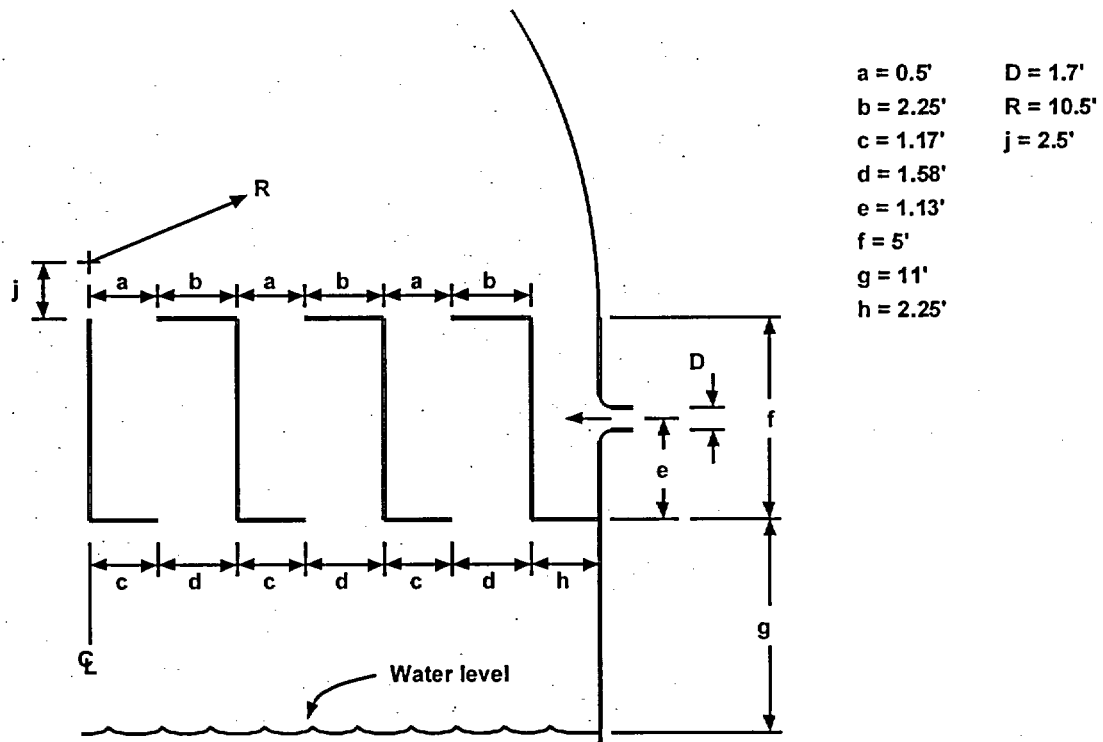


Figure 2: Steam dome and dryer dimensions.

Input Pressure Data

Exelon has mounted pressure transducers on the main steam lines at the main steam venturi and upstream of the turbine (turbine instrument lines). The data sets provided are tabulated below on Table 1. All data provided were taken at the end of instrument lines whose lengths were specified. Lines were assumed filled with water and the data corrected for the instrument line effects of line length, acoustic speed, and losses along the line, by correcting the data in frequency space and then reconstructing the time signal at the instrument line location on the main steam line. Corrections are significant at frequencies associated with the 1/4, 3/4, 5/4, etc. standing wave frequencies of the instrument lines. The resulting pressure time histories and Power Spectral Density functions (PSDs) are shown on Figures 4 and 5. The respective captions on these figures are read as follows. From Figure 4-a, for example, the label "30B: 11.60 Turbine" denotes that the data set number is "30" (see Table 1) taken on the "B" steam line at a steam mass flow rate of 11.60×10^6 lbm/hr. The sensor location is at the main steam line "turbine" location. Data at only one power setting were provided for DR2.

From work with these data sets, it is known that the largest dryer loads are correlated with the highest rms pressure levels. Sister plants are known to have maximum steam flow rates of 11.95×10^6 lbm/hr. It is therefore possible that the loads analyzed herein are not bounding.

Table 1
SUMMARY OF DRESDEN 2 DATA SETS

Data Set #	Steam Flow (10^6 lbm/hr)	Location	Date/Time	Data Rate (samples/sec)	Figure #
30	11.60	Turbine B & C	12/04 14:51	500	4-a, b
31	11.60	Venturi A, B, C & D	12/04 14:51	500	5-a, b, c, d

Model Validation

Referring to Table 1 it may be seen that the four venturi pressure fluctuations were recorded simultaneously, and two of the four turbine pressure fluctuations were recorded simultaneously. The main steam venturi measurements were used to drive the circuit model of the system, and predict the average root mean square pressure measured by the four turbine instruments at the same power settings. These averages are shown in Table 2.

It should be noted that the turbine instrumentation showed extremely narrow spikes at precisely 20 and 40 Hz. These spikes are believed to be induced by the strong electro-magnetic field of the turbine. The spikes were removed from the data analyzed by dropping the Fourier coefficients of the time series between 19-21 and 39-41 Hz.

The venturi in-phase data set was input into the model, and frictional damping was used in the main steam lines to predict the average root mean square pressure at the turbine instrument lines. The four venturi data sets were used simultaneously in the acoustic circuit analysis, to determine sources at the main steam line D ring junction. The friction factor used is summarized in Table 3.

Table 2
SUMMARY OF DRESDEN 2 RMS PRESSURE VALUES AT THE TURBINE
INSTRUMENT LINES

Run	Steam Flow (10^6 lbm/hr)	B Line P_{RMS} (psid)	C Line P_{RMS} (psid)	Average (psid)
30	11.60	1.24	1.22	1.23

Table 3
SUMMARY OF DRESDEN 2 DAMPING MODIFICATIONS TO PREDICT THE RMS
PRESSURE VALUES AT THE TURBINE INSTRUMENT LINES

Steam Flow (10^6 lbm/hr)	Multiplier on Friction Factor	Turbine Inlet Predicted rms (psid)	Turbine Inlet Measured rms (psid)
11.60	1.0	1.90	1.23

Results

The model (subject to the approximations and limitations described above) can now predict the pressure time histories in the reactor steam space as a function of position and time. Shown in Figure 6 is the prediction of steam dome pressure time history and PSD at a steam flow rate of 11.60×10^6 lbm/hr. Note that the PSD levels are very low, and little energy exists in the 20-30 Hz frequency band.

Dryer Hydrodynamic Forcing

Pressure differences are now computed across dryer components, and these loads and locations are described in the Appendix and are transmitted separately. In this section we will discuss these loads.

The analysis discussed above shows the maximum predicted load occurs on the cover plate located at the 270° position. The differential pressure time history and associated PSD are shown in Figure 7. Here, clearly, is a load at approximately 28.5 Hz, which should be compared with the pressure fluctuation in the steam dome (Figure 6), which is lower by nearly an order of magnitude. This indicates excitation of the steam above and below the dryer in a mode that would be difficult to anticipate by inspection of the dryer and steam dome geometry. It is also noted that unless the phasing of fluctuations in the main steam lines were such that signals were out of phase in general, the steam dome is a pressure node in the system. The peak is centered at 28.5 Hz.

Differential pressure loads for other dryer components computed at the center of the component are shown in Figures 8 to 14 for a steam flow rate of 11.60×10^6 lbm/hr. In general the loads decrease radially inboard into the dryer components away from the main steam line inlets, but not monotonically. This again is an indication that the acoustic oscillation about the dryer assembly is complex.

Conclusions

1. The acoustic circuit analysis used with plant data
 - a) predicts the maximum loading on the dryer occurs predominantly at a single frequency, 28.5 Hz in the 0 to 50 Hz frequency range.
 - b) predicts that the loads on dryer components are largest for components nearest the main steam nozzles and decrease for components near the center of the reactor vessel.

- c) predicts that the highest peak differential pressure to be found on any dryer component at a steam flow rate of 11.60×10^6 lbm/hr is instantaneously 1.3 psid (Figure 7), with a rms differential pressure of 0.40 psid.
2. While the load definition given herein is judged to be the best that could be obtained with existing data and plant description, improvement would result from obtaining data at other operating steam flow rates. In particular, data at maximum steam flow rates are likely to provide higher dryer loads.

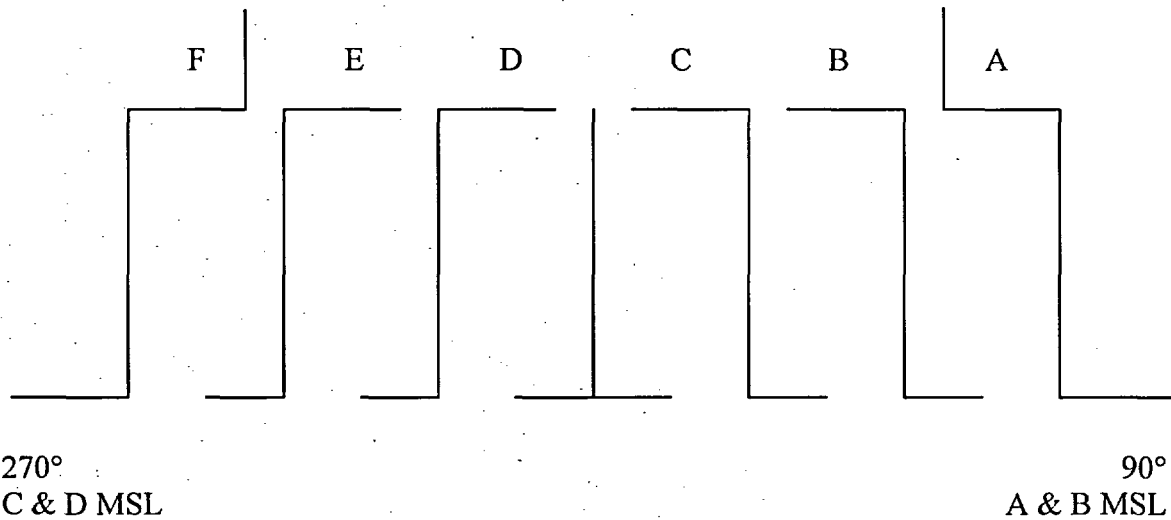
Recommendations

As confidence grows that the loads transfer methodology is valid and appropriate, scoping work should be undertaken to ascertain required changes to the circuit analysis to make it appropriate to compute higher frequency dryer loads.

APPENDIX

PREDICTIONS OF PRESSURE TIME HISTORY IN THE STEAM DOME

Three ASCII data files contain the time history data for the predictions of differential pressure (psid) across the various plates in the dryer. A schematic of the geometry looks like this:



The pressure differences are computed by subtracting the pressure below the plate from the pressure above the plate (for horizontal plates), and subtracting the pressure to the right of the plate (in the above schematic) from the pressure to the left of the plate (for vertical plates).

The file time31bottom.txt contains the following columns of data for the power setting of 11.60×10^6 lbm/hr:

#	Contents
1	time (sec) to 20.48 sec
2	pressure difference at the left edge of the 270° cover plate below entrance to MSL C
3	pressure difference at the right edge of the 270° cover plate below entrance to MSL C
4	pressure difference at the left edge of the 270° cover plate below entrance to MSL D
5	pressure difference at the right edge of the 270° cover plate below entrance to MSL D
6	pressure difference at the left edge of the F bottom plate
7	pressure difference at the right edge of the F bottom plate
8	pressure difference at the left edge of the E bottom plate
9	pressure difference at the right edge of the E bottom plate

- 10 pressure difference at the left edge of the D bottom plate
- 11 pressure difference at the right edge of the D bottom plate (center)
- 12 pressure difference at the left edge of the C bottom plate (center)
- 13 pressure difference at the right edge of the C bottom plate
- 14 pressure difference at the left edge of the B bottom plate
- 15 pressure difference at the right edge of the B bottom plate
- 16 pressure difference at the left edge of the A bottom plate
- 17 pressure difference at the right edge of the A bottom plate
- 18 pressure difference at the left edge of the 90° cover plate below entrance to MSL A
- 19 pressure difference at the right edge of the 90° cover plate below entrance to MSL A
- 20 pressure difference at the left edge of the 90° cover plate below entrance to MSL B
- 21 pressure difference at the right edge of the 90° cover plate below entrance to MSL B

The file time31vertical.txt contains the following columns of data for the power setting of 11.60×10^6 lbm/hr:

- | # | Contents |
|----|--|
| 1 | time (sec) to 20.48 sec |
| 2 | pressure difference at the top edge of the 270° outer hood opposite entrance to MSL C |
| 3 | pressure difference at the bottom edge of the 270° outer hood opposite entrance to MSL C |
| 4 | pressure difference at the top edge of the 270° outer hood opposite entrance to MSL D |
| 5 | pressure difference at the bottom edge of the 270° outer hood opposite entrance to MSL D |
| 6 | pressure difference at the top edge of the vertical plate between F and E |
| 7 | pressure difference at the bottom edge of the vertical plate between F and E |
| 8 | pressure difference at the top edge of the vertical plate between E and D |
| 9 | pressure difference at the bottom edge of the vertical plate between E and D |
| 10 | pressure difference at the top edge of the vertical plate between D and C |
| 11 | pressure difference at the bottom edge of the vertical plate between D and C |
| 12 | pressure difference at the top edge of the vertical plate between C and B |
| 13 | pressure difference at the bottom edge of the vertical plate between C and B |
| 14 | pressure difference at the top edge of the vertical plate between B and A |
| 15 | pressure difference at the bottom edge of the vertical plate between B and A |
| 16 | pressure difference at the top edge of the 90° outer hood opposite entrance to MSL A |
| 17 | pressure difference at the bottom edge of the 90° outer hood opposite entrance to MSL A |
| 18 | pressure difference at the top edge of the 90° outer hood opposite entrance to MSL B |

- 19 pressure difference at the bottom edge of the 90° outer hood opposite entrance to MSL B

The file time31top.txt contains the following columns of data for the power setting of 11.60×10^6 lbm/hr:

#	Contents
1	time (sec) to 20.48 sec
2	pressure difference at the left edge of the F top plate
3	pressure difference at the right edge of the F top plate
4	pressure difference at the left edge of the E top plate
5	pressure difference at the right edge of the E top plate
6	pressure difference at the left edge of the D top plate
7	pressure difference at the right edge of the D top plate (center)
8	pressure difference at the left edge of the C top plate (center)
9	pressure difference at the right edge of the C top plate
10	pressure difference at the left edge of the B top plate
11	pressure difference at the right edge of the B top plate
12	pressure difference at the left edge of the A top plate
13	pressure difference at the right edge of the A top plate
14	pressure difference on the 270° skirt
15	pressure difference at the 90° skirt

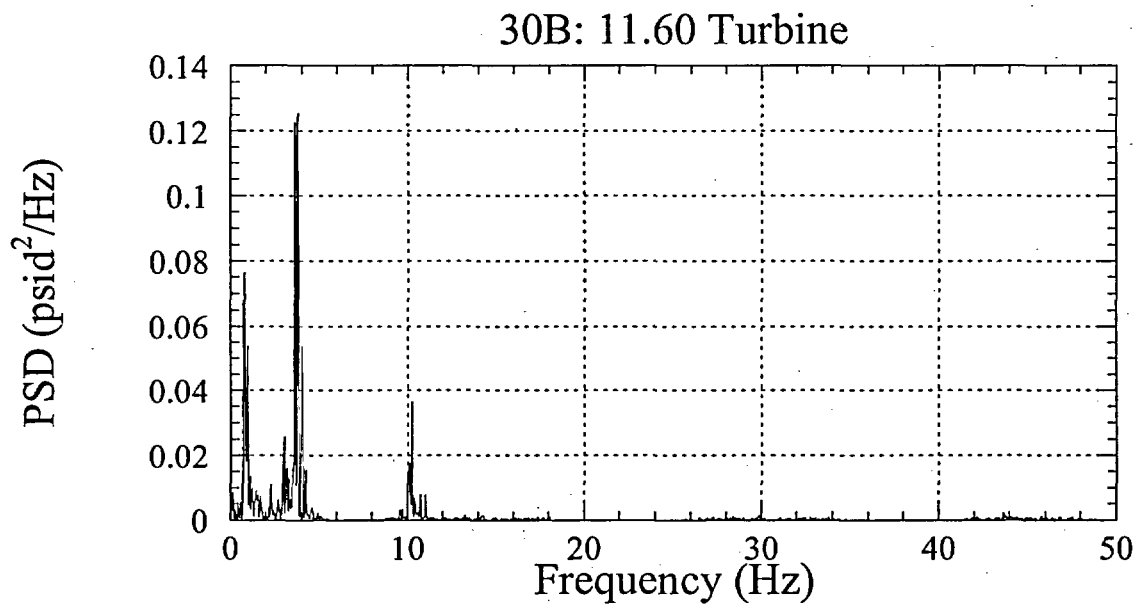
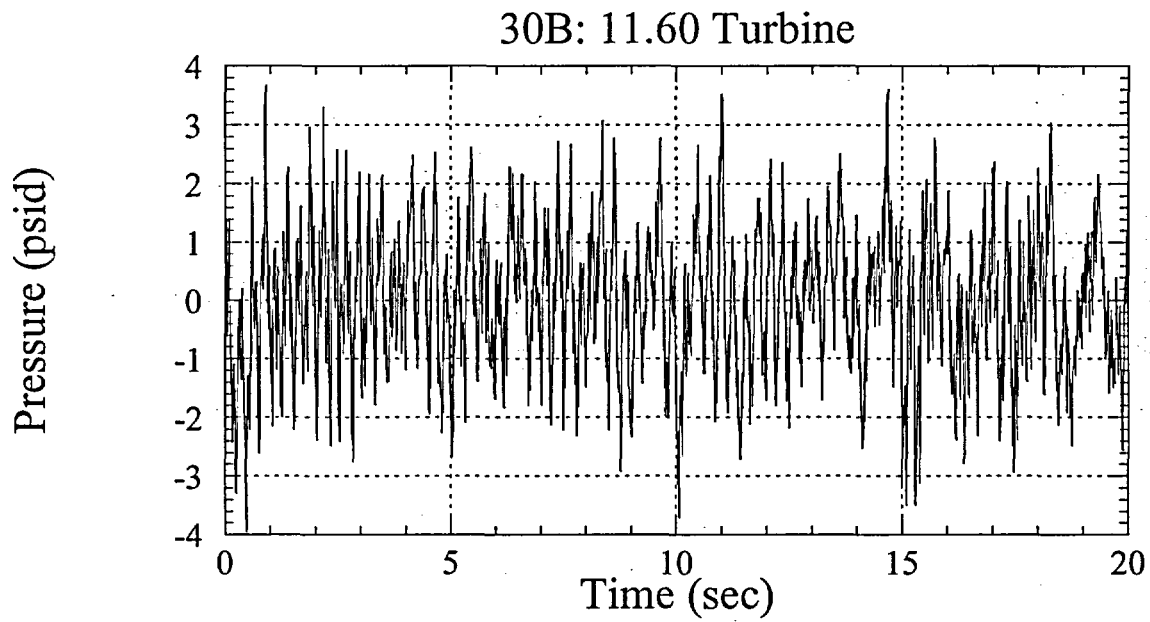


Figure 4-a.

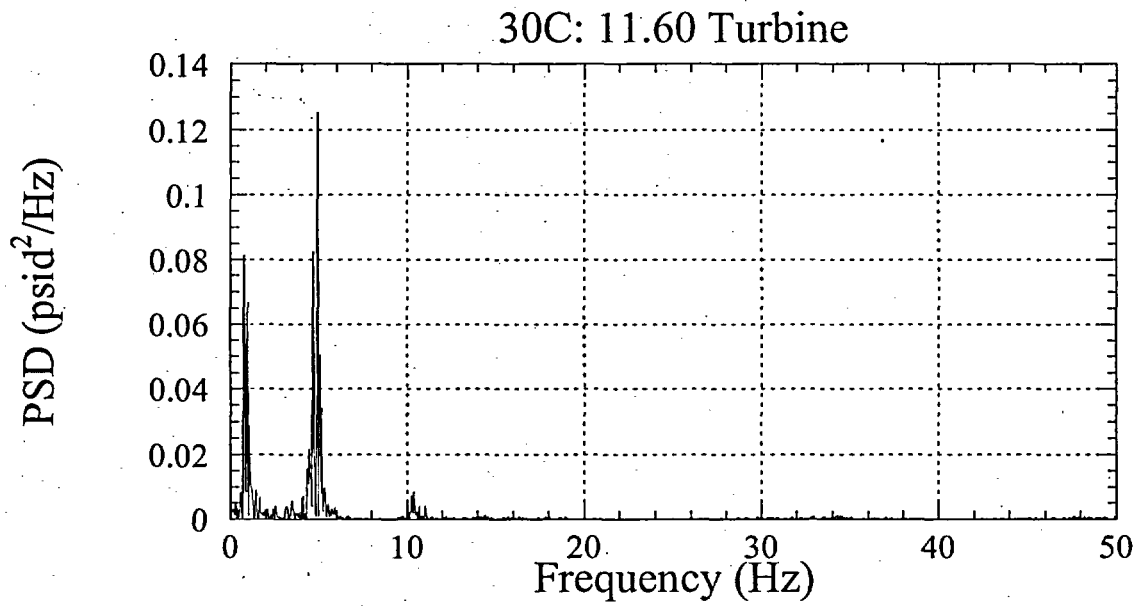
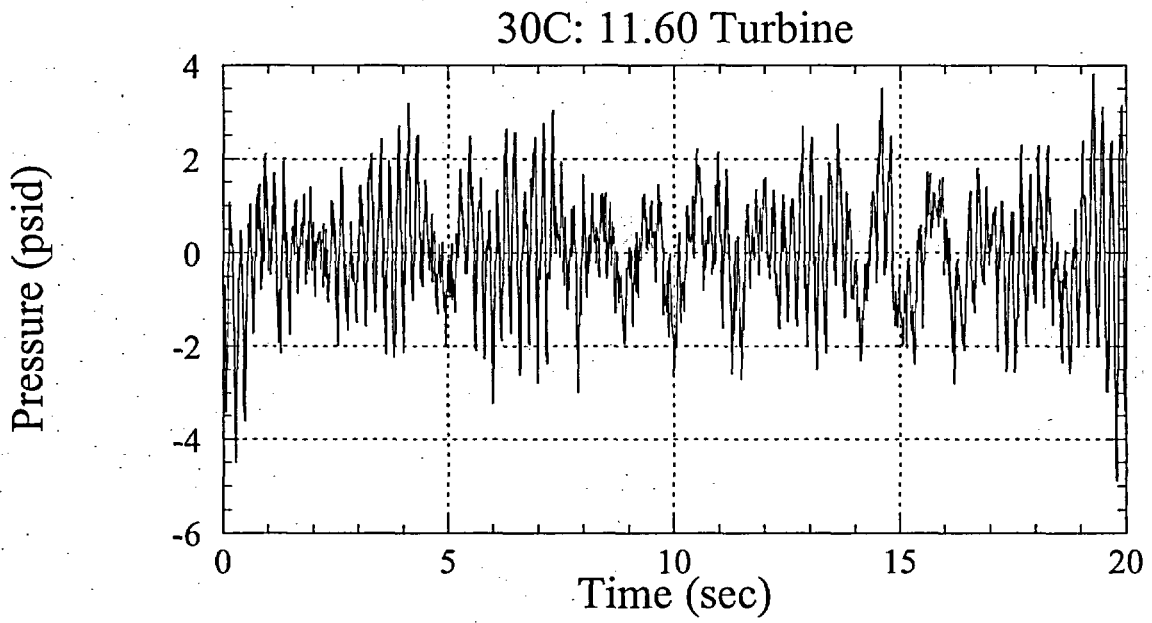


Figure 4-b.

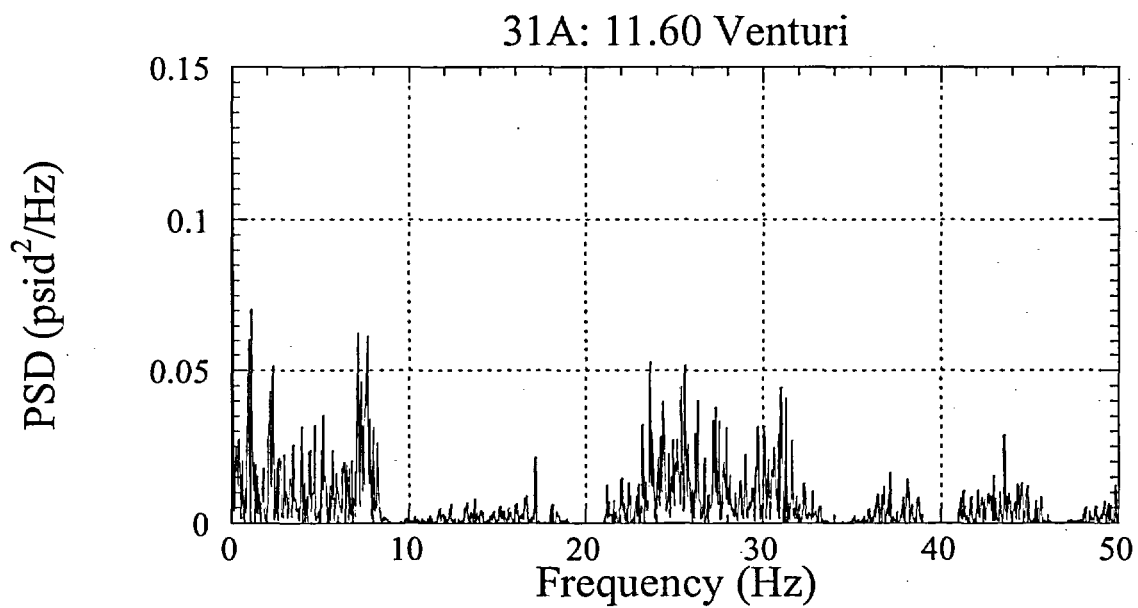
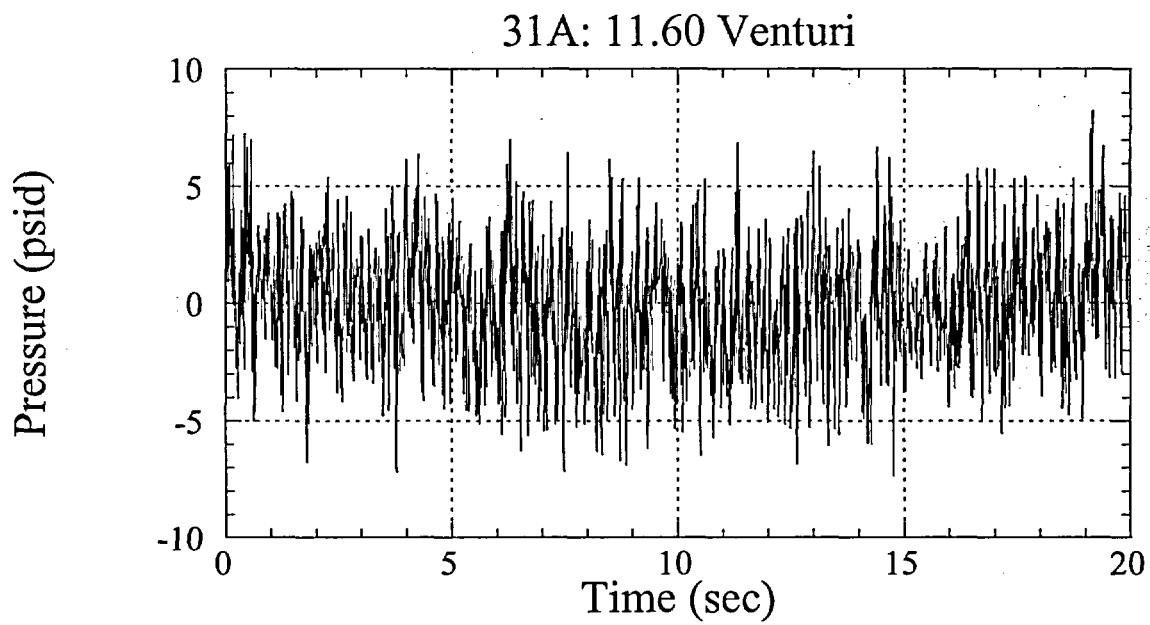


Figure 5-a.

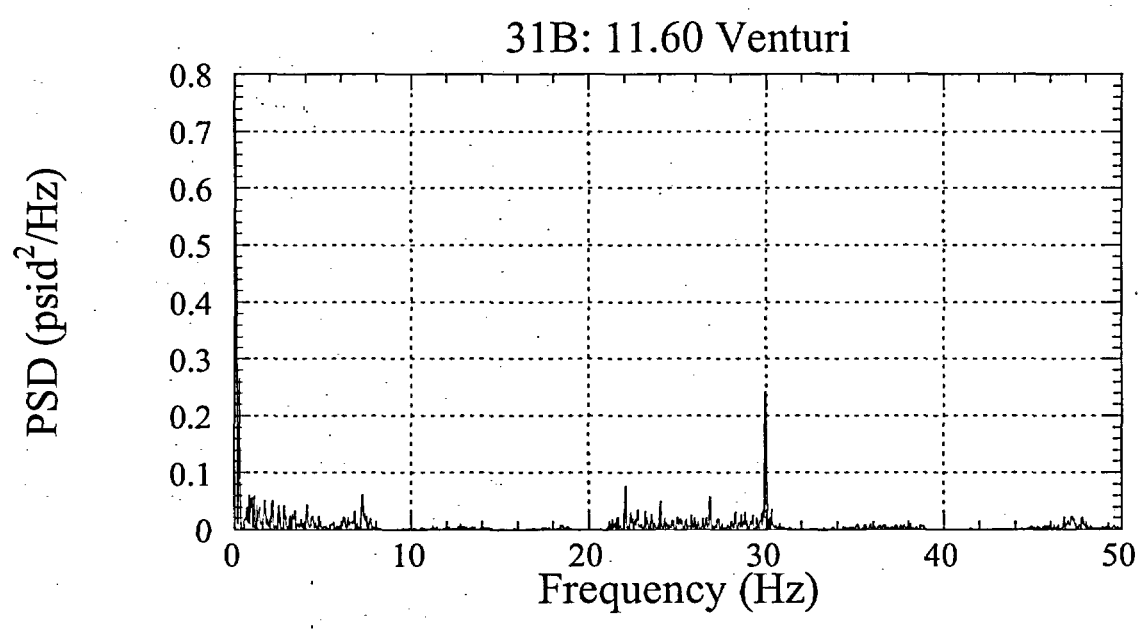
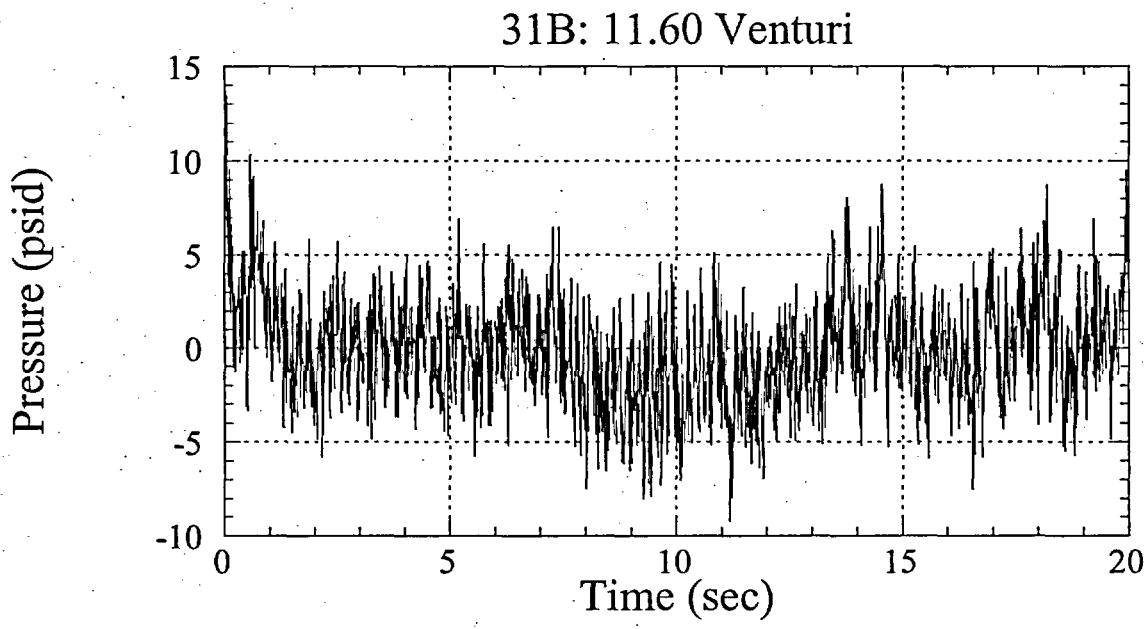


Figure 5-b.

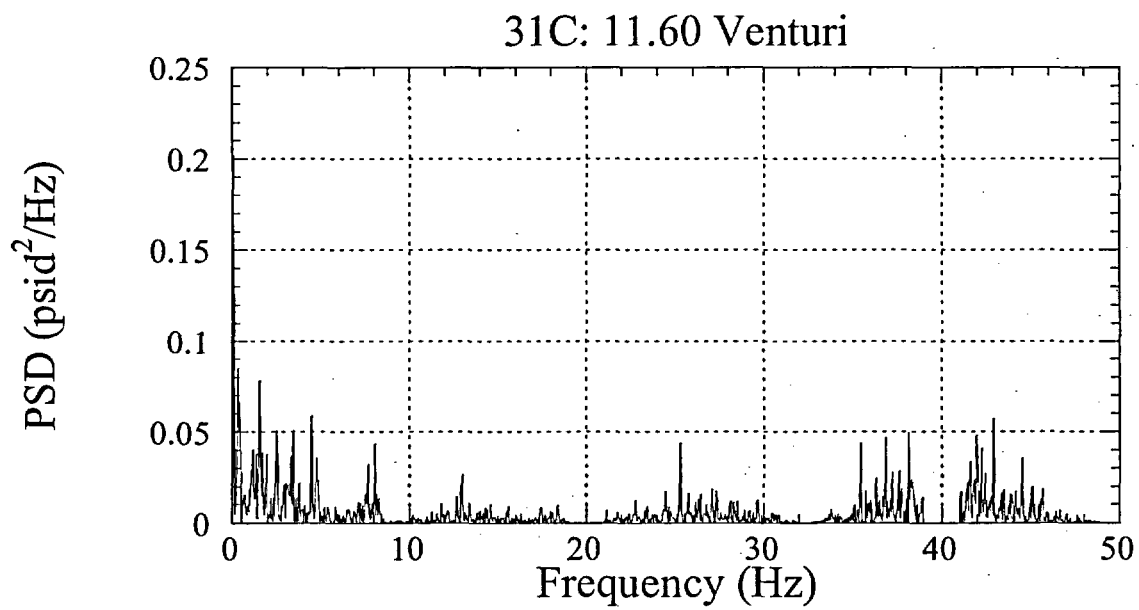
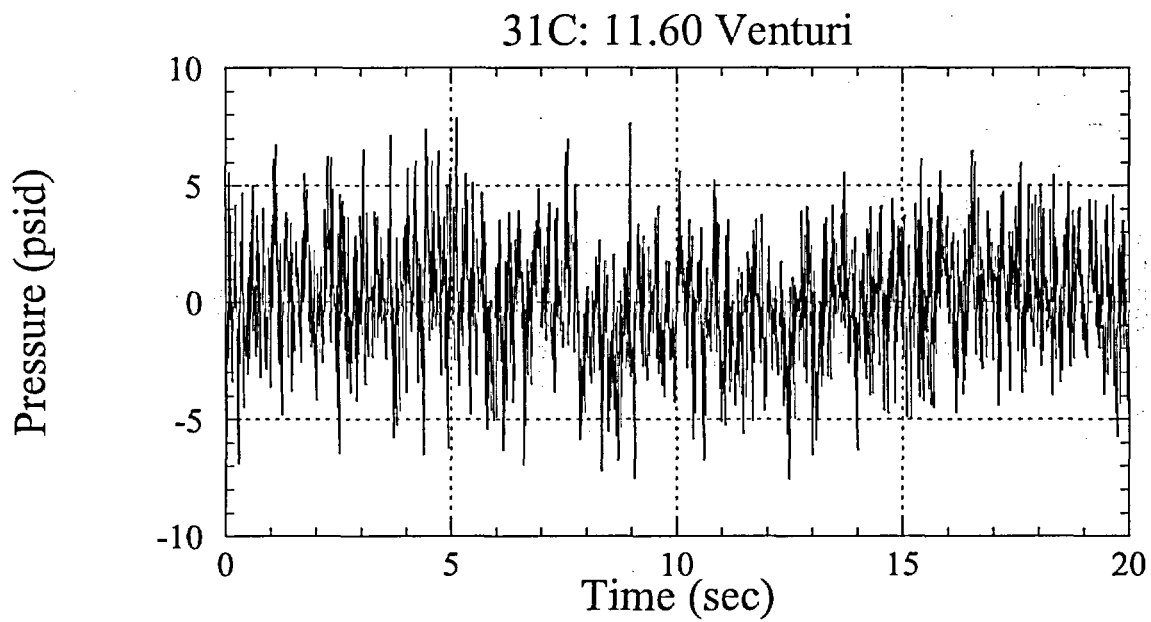


Figure 5-c.

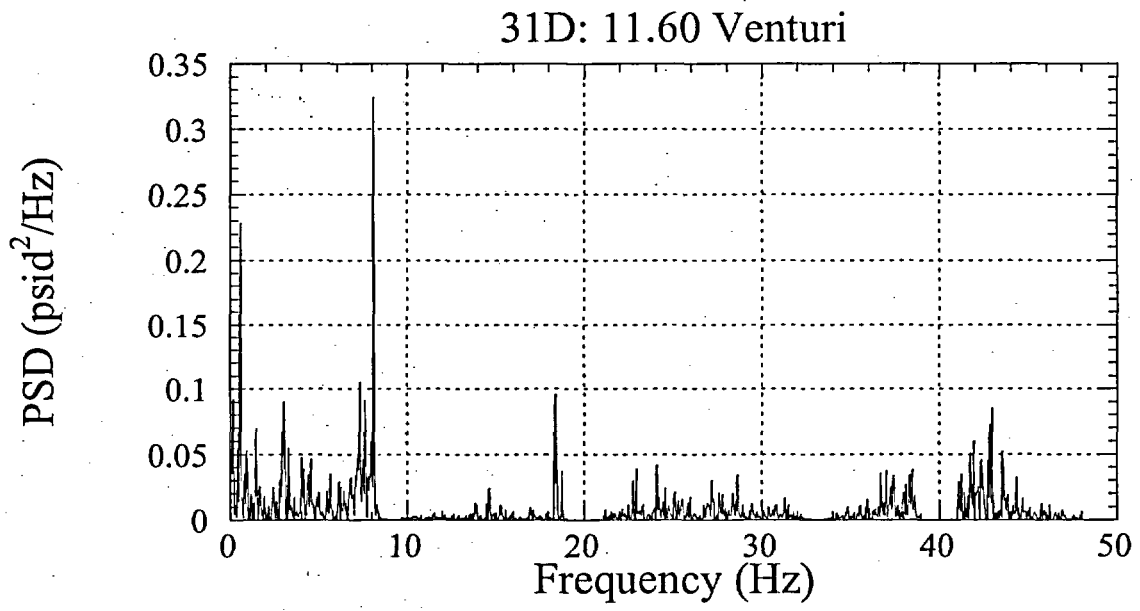
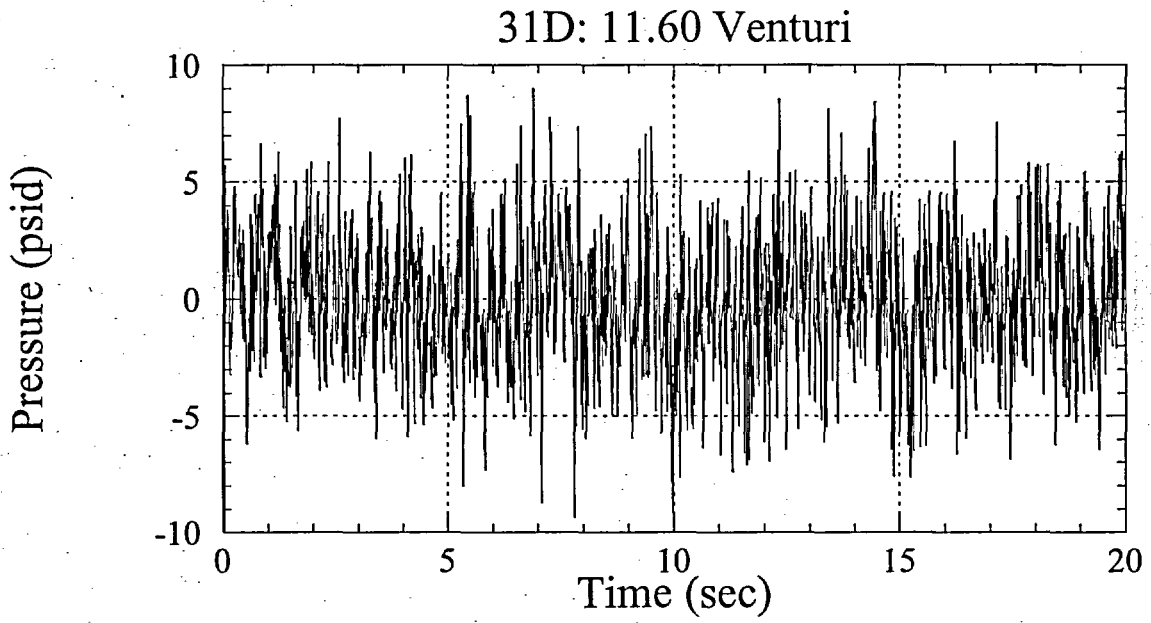


Figure 5-d.

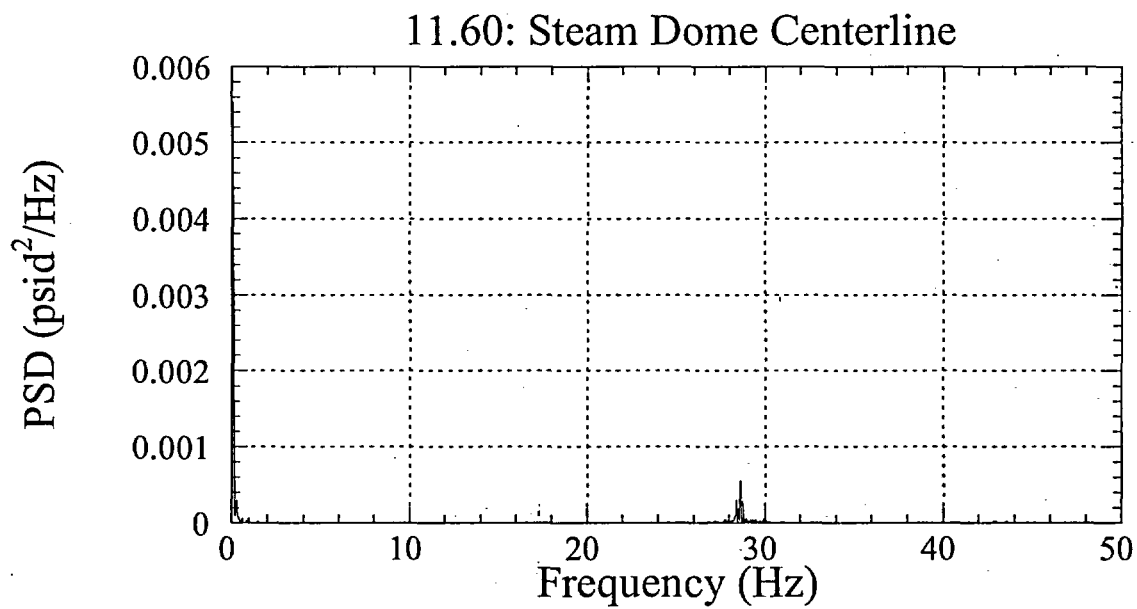
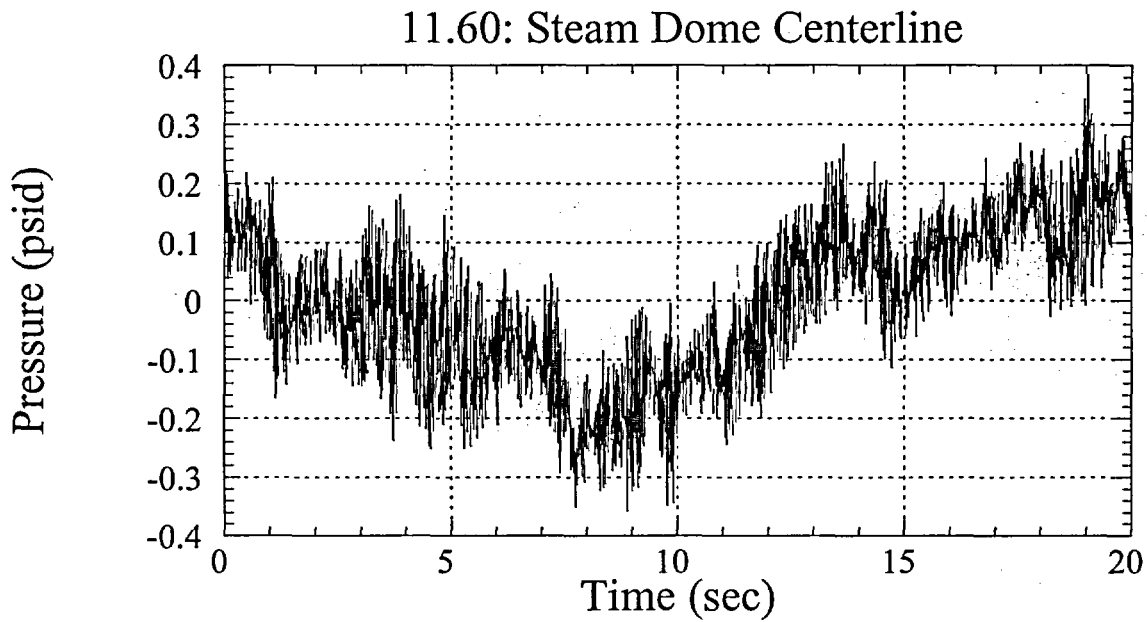


Figure 6. Predicted steam dome centerline pressures and associated PSD at a steam flow rate of 11.60×10^6 lbm/hr.

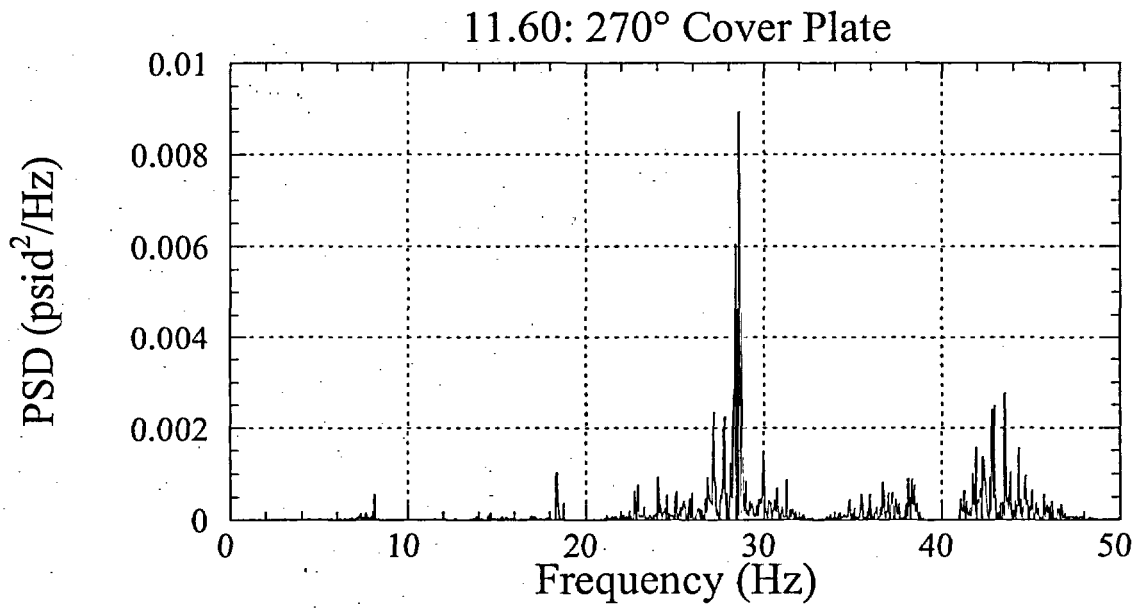
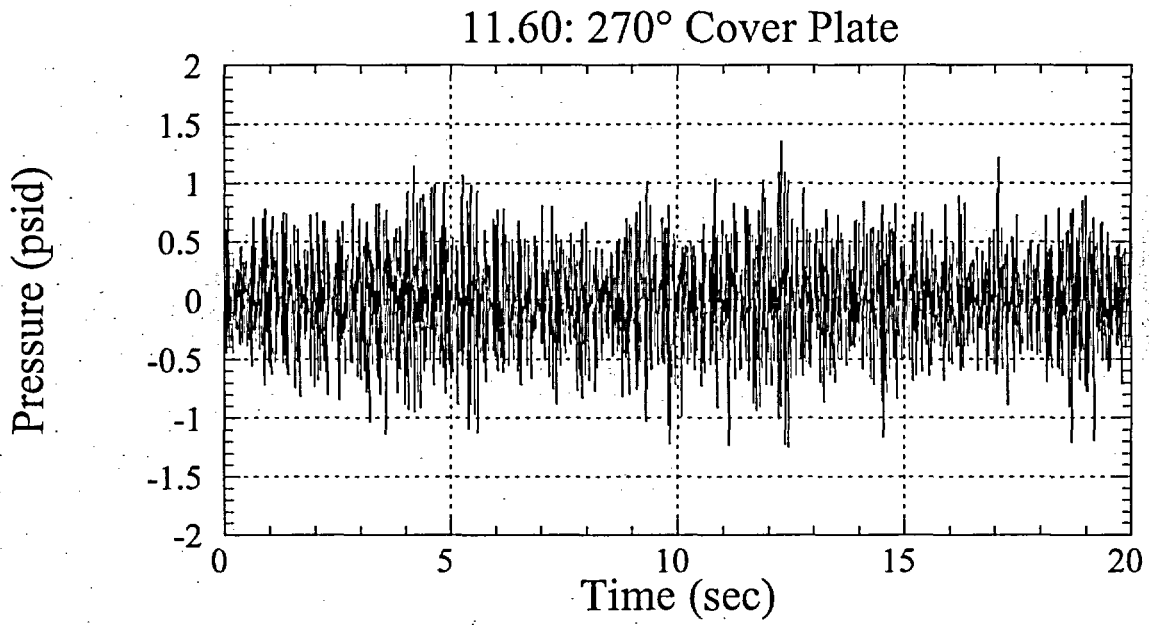


Figure 7. Maximum differential pressure load predicted across a dryer component.

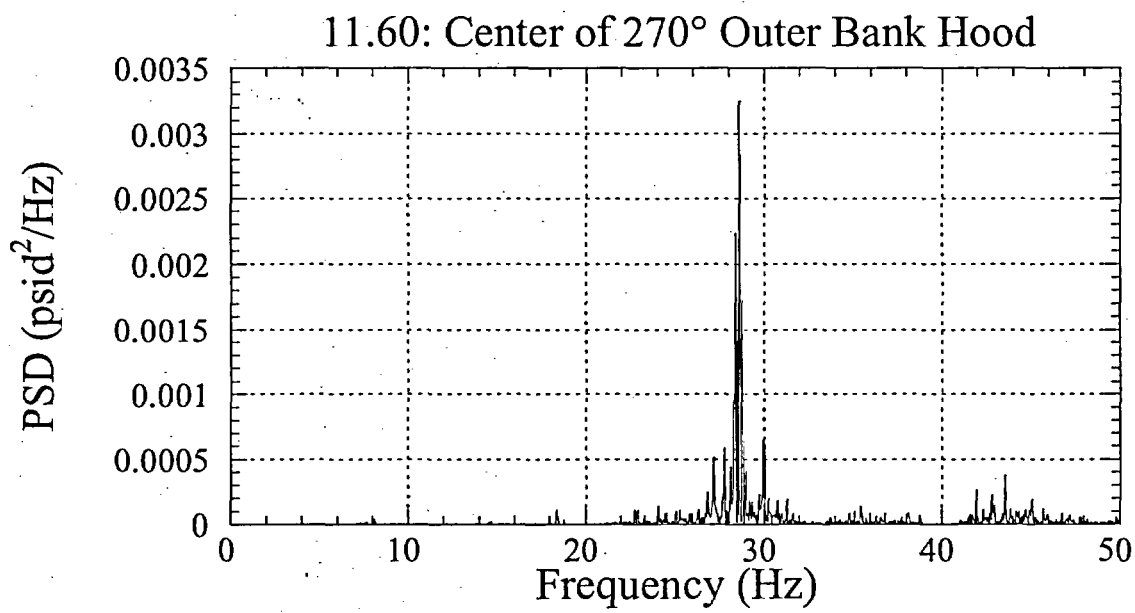
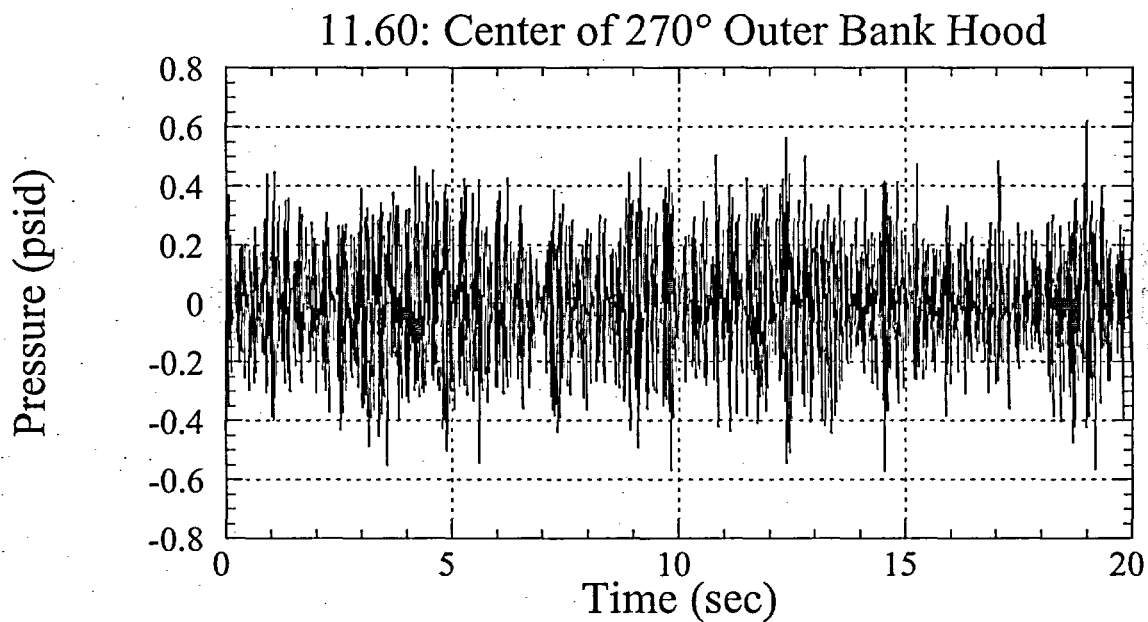


Figure 8.

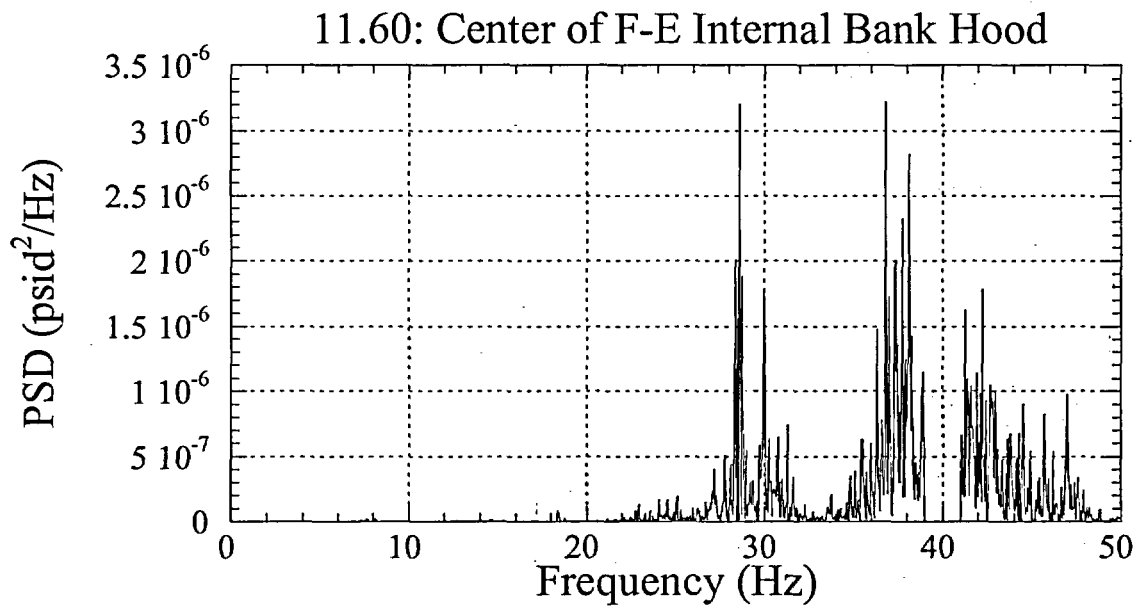
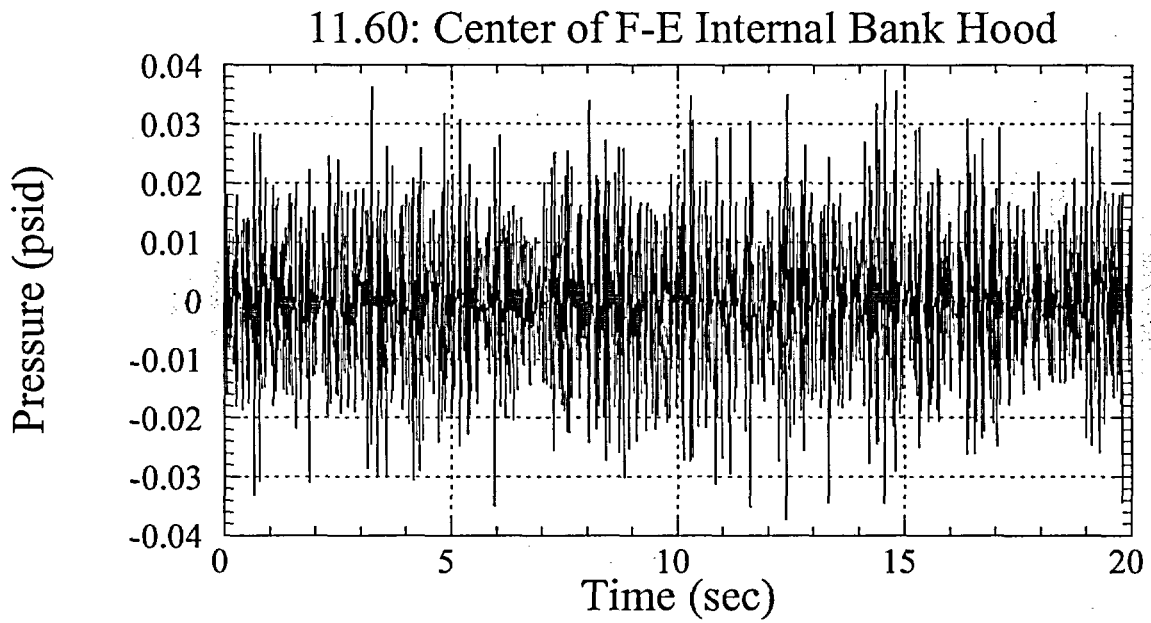


Figure 9.

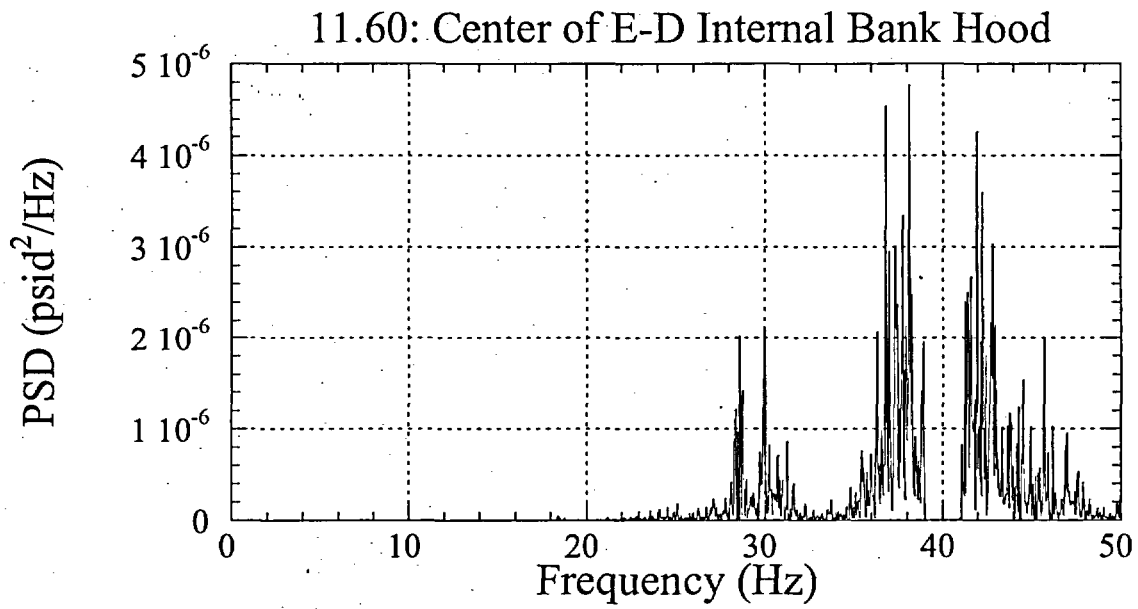
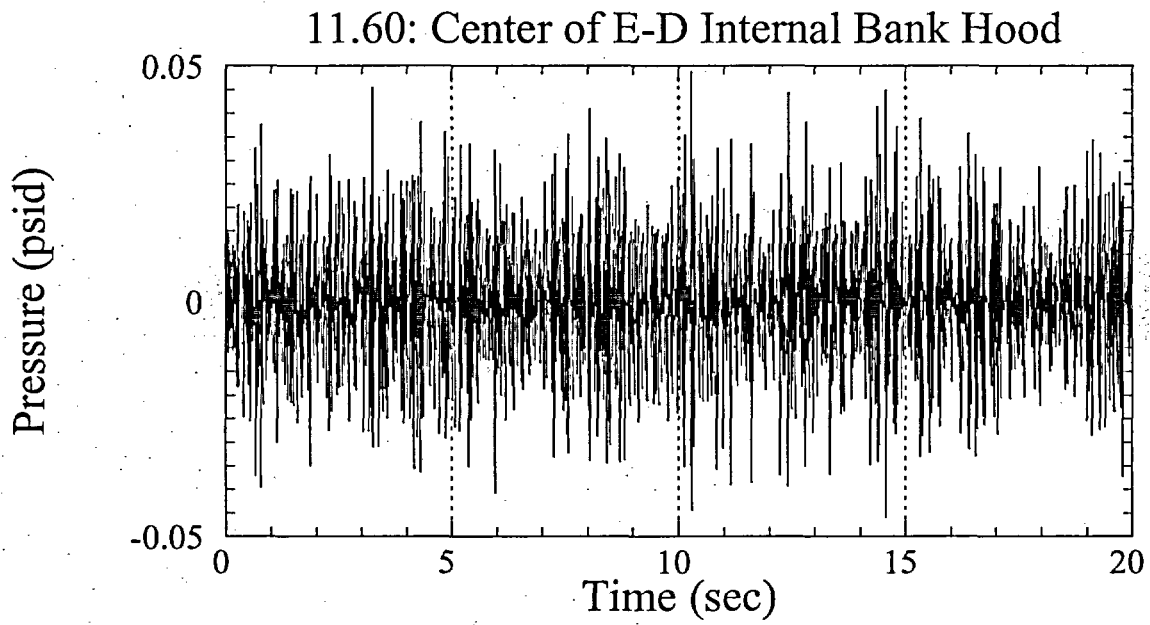


Figure 10.

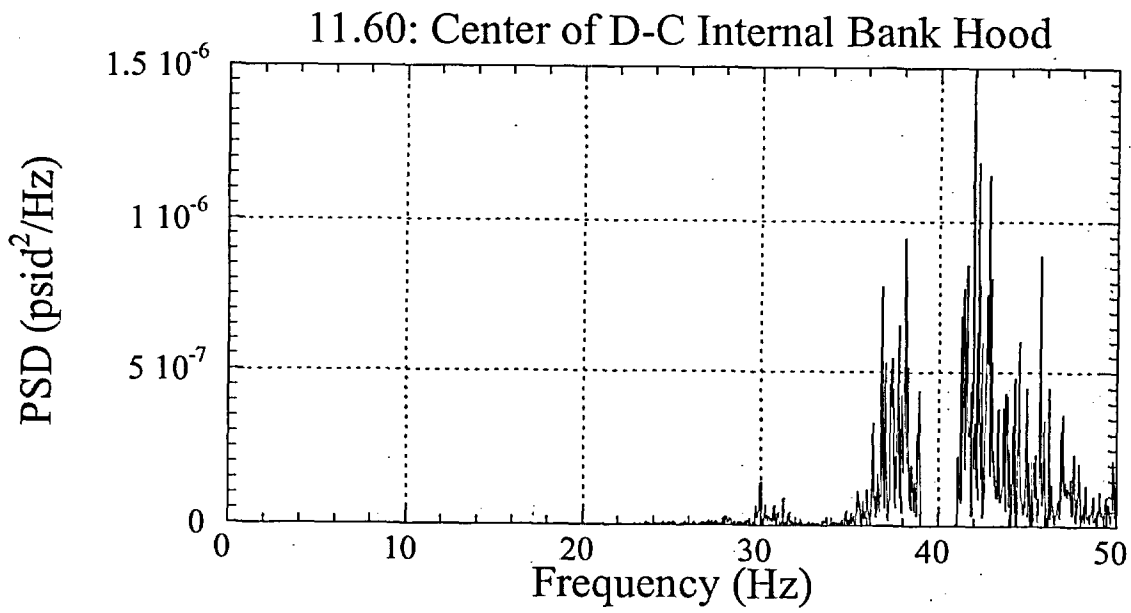
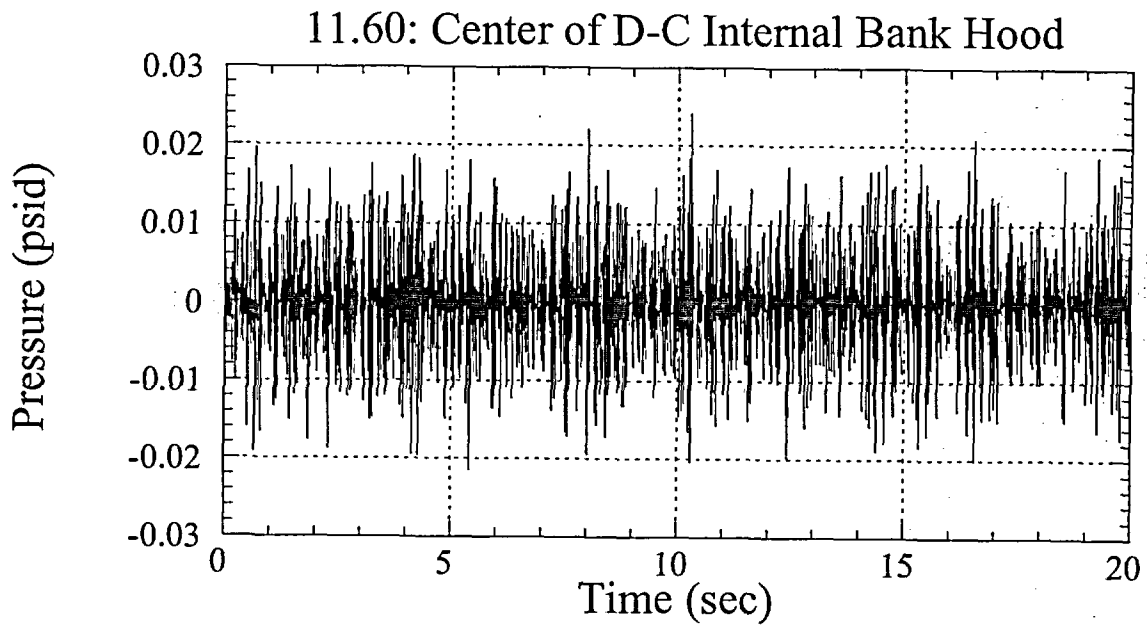


Figure 11.

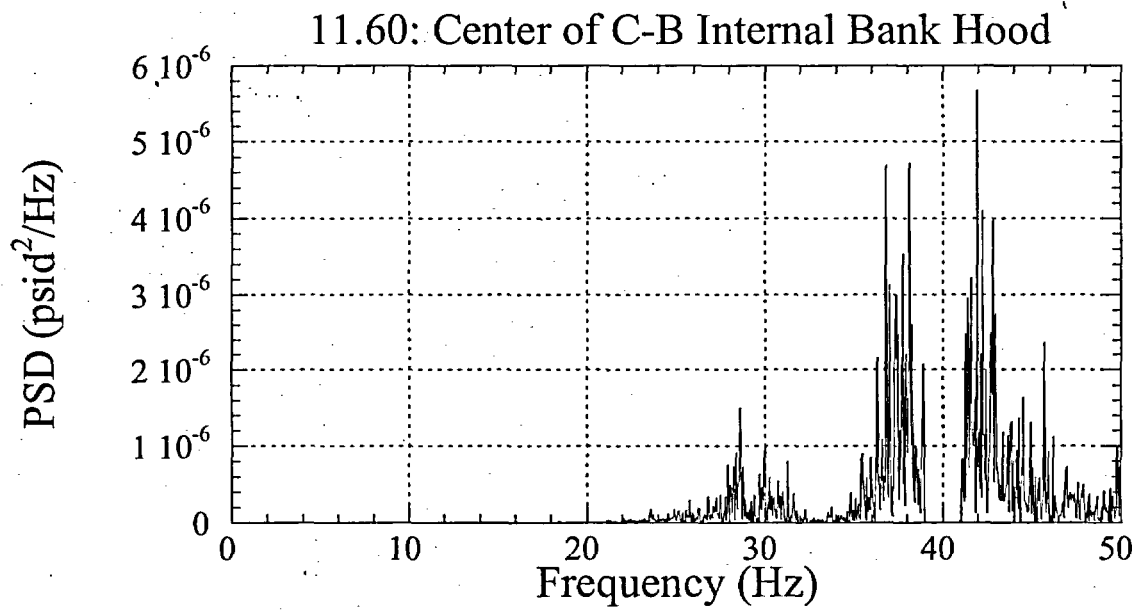
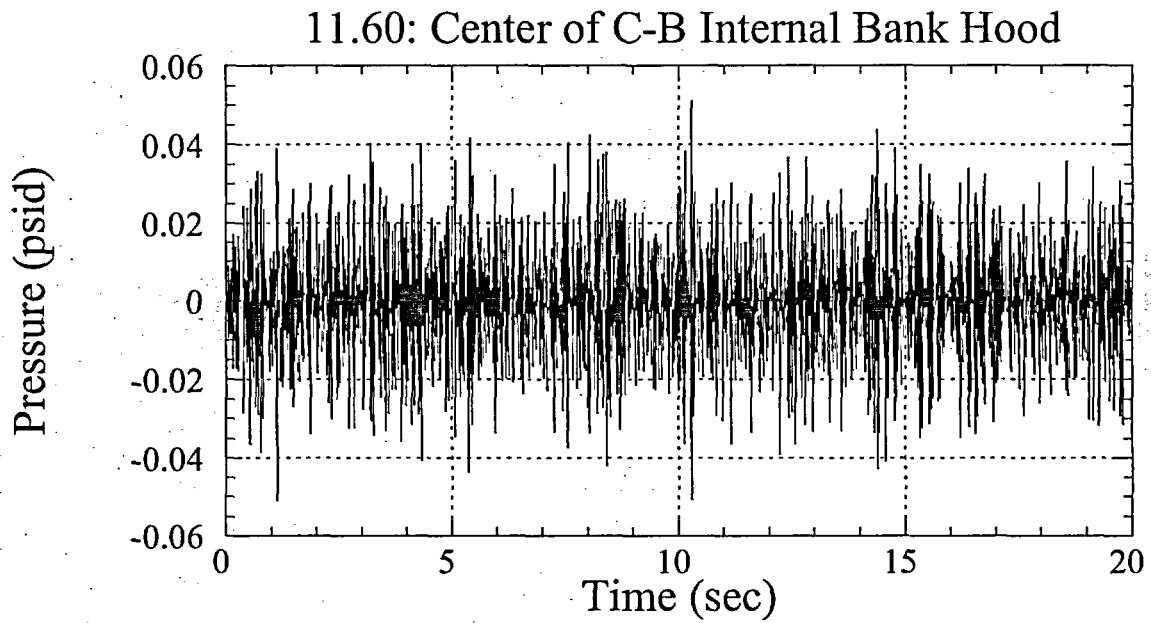


Figure 12.

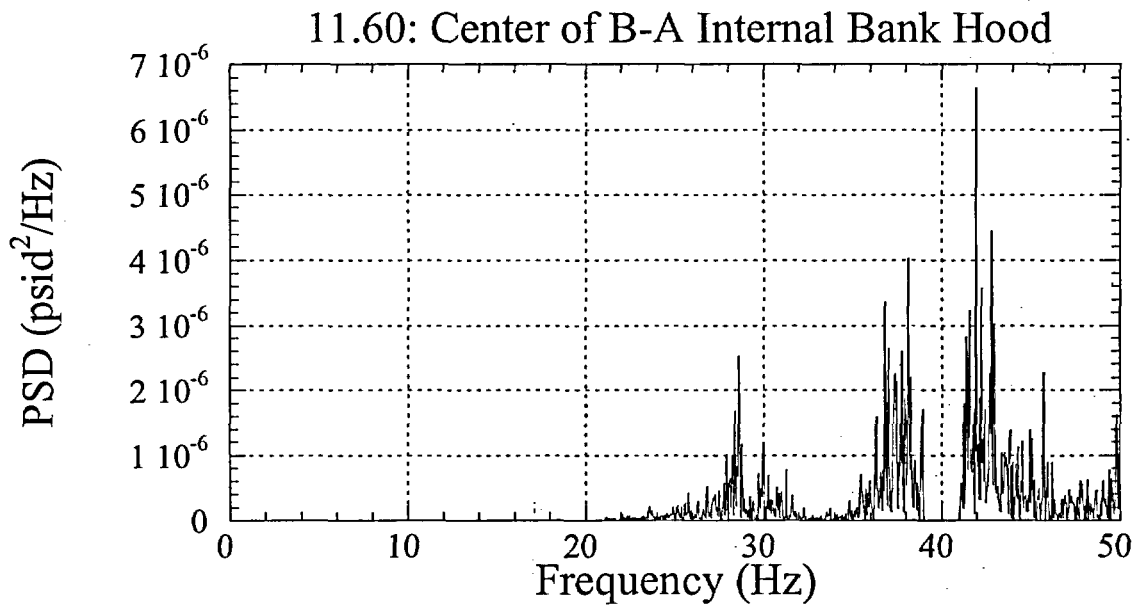
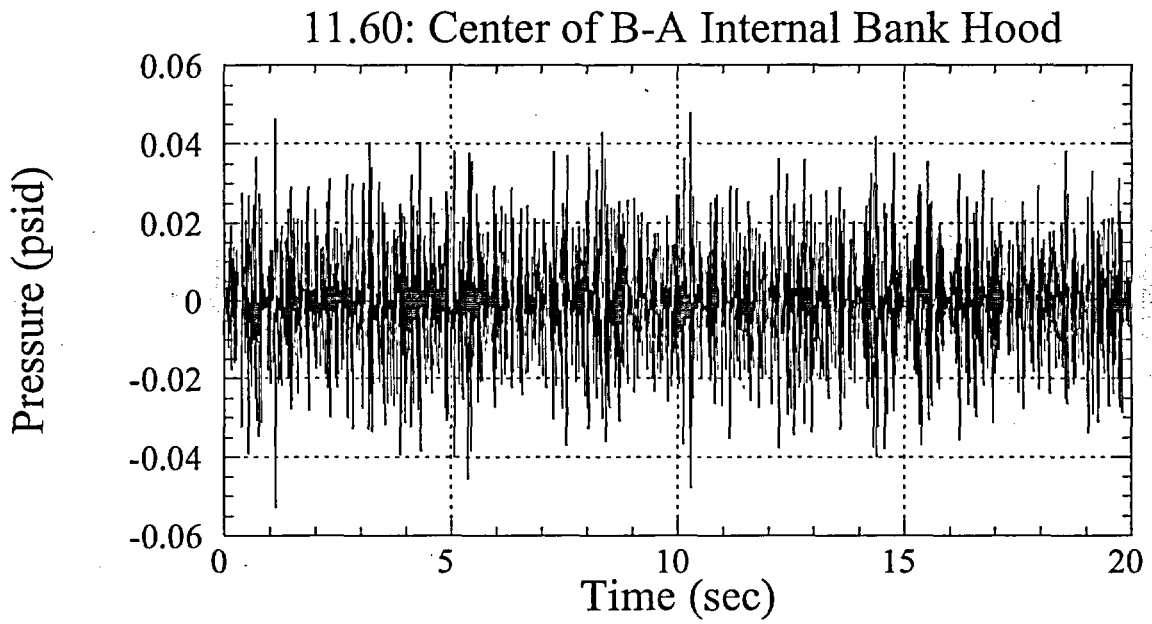


Figure 13.

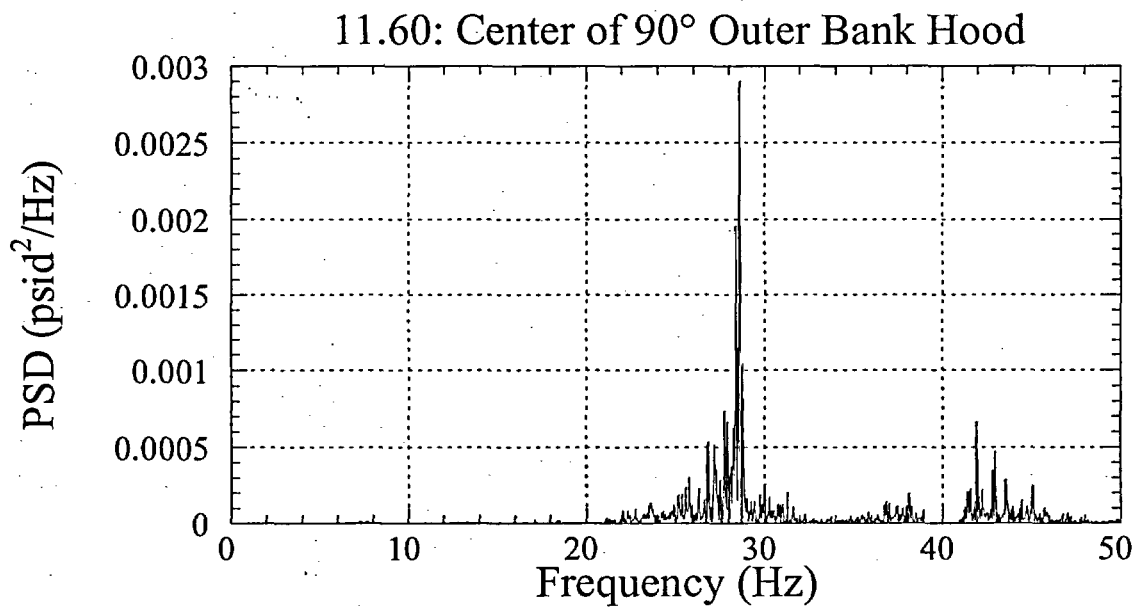
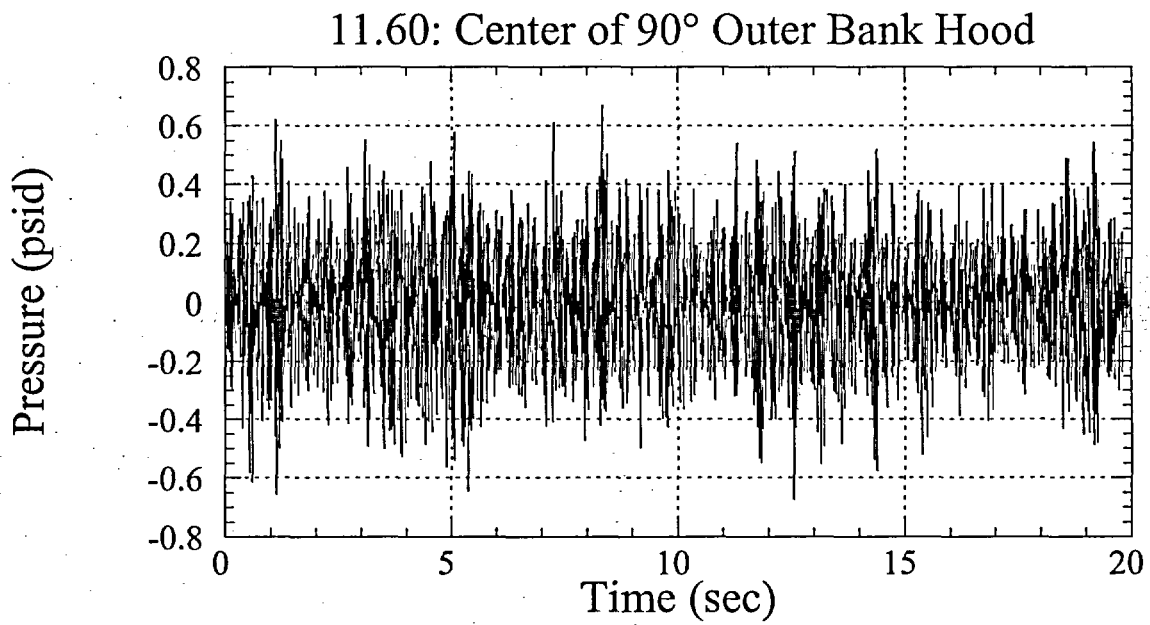


Figure 14.

Hydrodynamic Loads on Dresden Unit 3 Steam Dryer

Final Report

Revision 3

Prepared by

Continuum Dynamics, Inc.
34 Lexington Avenue
Ewing, NJ 08618

Prepared under Purchase Order No. 64992 for

Exelon Generation LLC
4300 Winfield Road
Warrenville, IL 60555

Approved by

Alan Bilanin

Alan J. Bilanin

May 2004

Object

In plant measured pressure oscillation data in main steam lines of Dresden Unit 3 (DR3) are used to force a dynamic model of the steam system. The model is then used to predict the fluctuating pressures across components of the steam dryer in the reactor vessel. This effort provides Exelon with a dryer load definition which comes directly from measured data. The hydrodynamic load data then will be used by a structural analyst to assess the structural adequacy of the "as built" steam dryer in DR3.

Physical Observations

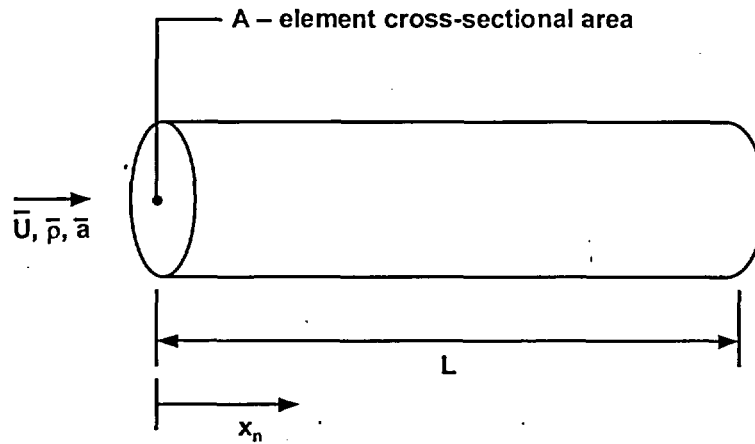
Analysis by others, of dryer failure at Quad Cities Unit 2 (QC2) during the summer of 2003, used the observed fatigue dryer damage to back calculate a structural load which was consistent with this damage. Fatigue damage, however, is dependent upon both magnitude of load and frequency of application. The analysis was not able to identify discrete frequencies and therefore recommended that a flat spectrum be used with an amplitude which was determined to be consistent with the observed damage. This flat spectrum is equivalent to the assumption that the forcing is random, in spite of the fact that the subscale tests conducted by others indicated that discrete frequencies were observed in the steam lines and the reactor steam dome. Exelon obtained unsteady pressure data in the plant (DR3) during operation, and the effort reported herein is the analysis of these data. Contrary to the assumption of a flat loading spectrum, the data show that there are discrete deterministic phenomenon at work in the steam dome and main steam lines that are responsible for the loading on the dryer. This report quantifies this load from full scale test data.

Modeling Considerations

Pulsation in a single phase compressible medium, where acoustic wavelengths are long compared to component dimensions and in particular long compared to transverse dimensions (directions perpendicular to the primary flow directions), lend themselves to an analysis methodology known as acoustic circuit analysis. If the analysis is restricted to frequencies below 50 Hz, acoustic wavelengths are approximately 30 feet in length and wavelengths are long compared to most components of interest.

Acoustic circuit analysis divides the system to be analyzed into elements which are characterized as sketched below in a length (L), cross sectional area (A), mean density ($\bar{\rho}$), mean flow velocity (\bar{U}) and mean acoustic speed (\bar{a})

nth-element



It can be shown that the fluctuating pressure P' and velocity u'_n in this nth element must satisfy

$$P'_n = (A_n e^{ik_{1n}X_n} + B_n e^{ik_{2n}X_n}) e^{i\omega t}$$

$$u'_n = \frac{1}{-\omega\rho} (A_n k_{1n} e^{ik_{1n}X_n} + B_n k_{2n} e^{ik_{2n}X_n}) e^{i\omega t}$$

where harmonic time dependence of the form $e^{i\omega t}$ has been assumed. The wave numbers k_{1n} and k_{2n} are the two complex roots of

$$k_n^2 + i4f_n \frac{|\bar{U}_n|}{D_n a} (\omega + \bar{U}_n k_n) - \frac{\omega}{a} (\omega + \bar{U}_n k_n) = 0$$

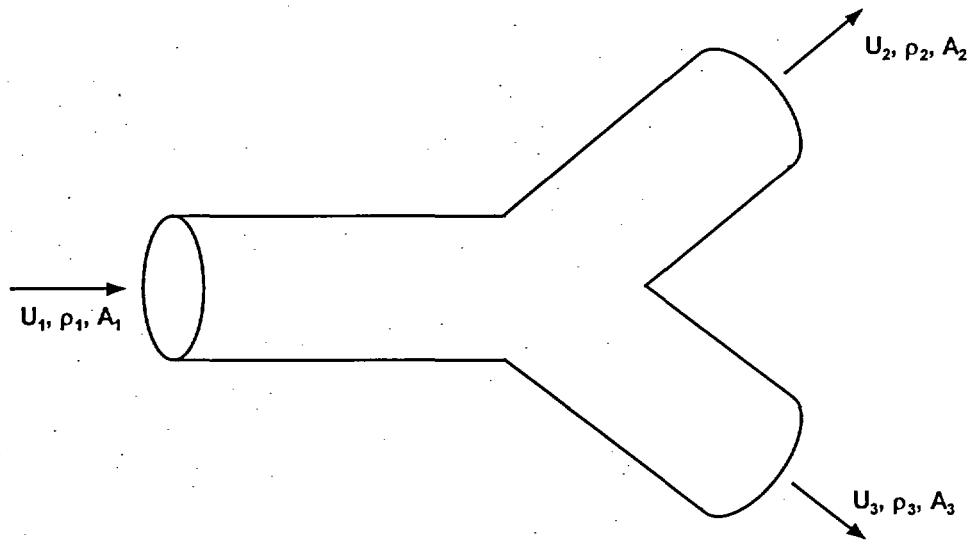
where f_n - pipe friction factor for element n
 D_n - hydrodynamic diameter for element n
 $i = \sqrt{-1}$

A_n and B_n are constants which are a function of frequency and are determined by satisfying continuity of pressure at element junctions and mass conservation at a junction.

Mass conservation at a junction requires that (see sketch below)

$$\rho_1 U_1 A_1 = \rho_2 U_2 A_2 + \rho_3 U_3 A_3$$

where $()_m$ refer to each segment.



The flow passages for the DR3 reactor and main steam lines are discretized into 78 elements and the resulting system can be driven with prescribed shear layer motions at geometric discontinuities. These discontinuities exist in the steam delivery system where convective velocities are high.

One source of energy transfer from the main steam velocity to unsteady motion results from the impingement of the shear layer in the main steam line over the 30 inch diameter D ring junction. This oscillation of the shear layer over the cavity formed by the D ring header has an empirically determined preferred frequency of oscillation (f) of

$$f = 0.44 \frac{\bar{U}}{D}$$

The preferred driving frequency with a main steam velocity at this junction of 145 ft/sec and $D = 2.5$ ft is 25.5 Hz. As will be shown, the plant data suggest that energy does indeed exist at this frequency in the main steam lines. The circuit analysis should tell whether the energy at this frequency can propagate into the reactor dome.

Model Discretization

The 78 elements which are used to model the dynamics of the steam system are sketched schematically below and physical dimensions used in defining the individual elements are shown in Figures 2 and 3. The dimensions used were the best available at the time of analysis.

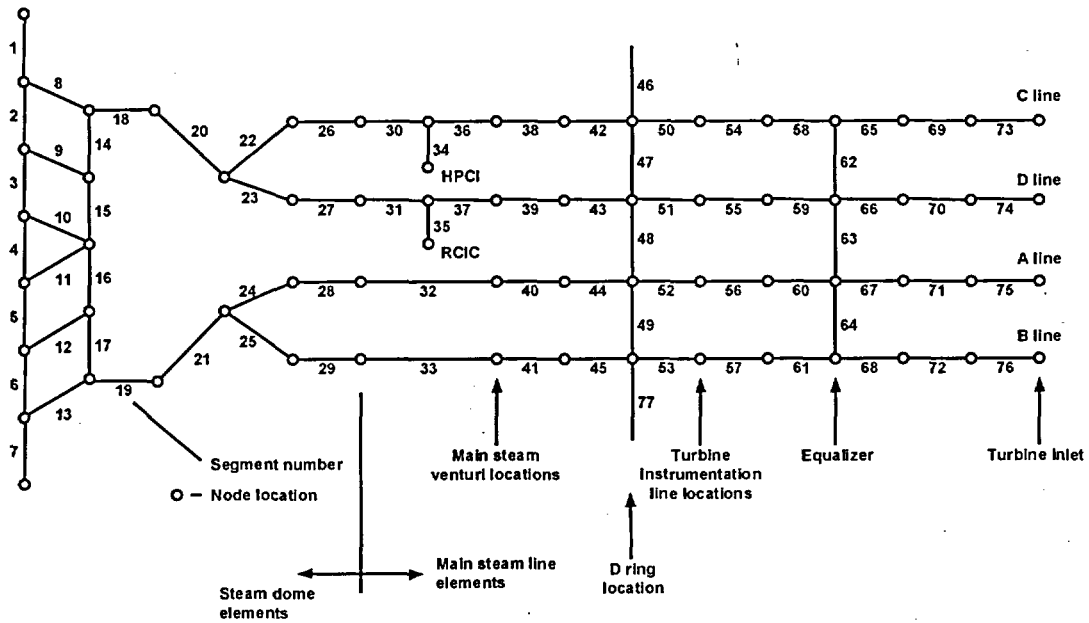


Figure 1: Schematic of the elements used in the acoustic circuit analysis.

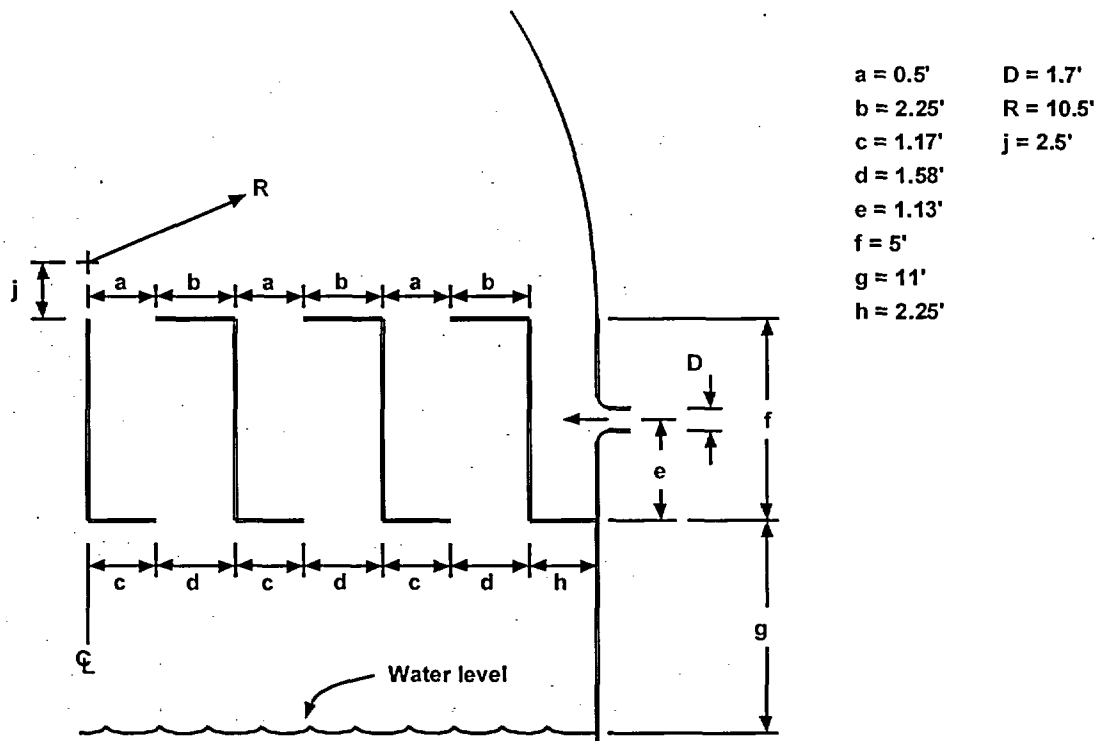


Figure 2: Steam dome and dryer dimensions.

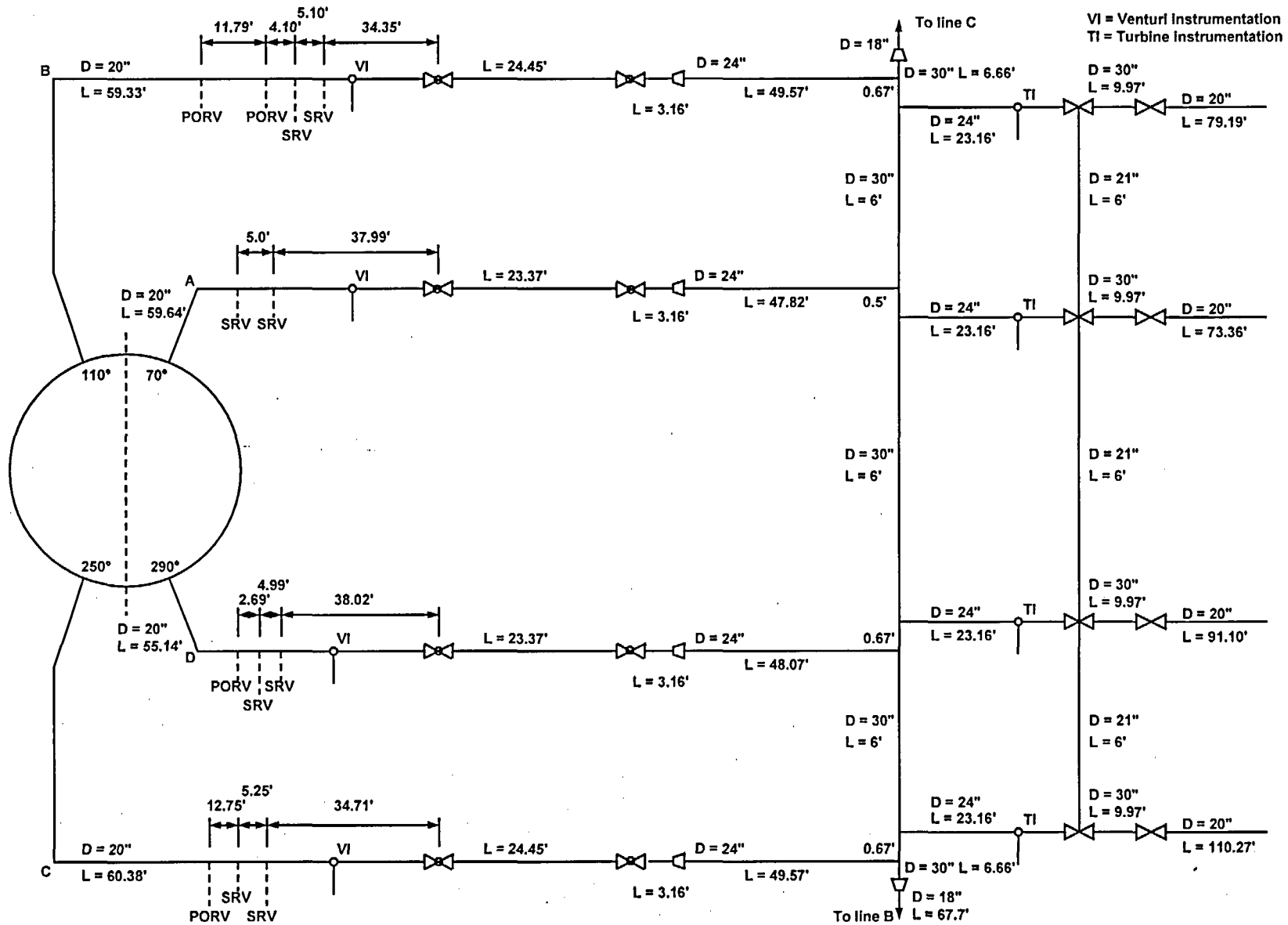


Figure 3: Piping geometry to be used in the circuit analysis (DR3).

Input Pressure Data

Exelon has mounted pressure transducers on the main steam lines at the main steam venturi and upstream of the turbine (turbine instrument lines). The data sets provided are tabulated below on Table 1. All data provided were taken at the end of instrument lines whose lengths were specified. Lines were assumed filled with water and the data corrected for the instrument line effects of line length, acoustic speed, and losses along the line, by correcting the data in frequency space and then reconstructing the time signal at the instrument line location on the main steam line. Corrections are significant at frequencies associated with the 1/4, 3/4, 5/4, etc. standing wave frequencies of the instrument lines. The resulting pressure time histories and Power Spectral Density functions (PSDs) are shown on Figures 4 to 17. The respective captions on these figures are read as follows. From Figure 4-a, for example, the label "21A: 9.86 Venturi" denotes that the data set number is "21" (see Table 1) taken on the "A" steam line at a steam mass flow rate of 9.86×10^6 lbm/hr. The sensor location is at the main steam line "venturi" location.

In an effort to illustrate the relationship between mean steam flow rate and pressure oscillation level, the rms pressure at the venturi on main steam line D was plotted as a function of mean steam flow rate on Figure 18 (the C and D lines were chosen, since by observation the oscillations are largest in these lines). It may be seen that the rms pressure fluctuations on the plotted main steam lines are an increasing function of mean steam flow rate.

From work with these data sets, it is known that the largest dryer loads are correlated with the highest rms pressure levels. It is therefore anticipated that the largest dryer load occurs in these data at a mean steam flow rate of 11.63×10^6 lbm/hr. It is not known that this is the maximum steam flow rate possible in DR3, as sister plants have had maximum steam flow rates of 11.95×10^6 lbm/hr. If flow rates for DR3 higher than those reported here exist, the dryer load definition reported here may not be bounding.

Table 1
SUMMARY OF DRESDEN 3 DATA SETS

Data Set #	Steam Flow (10 ⁶ lbm/hr)	Location	Date/Time	Data Rate (samples/sec)	Figure #	Comments
21	9.86	Venturi A, B, C & D	11/21 07:39	500	4-a, b, c, d	1, 2
22	9.86	Turbine B & C	11/21 07:39	500	5-a, b	2
23	9.86	Venturi A, B, C & D	11/21 09:07	500	6-a, b, c, d	1, 2
24	9.86	Turbine B & C	11/21 09:07	500	7-a, b	2
32	10.22	Venturi A, B, C & D	12/22 12:40	500	8-a, b, c, d	1, 2
33	10.22	Turbine B & C	12/22 12:40	500	9-a, b	2
34	10.49	Venturi A, B, C & D	12/22 13:45	500	10-a, b, c, d	1, 2
35	10.49	Turbine B & C	12/22 13:45	500	11-a, b	2
36	11.00	Venturi A, B, C & D	12/22 15:50	500	12-a, b, c, d	1, 2
37	11.00	Turbine B & C	12/22 15:50	500	13-a, b	2
38	11.35	Venturi A, B, C & D	12/22 18:06	500	14-a, b, c, d	1, 2
39	11.35	Turbine B & C	12/22 18:06	500	15-a, b	2
40	11.63	Venturi A, B, C & D	12/22 19:30	500	16-a, b, c, d	1, 3
41	11.63	Turbine B & C	12/22 19:30	500	17-a, b	3

Comment 1: rms value computed on C and D venturi data

Comment 2: analyzed for dryer load but not reported here

Comment 3: used for dryer load definition

Model Validation

Referring to Table 1 there are seven data sets where the four venturi pressure fluctuations were recorded simultaneously, and two of the four turbine pressure fluctuations were recorded simultaneously. From Table 1 it may be seen that the pressures in the venturi instrument lines A through D were recorded simultaneously in Runs 21, 23, 32, 34, 36, 38, and 40 with corresponding turbine data in Runs 22, 24, 33, 35, 37, 39, and 41, respectively. The main steam venturi measurements were used to drive the circuit model of the system, and predict the average root mean square pressure measured by the four turbine instruments at the same power settings. These averages are shown in Table 2.

It should be noted that the turbine instrumentation showed extremely narrow spikes at precisely 20 and 40 Hz. These spikes are believed to be induced by the strong electromagnetic field of the turbine. The spikes were removed from the data analyzed by dropping the Fourier coefficients of the time series between 19-21 and 39-41 Hz.

The venturi in-phase data sets were input into the model, and frictional damping was adjusted in the main steam lines until the average root mean square pressure was predicted at the turbine instrument lines. No adjustment was made to the frictional damping at the lowest steam flow rate. The four venturi data sets were used simultaneously in the acoustic circuit analysis to determine sources at the main steam line D ring junction. The friction factors used are summarized in Table 3.

Table 2
SUMMARY OF DRESDEN 3 RMS PRESSURE VALUES AT THE TURBINE
INSTRUMENT LINES

Run	Steam Flow (10 ⁶ lbm/hr)	B Line P _{RMS} (psid)	C Line P _{RMS} (psid)	Average (psid)
22	9.86	1.16	1.23	1.20
24	9.86	1.15	1.06	1.11
33	10.22	2.80	1.48	2.24
35	10.49	2.82	1.59	2.29
37	11.00	3.09	2.17	2.67
39	11.35	2.90	1.73	2.39
41	11.63	2.85	1.67	2.33

Table 3
SUMMARY OF DRESDEN 3 DAMPING MODIFICATIONS TO PREDICT THE RMS
PRESSURE VALUES AT THE TURBINE INSTRUMENT LINES

Steam Flow (10 ⁶ lbm/hr)	Multiplier on Friction Factor	Turbine Inlet Predicted rms (psid)	Turbine Inlet Measured rms (psid)
9.86	1.00	1.71	1.20
9.86	1.00	1.52	1.11
10.22	1.60	2.25	2.24
10.49	1.50	2.30	2.29
11.00	1.52	2.67	2.67
11.35	1.34	2.39	2.39
11.63	1.30	2.33	2.33

Rev 3

Results

The model (subject to the approximations and limitations described above) can now predict the pressure time histories in the reactor steam space as a function of position and time. Shown in Figure 19 is the prediction of steam dome pressure time history and PSD at a steam flow rate of 11.63×10^6 lbm/hr. Note that the PSD levels are very low, and little energy exists in the 20-30 Hz frequency band.

Sensitivity

Calculations were performed to determine the sensitivity of peak differential pressure load, as a function of assumed friction factor. The sensitivity of the peak differential pressure load at the highest steam flow rate of 11.63×10^6 lbm/hr can be computed from

$$\Delta p_{\text{peak}} (\text{psid}) = -0.6(f - 1.0).$$

A 10% decrease of the friction factor from 1.0 to 0.9, increases the peak differential pressure load by 0.06 psid.

Rev 3

Dryer Hydrodynamic Forcing

Pressure differences are now computed across dryer components, and these loads and locations are described in the Appendix and are transmitted separately. In this section we will discuss these loads.

The analysis discussed above shows the maximum predicted load occurs on the cover plate located at the 270° position. The differential pressure time history and associated PSD are shown in Figure 20. Here, the load is maximum at 28.5 Hz, which should be compared with the pressure fluctuation in the steam dome (Figure 19) which is lower by one order of magnitude. This indicates excitation of the steam above and below the dryer in a mode that would be difficult to anticipate by inspection of the dryer and steam dome geometry. It is also noted that unless the phasing of fluctuations in the main steam lines were such that signals were out of phase in general, the steam dome is a pressure node in the system. The peak is not sharp and energy exists in the 22 – 33 Hz frequency interval.

Differential pressure loads for other dryer components computed at the center of the component are shown in Figures 21 to 27 for a steam flow rate of 11.63×10^6 lbm/hr. In general the loads decrease radially inboard into the dryer components away from the main steam line inlets, but not monotonically. This again is an indication that the acoustic oscillation about the dryer assembly is complex.

Conclusions

The acoustic circuit analysis used with plant data

- a) confirms that steam dryer hydrodynamic loads are highest at the highest reactor power setting.
- b) predicts the maximum loading on the dryer occurs predominantly at a single frequency, 28.5 Hz in the 0 to 50 Hz frequency range.
- c) predicts that the loads on dryer components are largest for components nearest the main steam nozzles and decrease for components near the center of the reactor vessel.
- d) may not determine the highest dryer load, if steam flow rates in excess of 11.63×10^6 lbm/hr are achieved in DR3.
- e) predicts that the highest peak differential pressure to be found on any dryer component at a steam flow rate of 11.63×10^6 lbm/hr is instantaneously 1.4 psid (Figure 20), with a rms differential pressure of 0.38 psid.

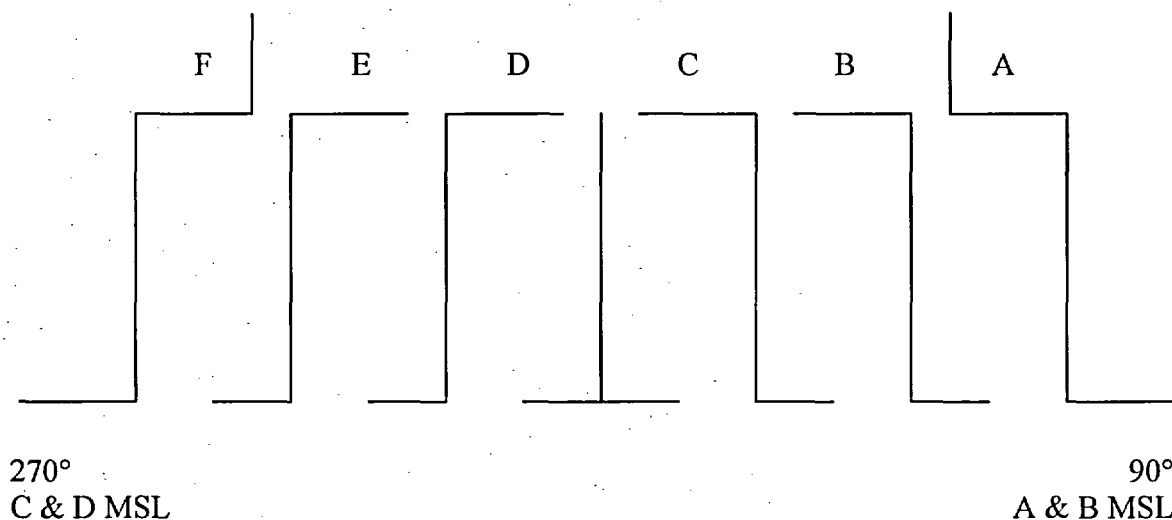
Recommendations

As confidence grows that the loads transfer methodology is valid and appropriate, scoping work should be undertaken to ascertain required changes to the circuit analysis to make it appropriate to compute higher frequency dryer loads.

APPENDIX

PREDICTIONS OF PRESSURE TIME HISTORY IN THE STEAM DOME

Three ASCII data files contain the time history data for the predictions of differential pressure (psid) across the various plates in the dryer. A schematic of the geometry looks like this:



The pressure differences are computed by subtracting the pressure below the plate from the pressure above the plate (for horizontal plates), and subtracting the pressure to the right of the plate (in the above schematic) from the pressure to the left of the plate (for vertical plates).

The file `time40bottom.txt` contains the following columns of data for the power setting of 11.63×10^6 lbm/hr:

#	Contents
1	time (sec) to 20.48 sec
2	pressure difference at the left edge of the 270° cover plate below entrance to MSL C
3	pressure difference at the right edge of the 270° cover plate below entrance to MSL C
4	pressure difference at the left edge of the 270° cover plate below entrance to MSL D
5	pressure difference at the right edge of the 270° cover plate below entrance to MSL D
6	pressure difference at the left edge of the F bottom plate
7	pressure difference at the right edge of the F bottom plate
8	pressure difference at the left edge of the E bottom plate
9	pressure difference at the right edge of the E bottom plate

- 10 pressure difference at the left edge of the D bottom plate
- 11 pressure difference at the right edge of the D bottom plate (center)
- 12 pressure difference at the left edge of the C bottom plate (center)
- 13 pressure difference at the right edge of the C bottom plate
- 14 pressure difference at the left edge of the B bottom plate
- 15 pressure difference at the right edge of the B bottom plate
- 16 pressure difference at the left edge of the A bottom plate
- 17 pressure difference at the right edge of the A bottom plate
- 18 pressure difference at the left edge of the 90° cover plate below entrance to MSL A
- 19 pressure difference at the right edge of the 90° cover plate below entrance to MSL A
- 20 pressure difference at the left edge of the 90° cover plate below entrance to MSL B
- 21 pressure difference at the right edge of the 90° cover plate below entrance to MSL B

The file time40vertical.txt contains the following columns of data for the power setting of 11.63×10^6 lbm/hr:

- | # | Contents |
|----|--|
| 1 | time (sec) to 20.48 sec |
| 2 | pressure difference at the top edge of the 270° outer hood opposite entrance to MSL C |
| 3 | pressure difference at the bottom edge of the 270° outer hood opposite entrance to MSL C |
| 4 | pressure difference at the top edge of the 270° outer hood opposite entrance to MSL D |
| 5 | pressure difference at the bottom edge of the 270° outer hood opposite entrance to MSL D |
| 6 | pressure difference at the top edge of the vertical plate between F and E |
| 7 | pressure difference at the bottom edge of the vertical plate between F and E |
| 8 | pressure difference at the top edge of the vertical plate between E and D |
| 9 | pressure difference at the bottom edge of the vertical plate between E and D |
| 10 | pressure difference at the top edge of the vertical plate between D and C |
| 11 | pressure difference at the bottom edge of the vertical plate between D and C |
| 12 | pressure difference at the top edge of the vertical plate between C and B |
| 13 | pressure difference at the bottom edge of the vertical plate between C and B |
| 14 | pressure difference at the top edge of the vertical plate between B and A |
| 15 | pressure difference at the bottom edge of the vertical plate between B and A |
| 16 | pressure difference at the top edge of the 90° outer hood opposite entrance to MSL A |
| 17 | pressure difference at the bottom edge of the 90° outer hood opposite entrance to MSL A |
| 18 | pressure difference at the top edge of the 90° outer hood opposite entrance to MSL B |

- 19 pressure difference at the bottom edge of the 90° outer hood opposite entrance to MSL B

The file time40top.txt contains the following columns of data for the power setting of 11.63×10^6 lbm/hr:

#	Contents
1	time (sec) to 20.48 sec
2	pressure difference at the left edge of the F top plate
3	pressure difference at the right edge of the F top plate
4	pressure difference at the left edge of the E top plate
5	pressure difference at the right edge of the E top plate
6	pressure difference at the left edge of the D top plate
7	pressure difference at the right edge of the D top plate (center)
8	pressure difference at the left edge of the C top plate (center)
9	pressure difference at the right edge of the C top plate
10	pressure difference at the left edge of the B top plate
11	pressure difference at the right edge of the B top plate
12	pressure difference at the left edge of the A top plate
13	pressure difference at the right edge of the A top plate
14	pressure difference on the 270° skirt
15	pressure difference at the 90° skirt

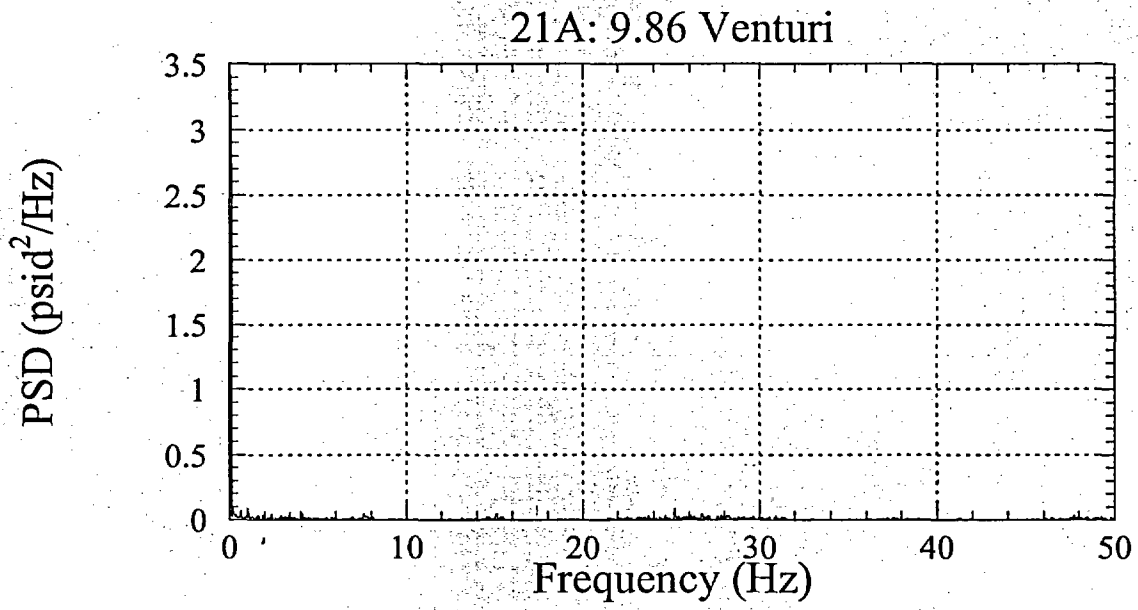
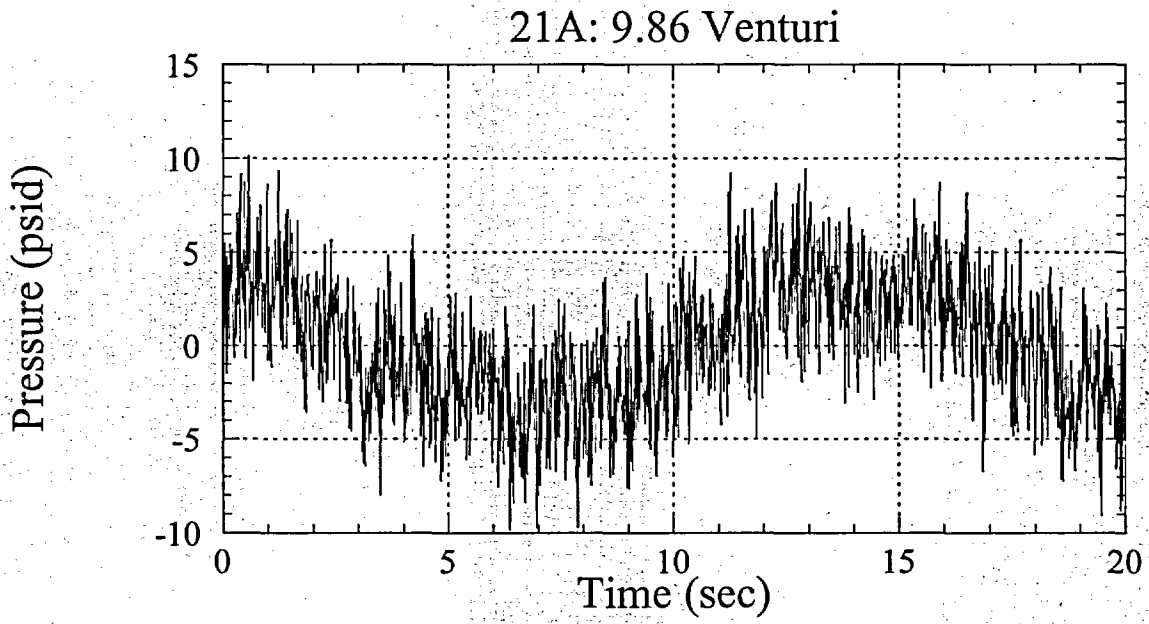


Figure 4-a.

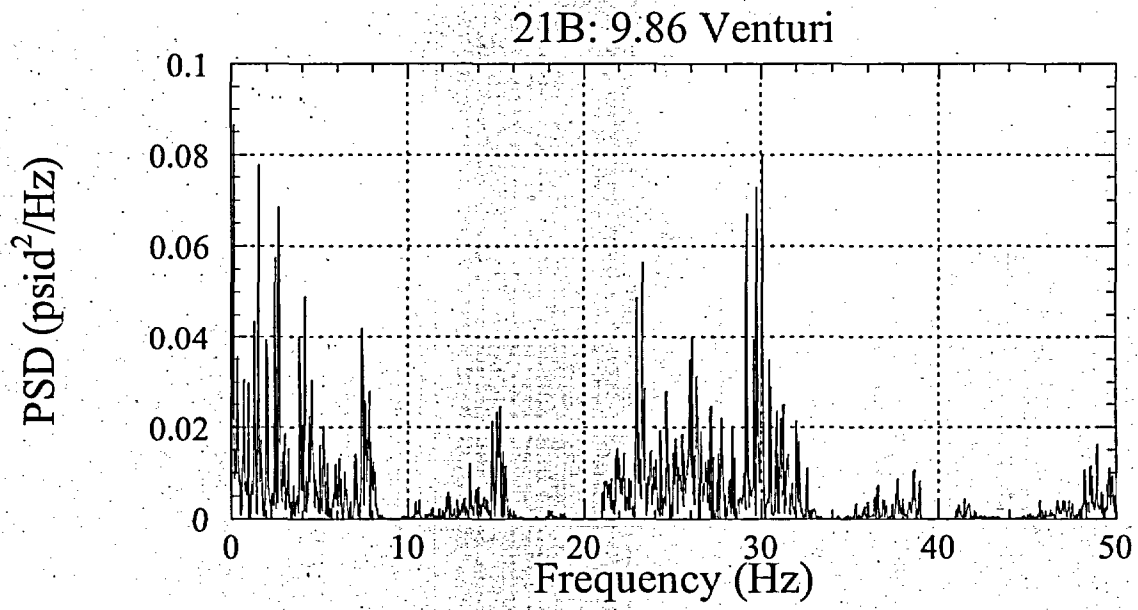
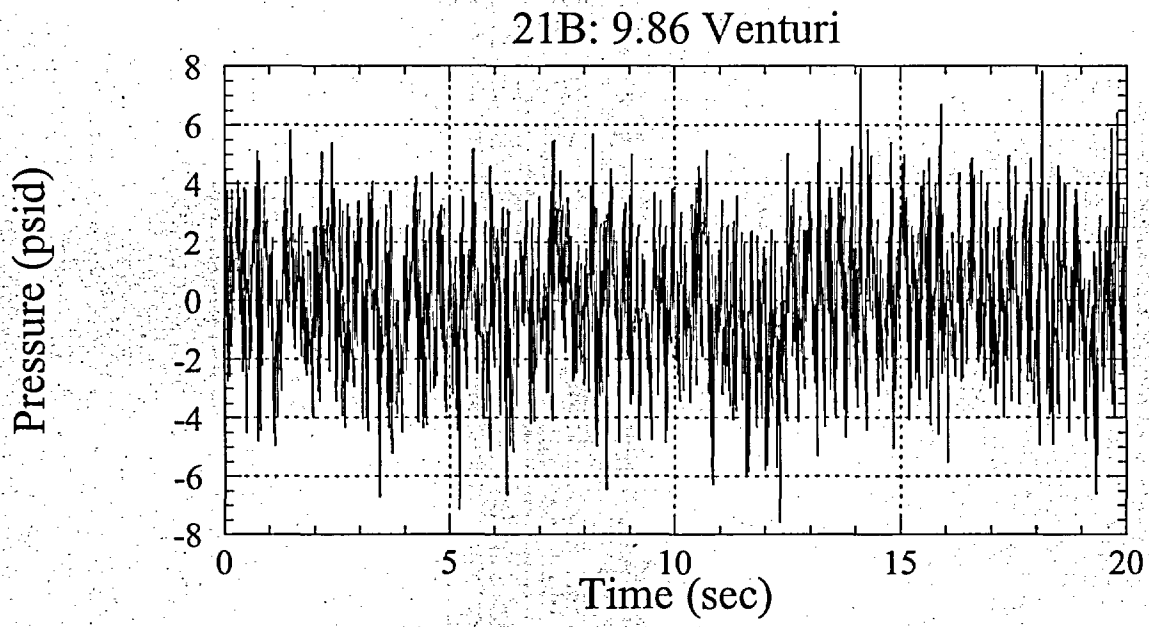


Figure 4-b.

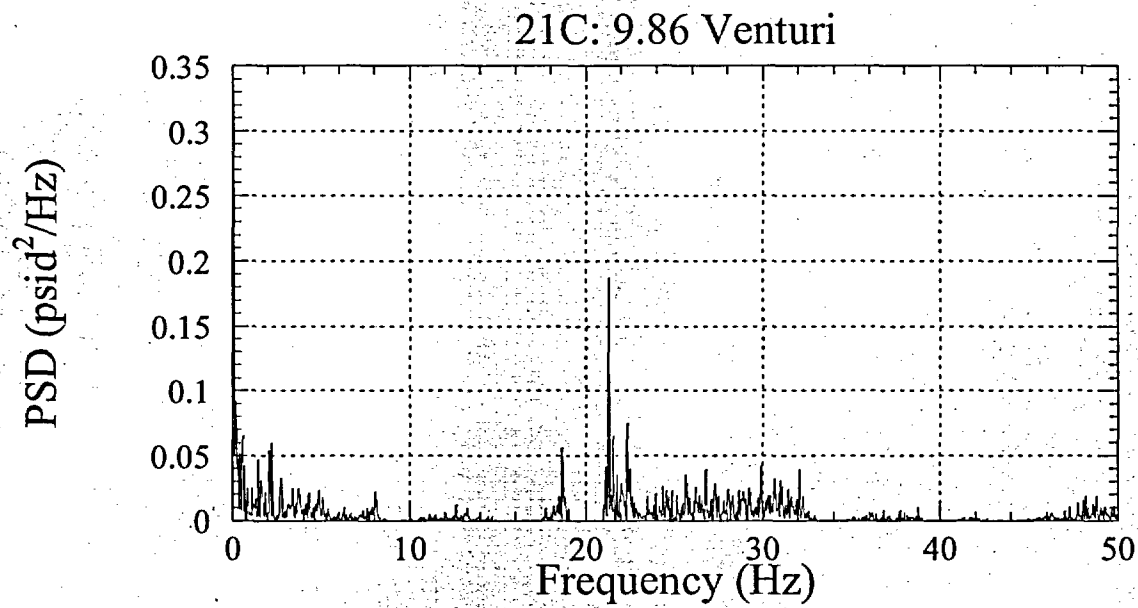
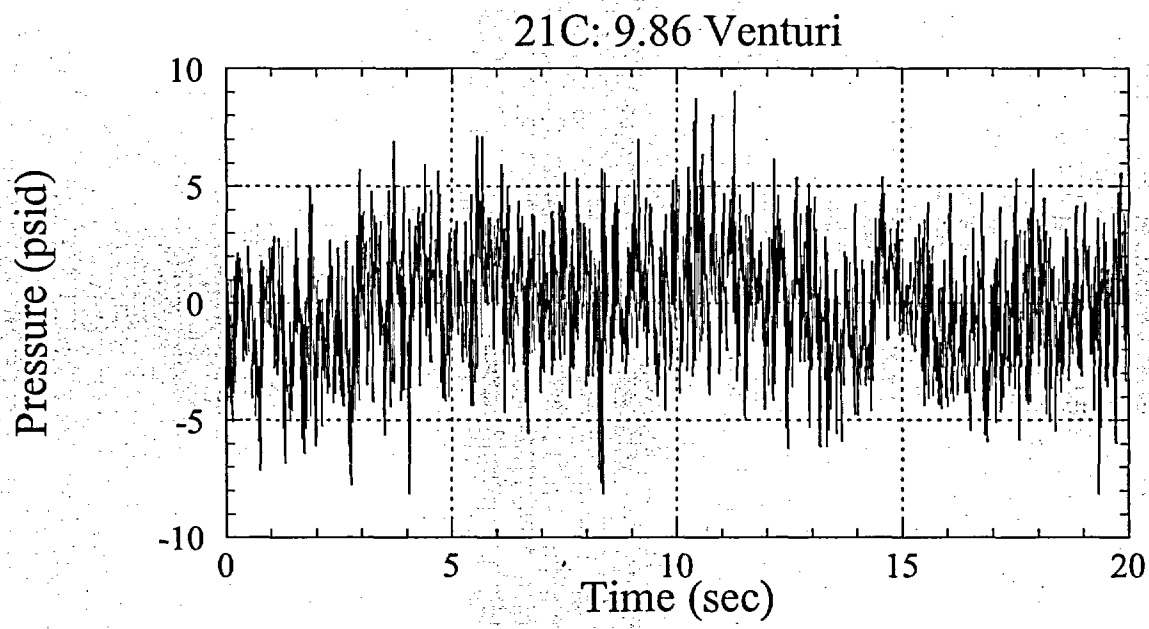


Figure 4-c.

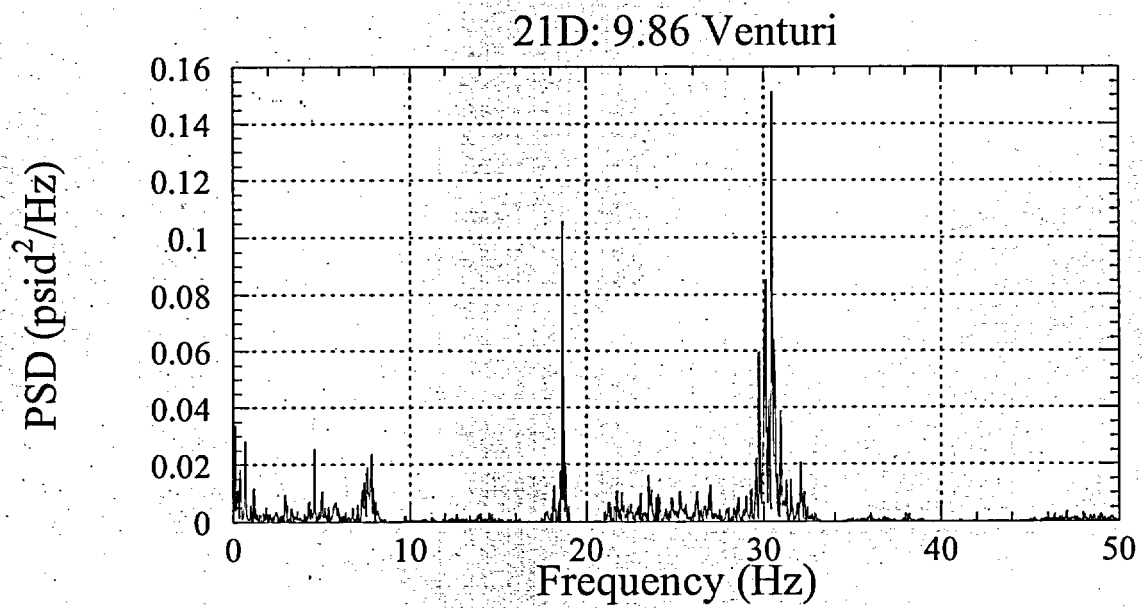
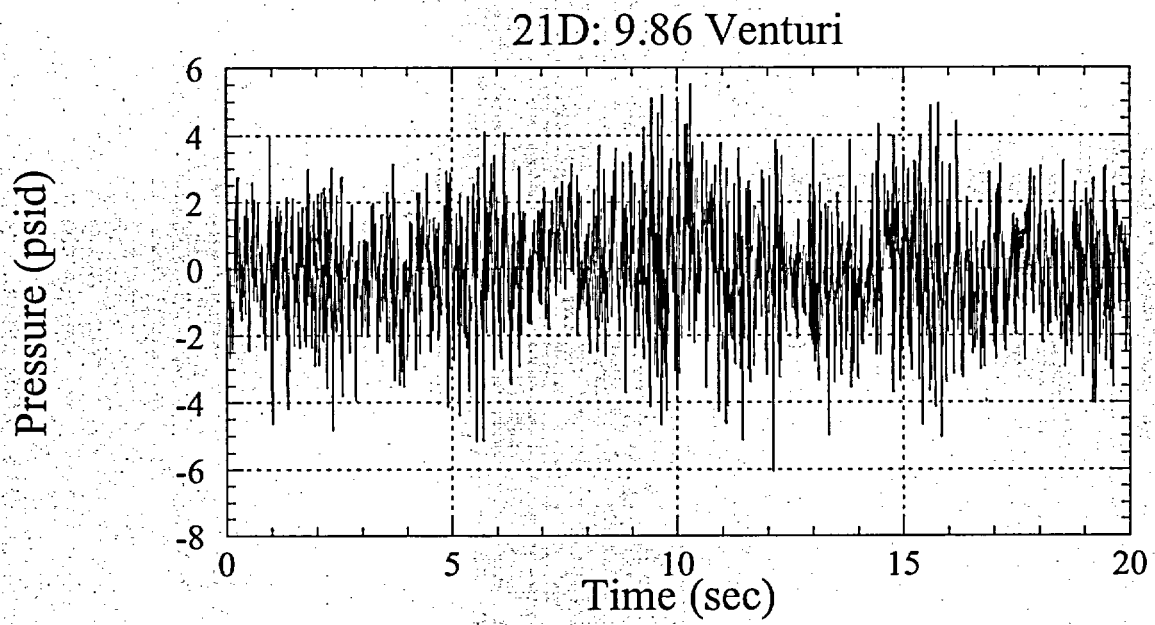


Figure 4-d.

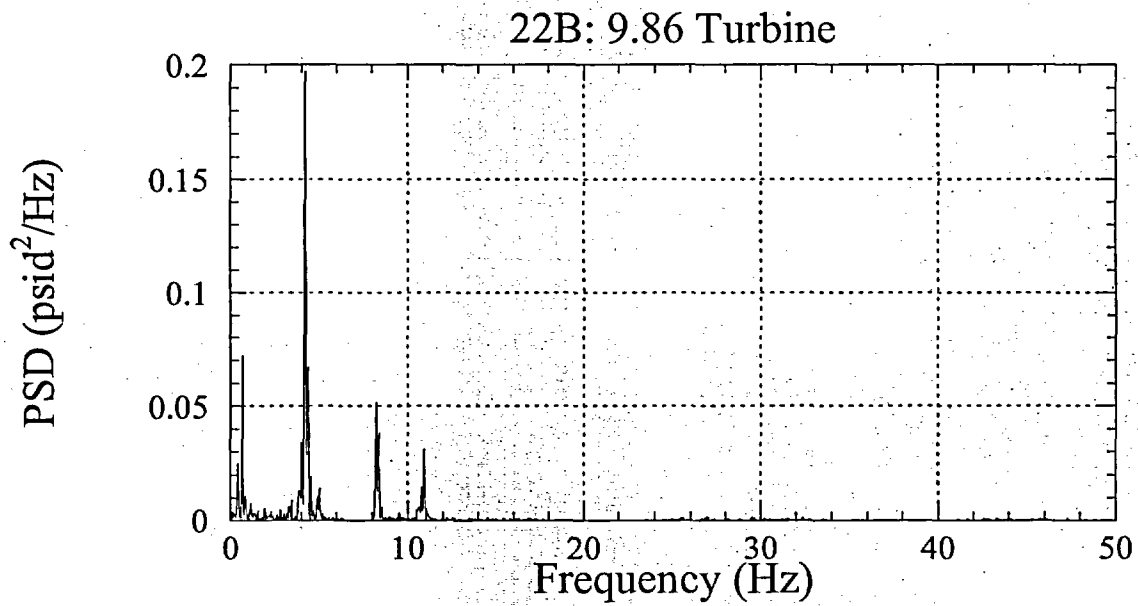
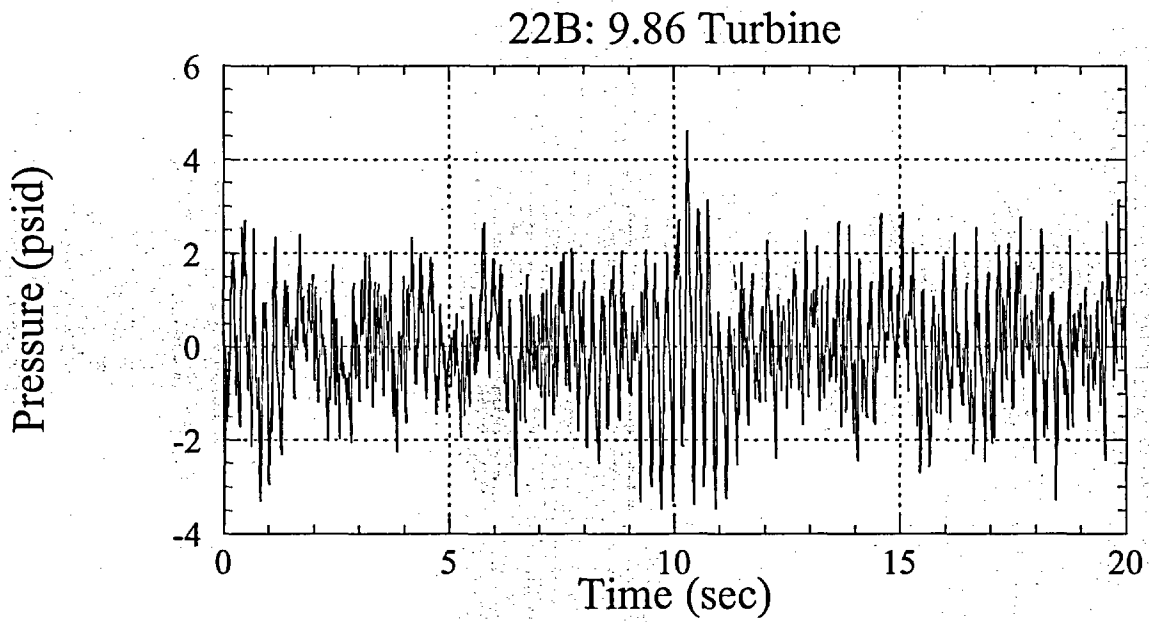


Figure 5-a.

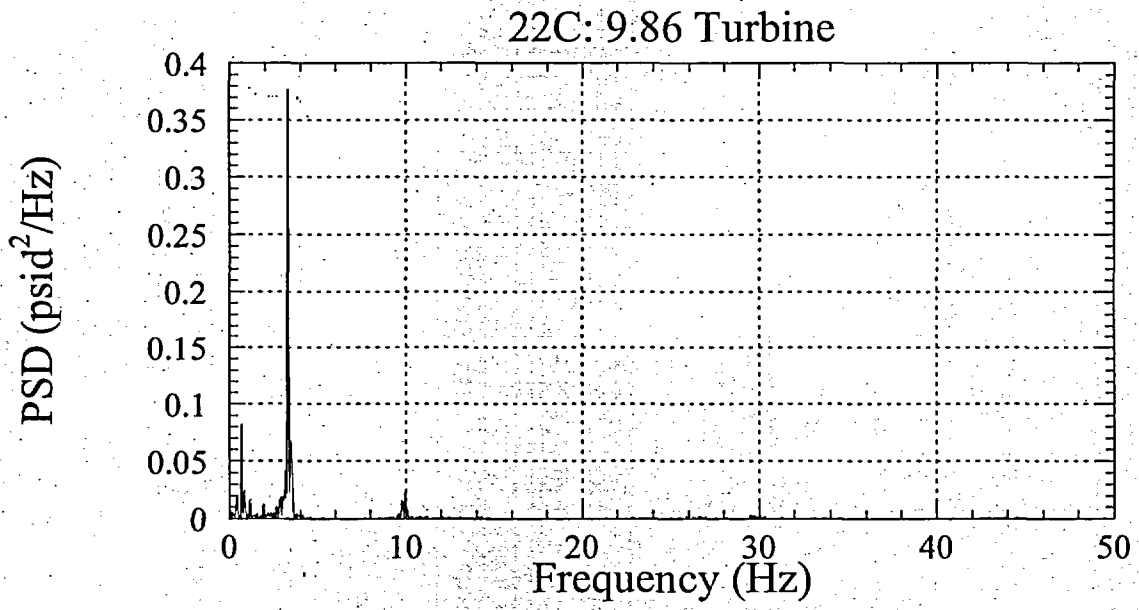
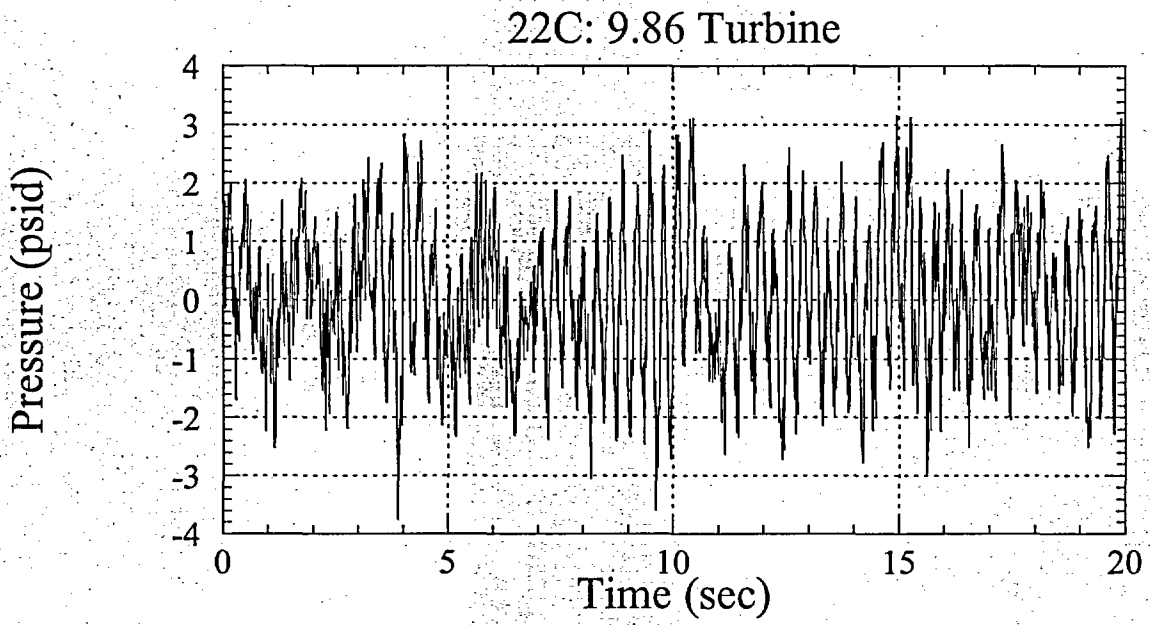


Figure 5-b.

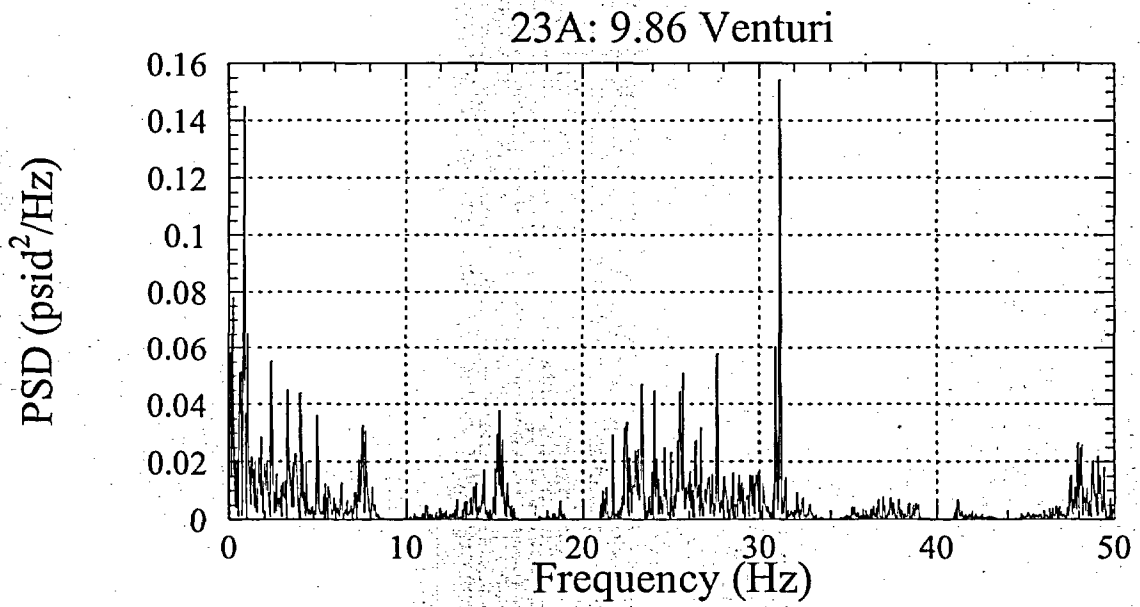
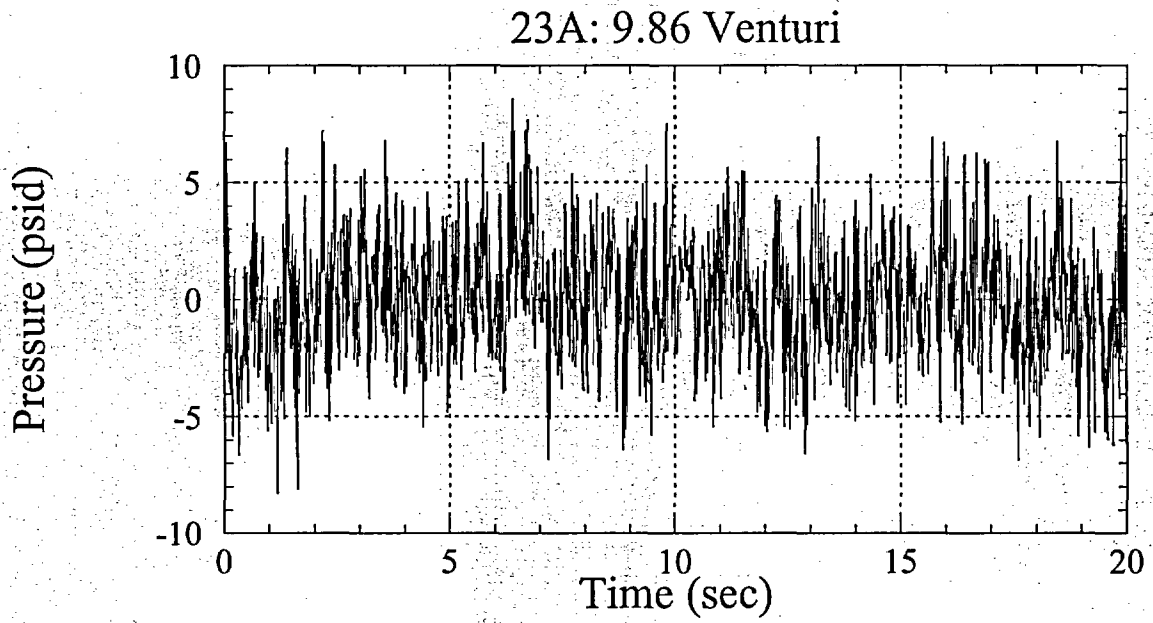


Figure 6-a.

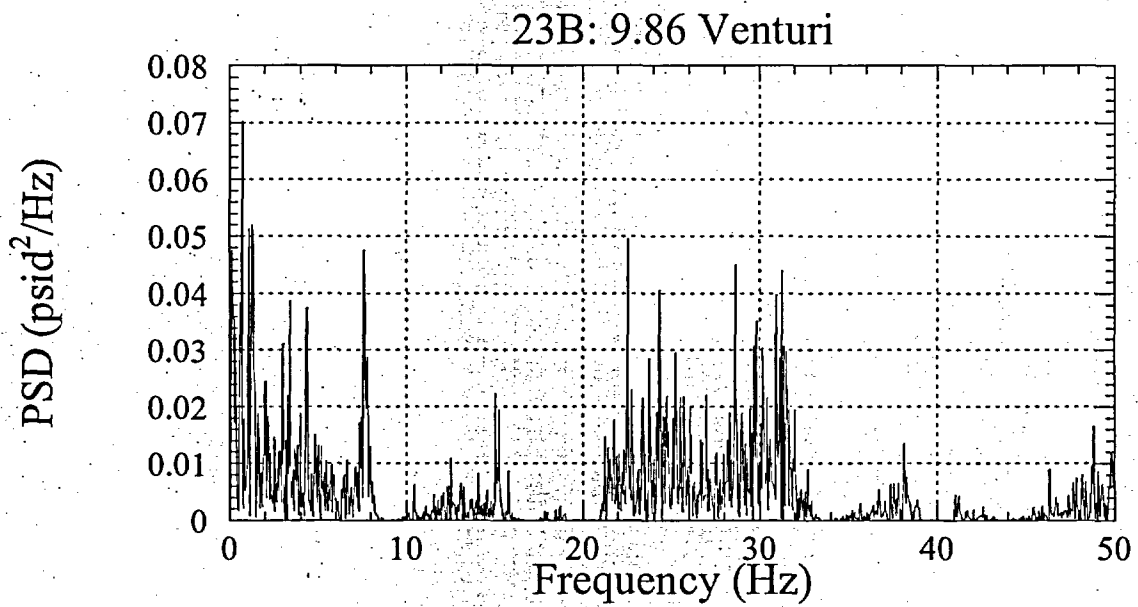
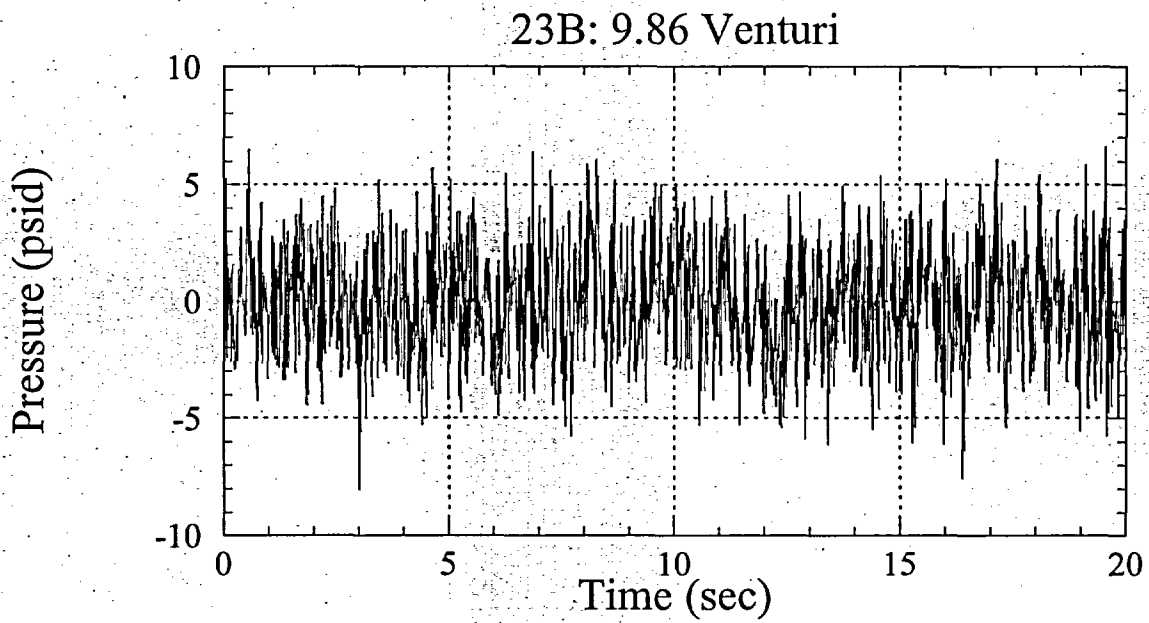


Figure 6-b.

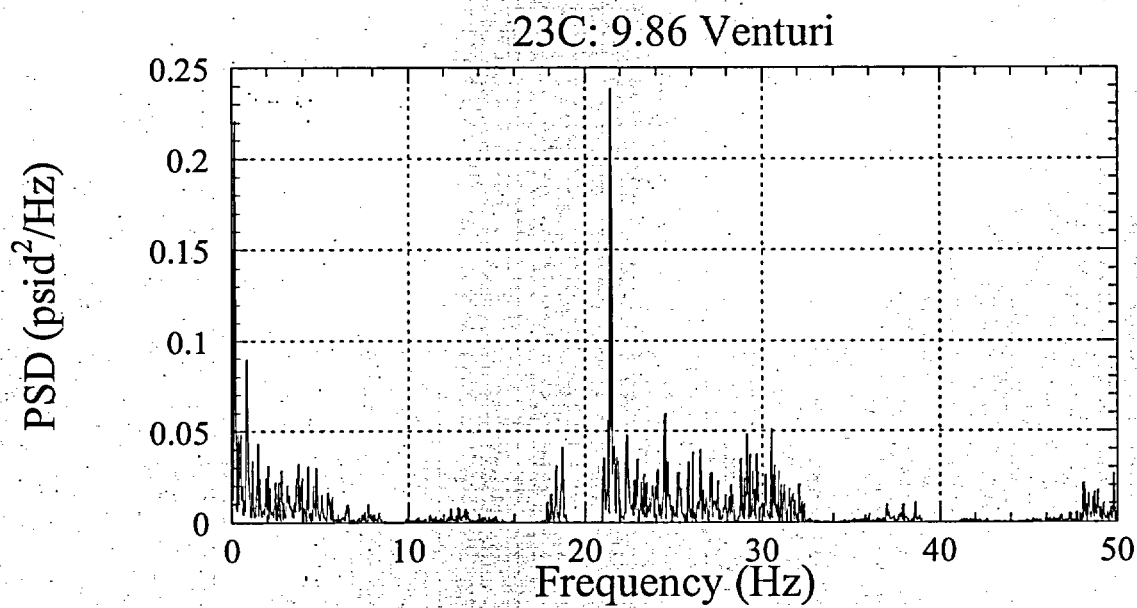
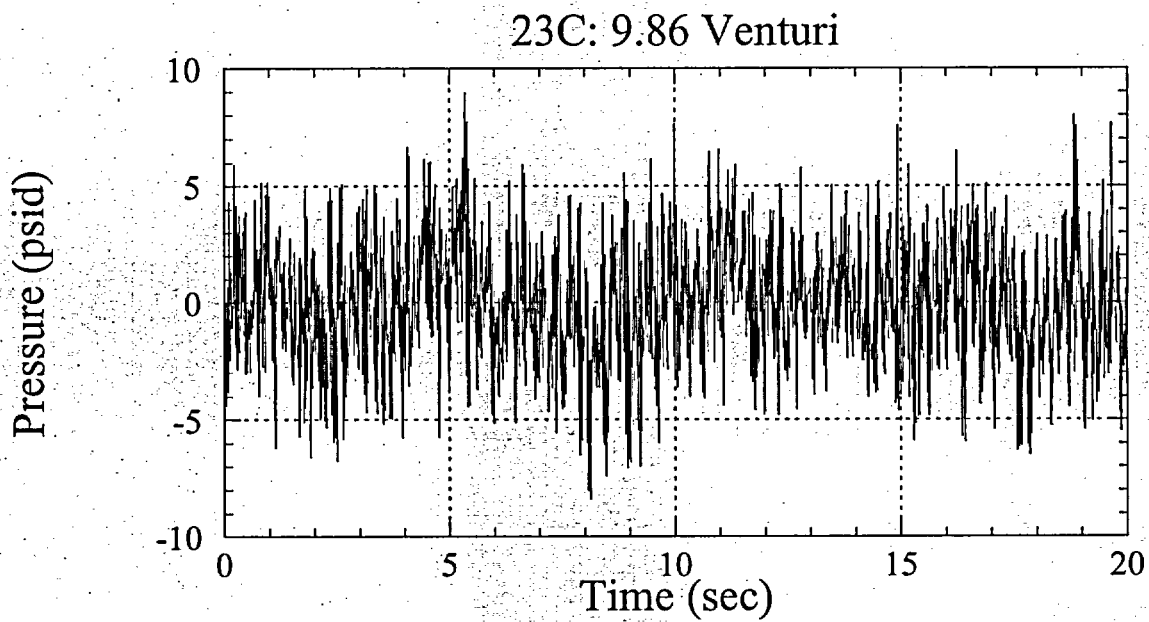


Figure 6-c.

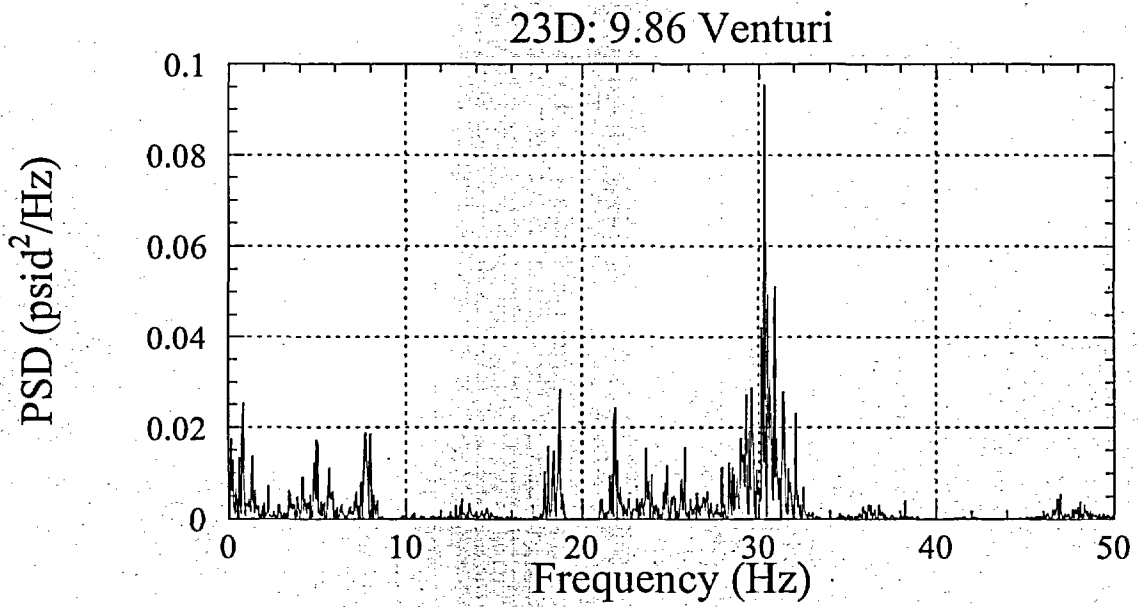
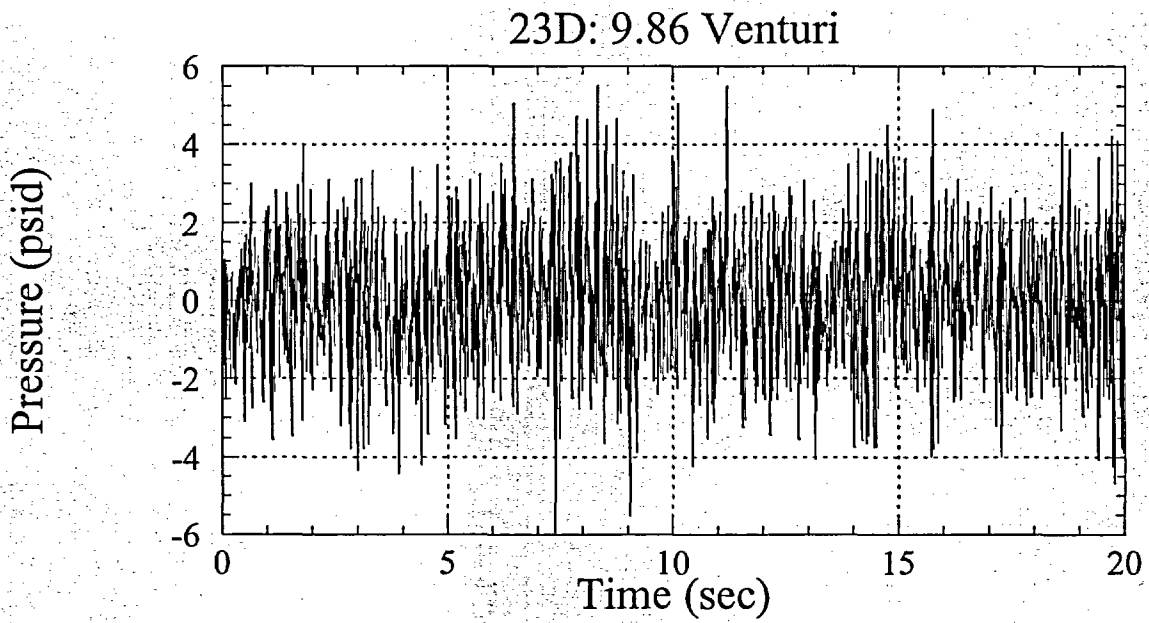


Figure 6-d.

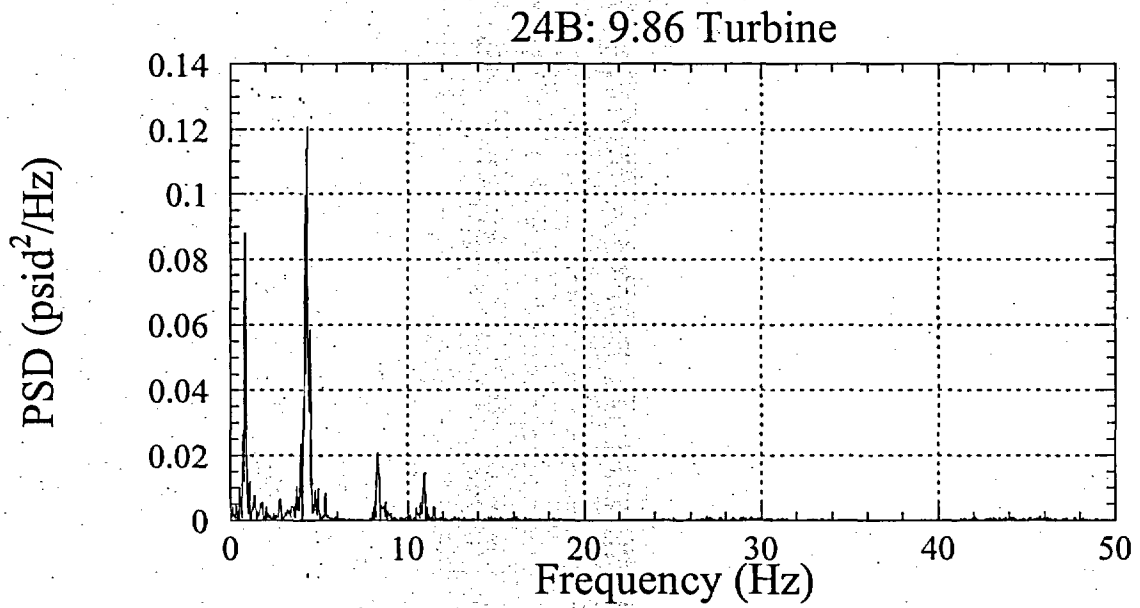
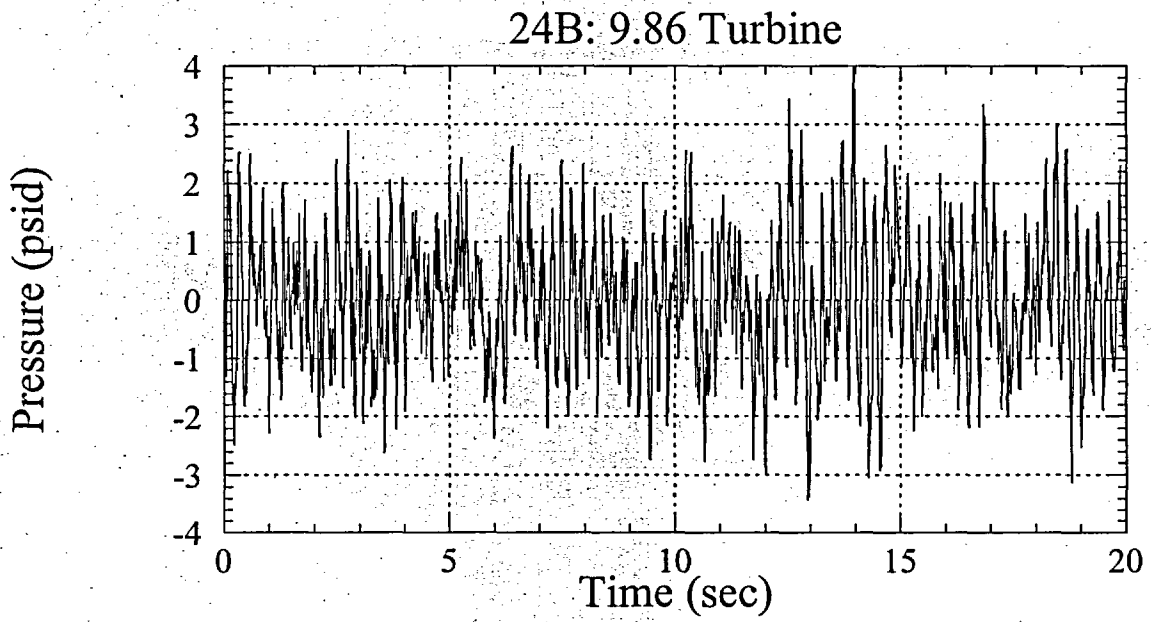


Figure 7-a.

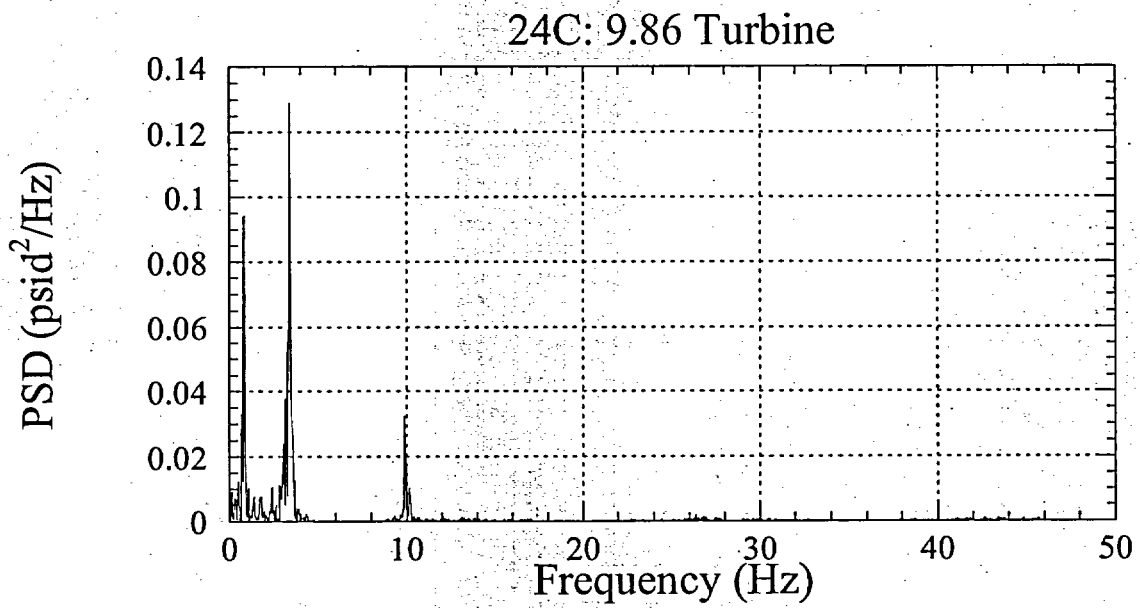
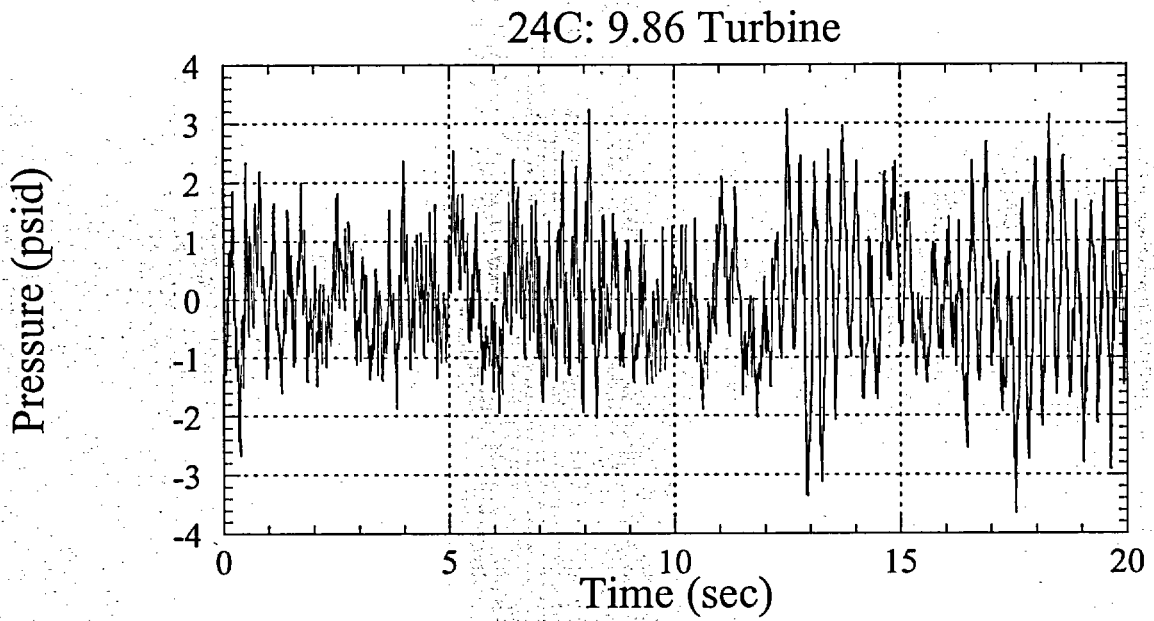


Figure 7-b.

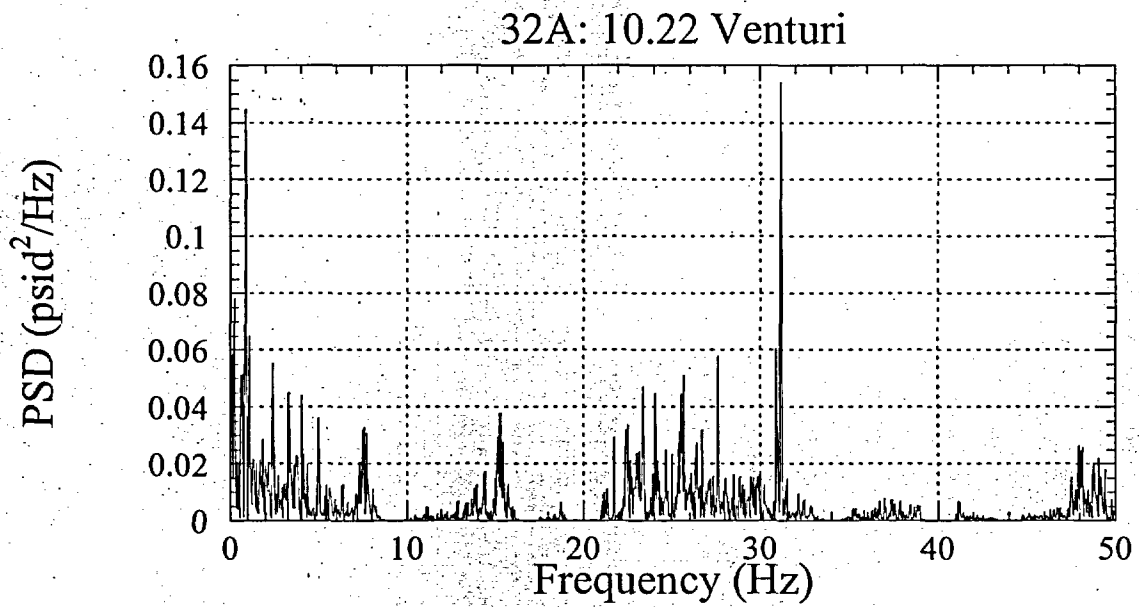
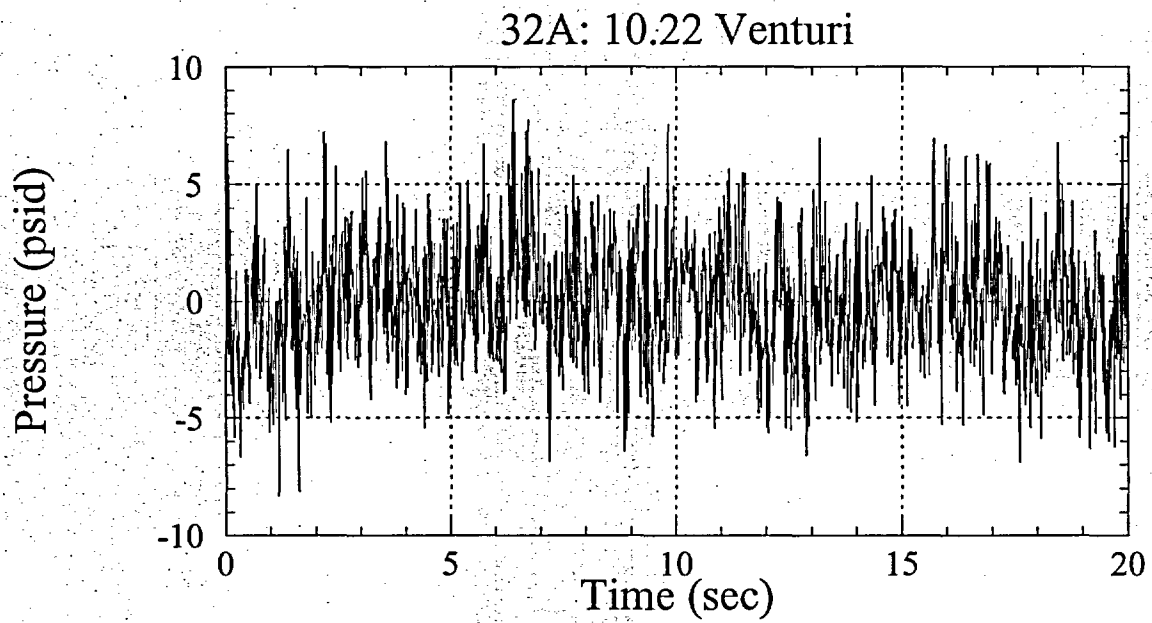


Figure 8-a.

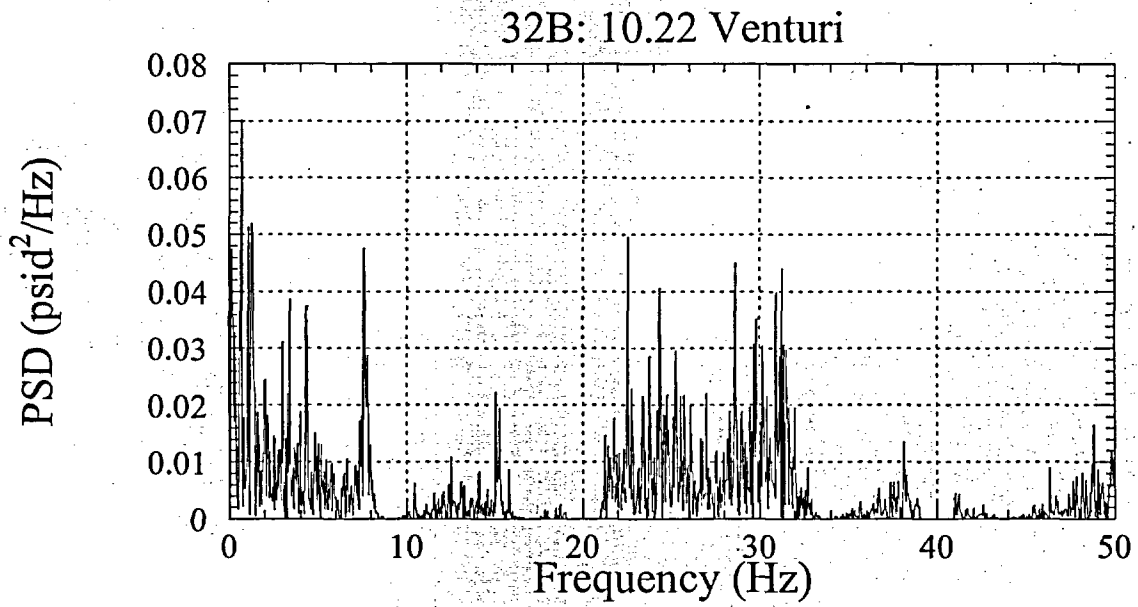
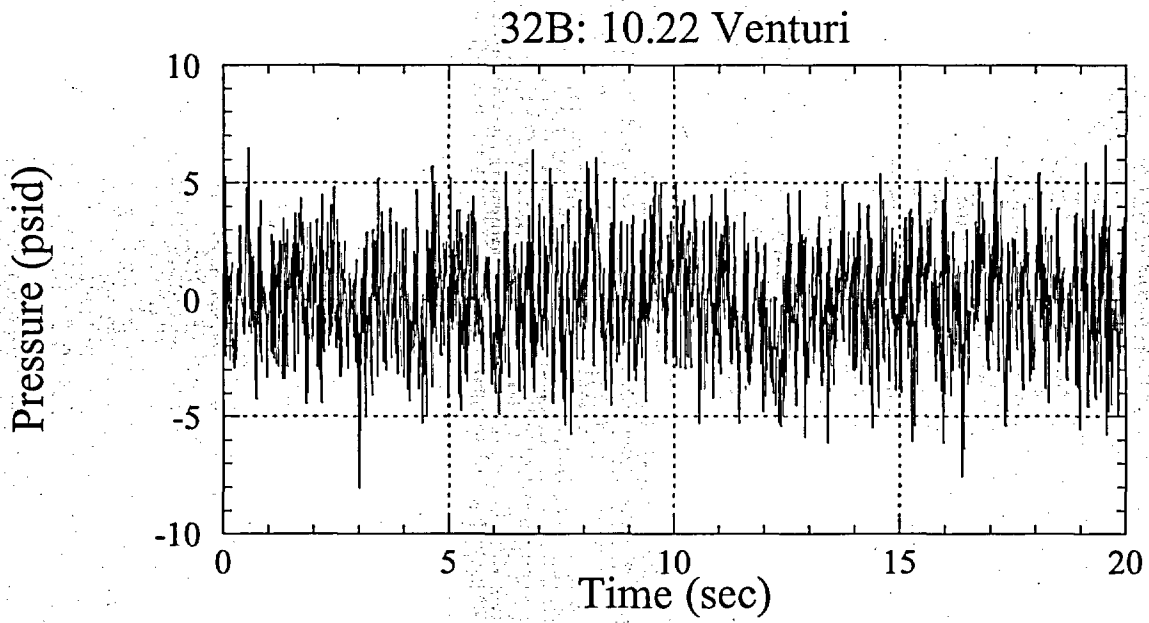


Figure 8-b.

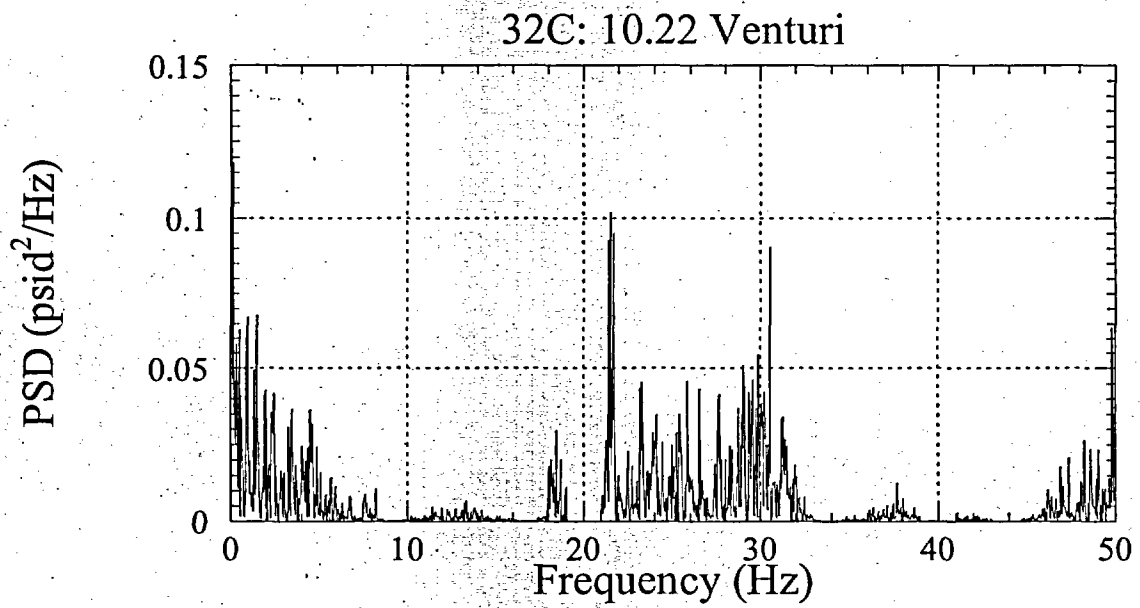
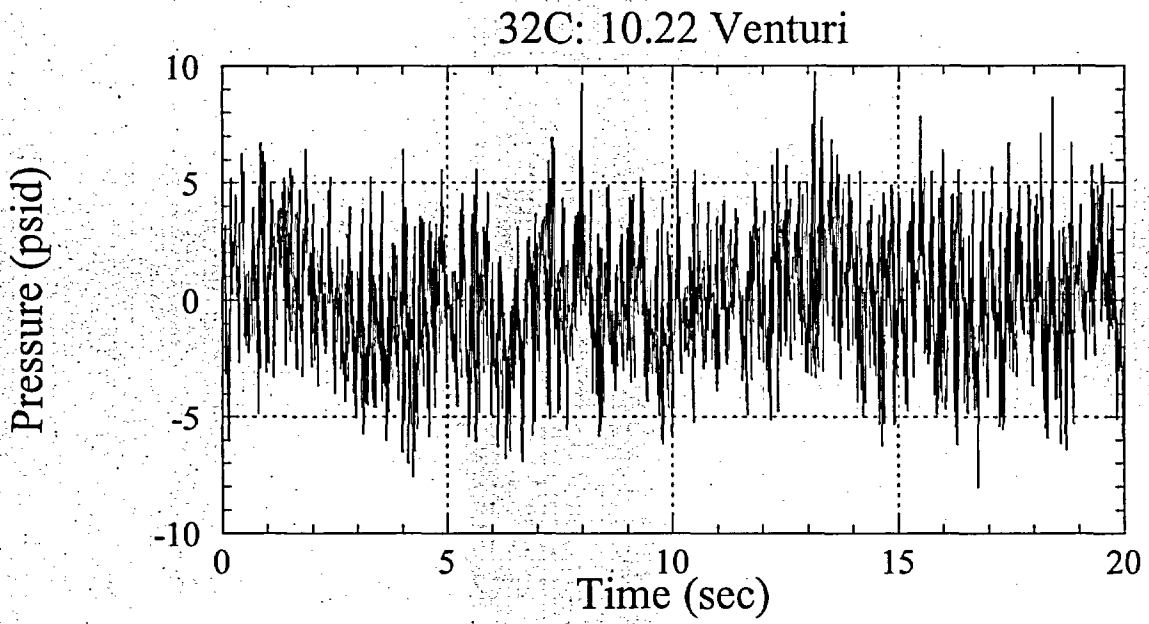


Figure 8-c.

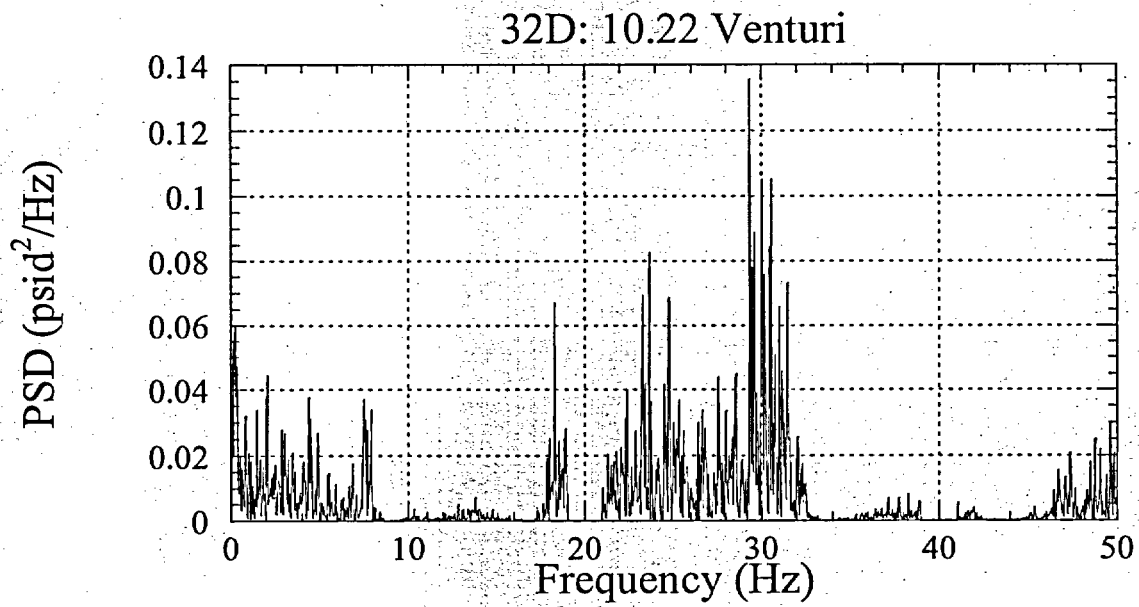
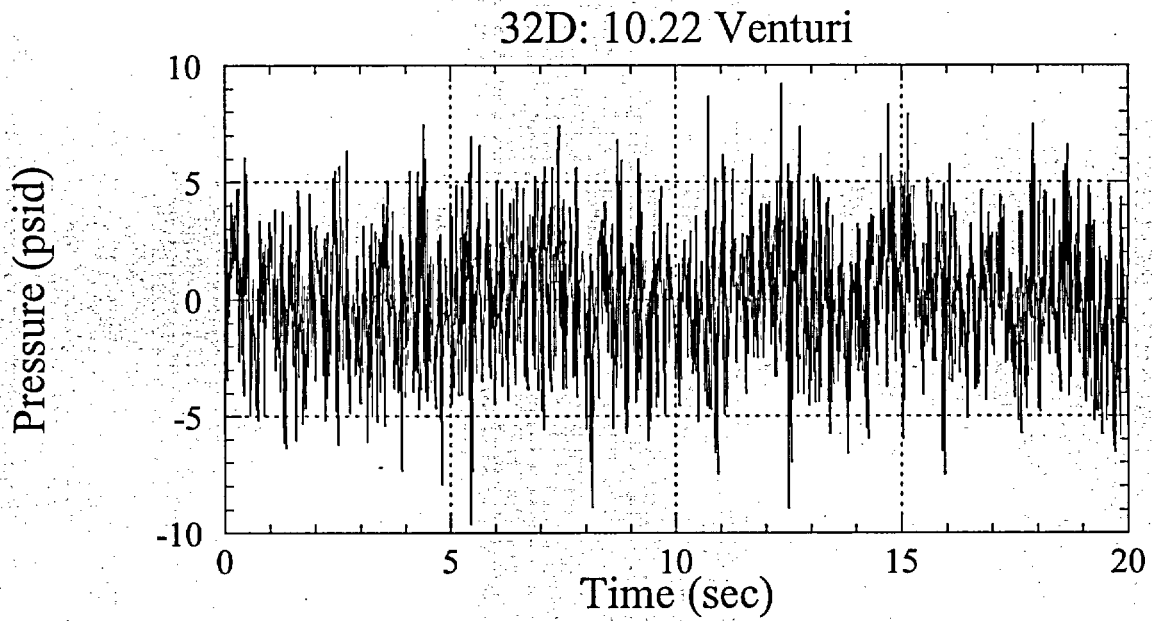


Figure 8-d.

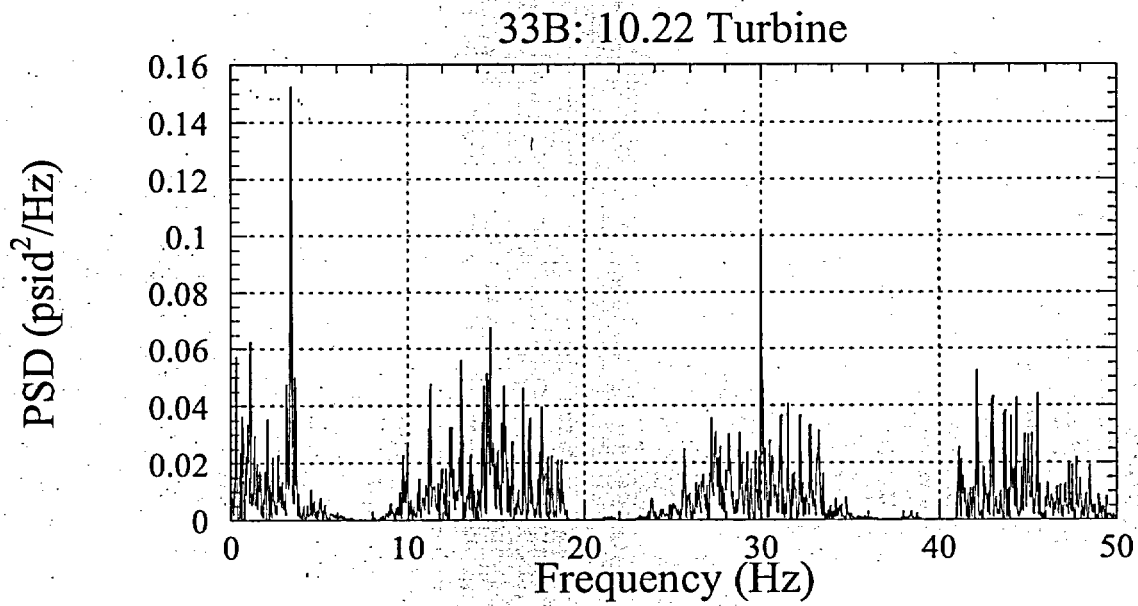
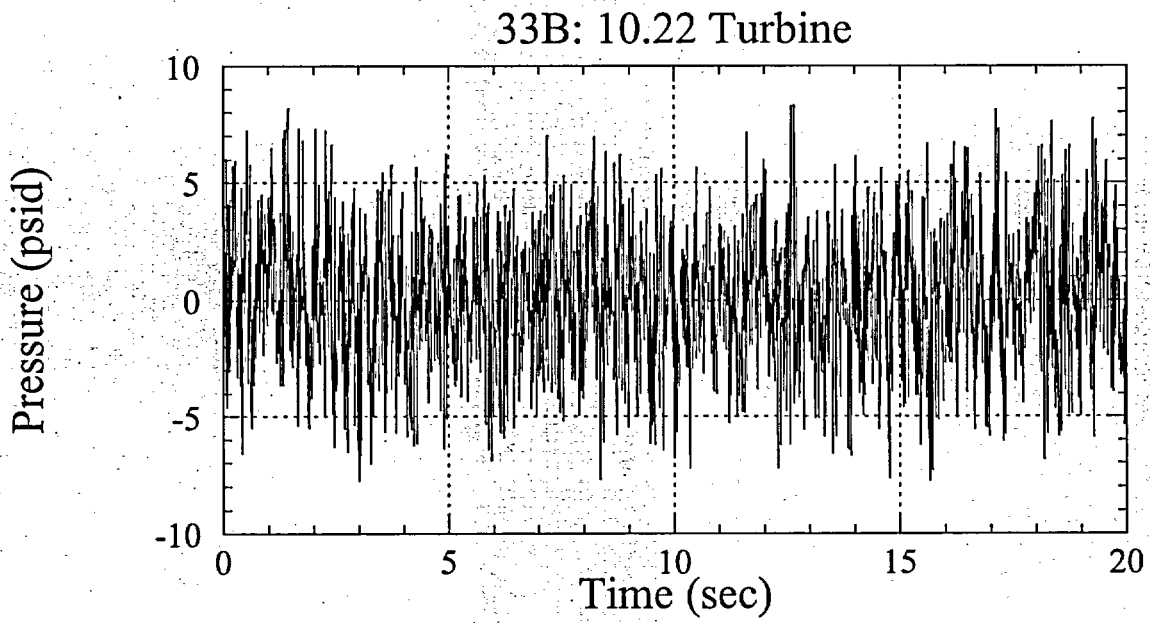


Figure 9-a.

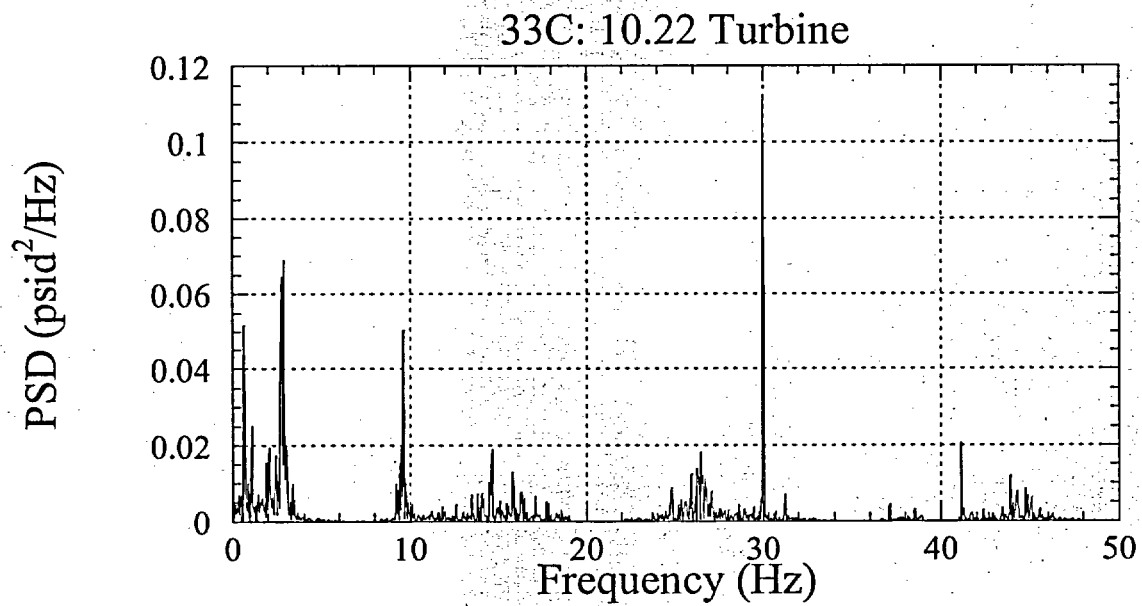
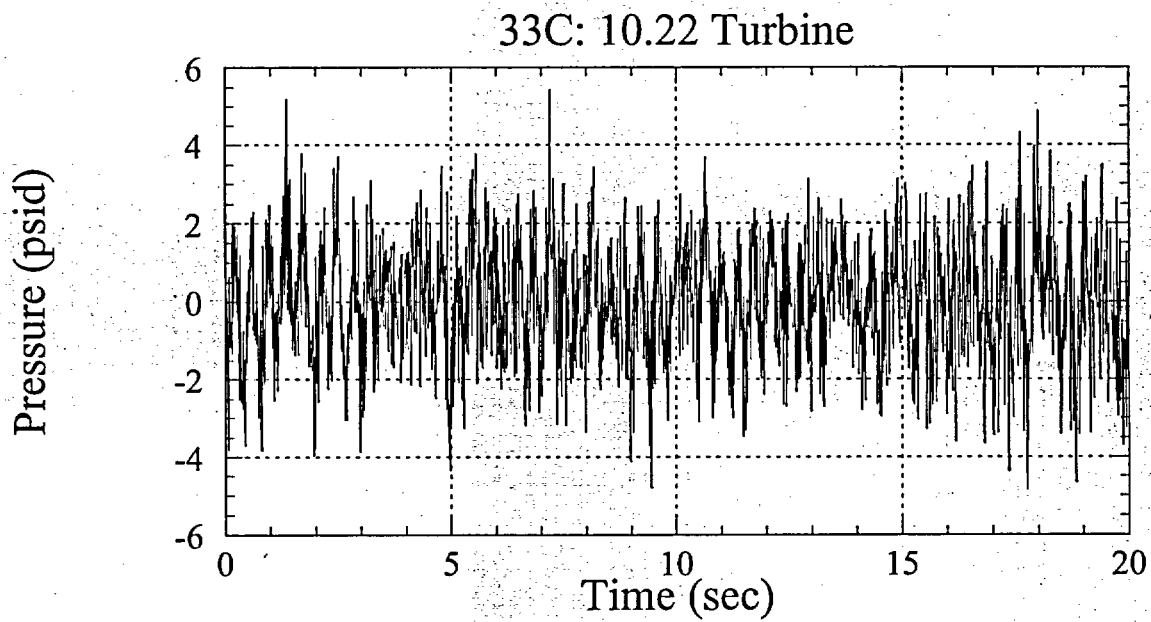


Figure 9-b.

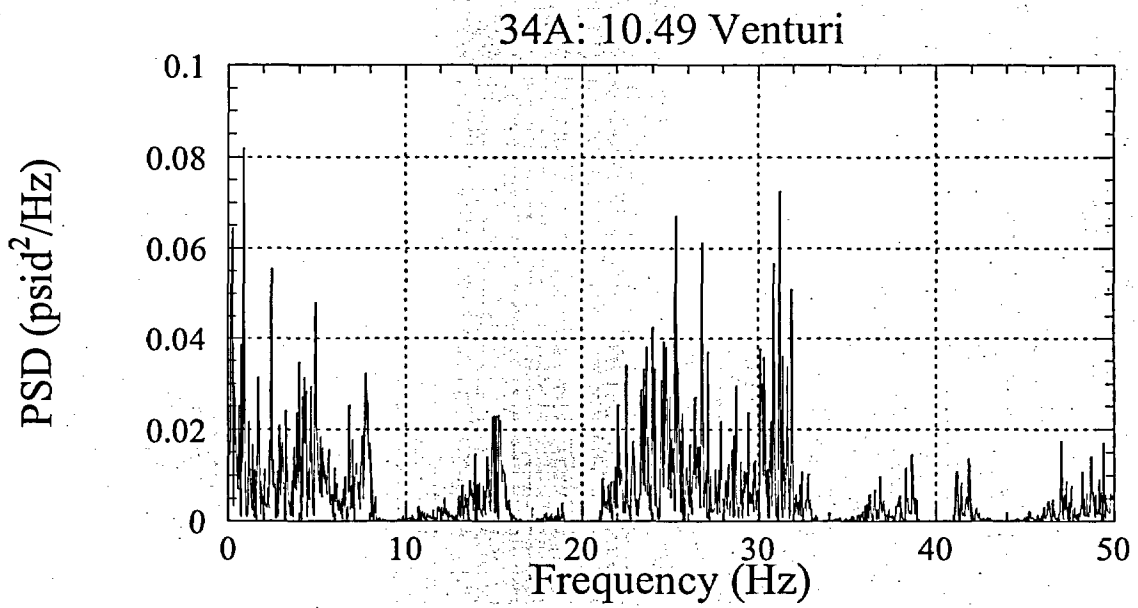
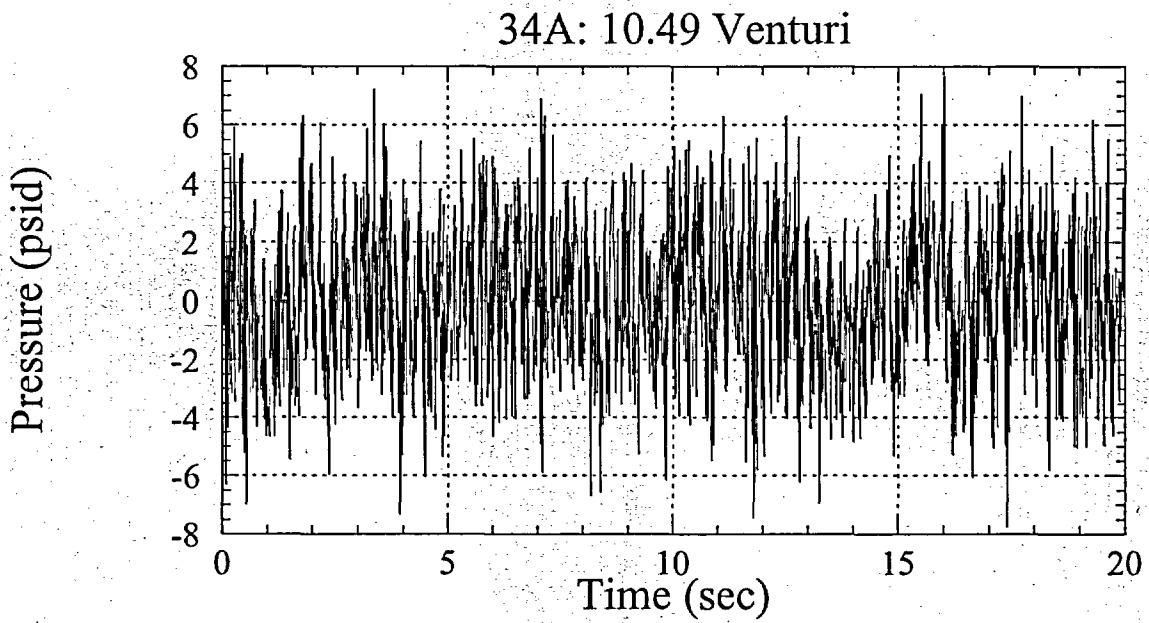


Figure 10-a.

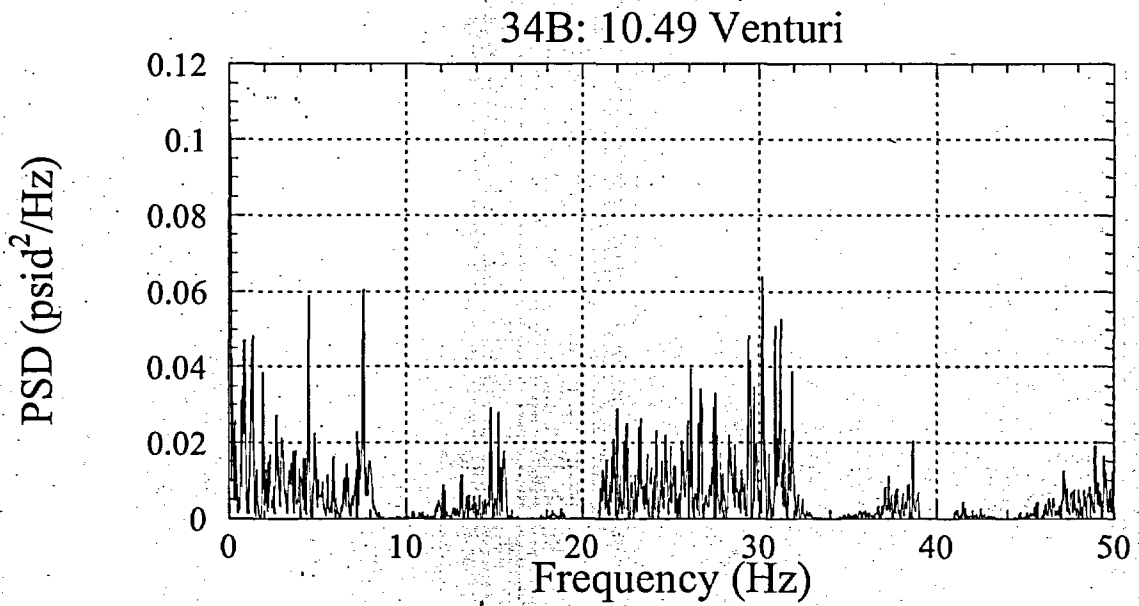
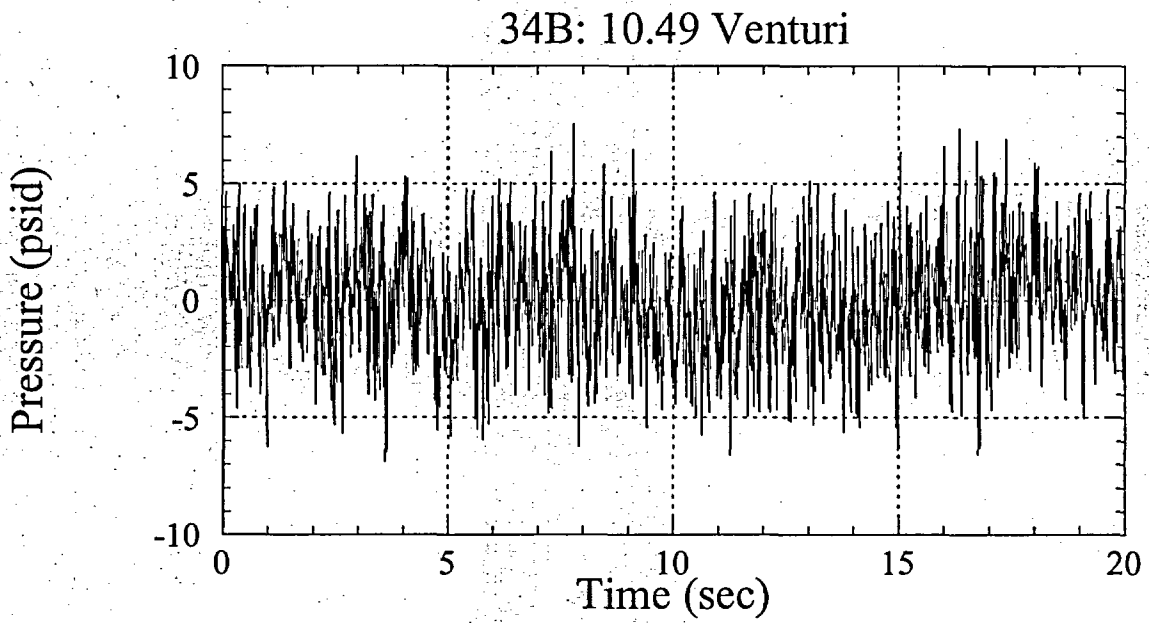


Figure 10-b.

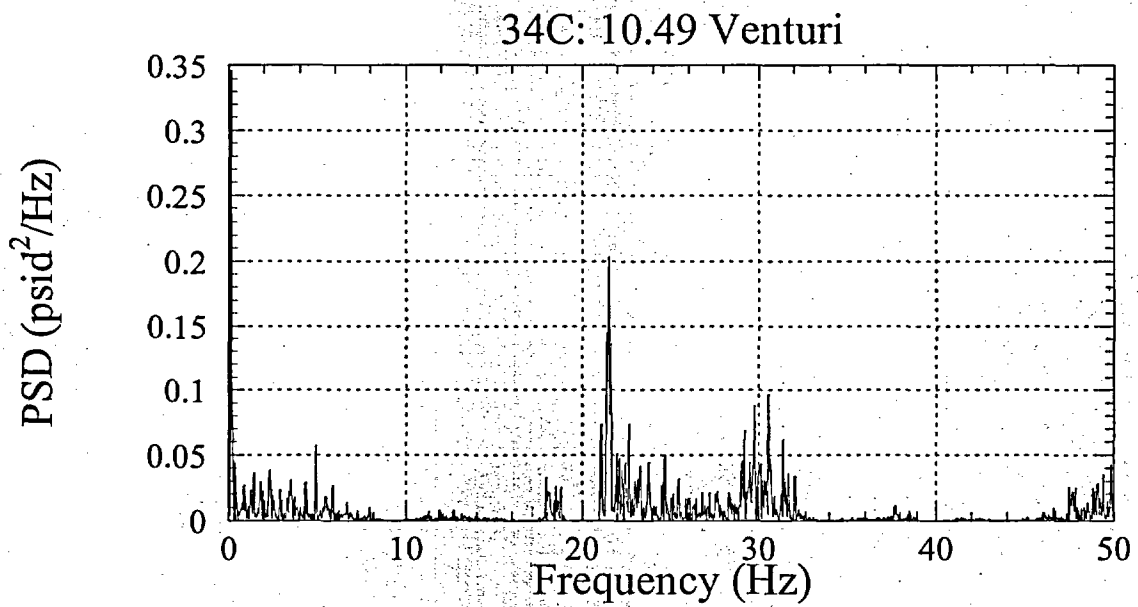
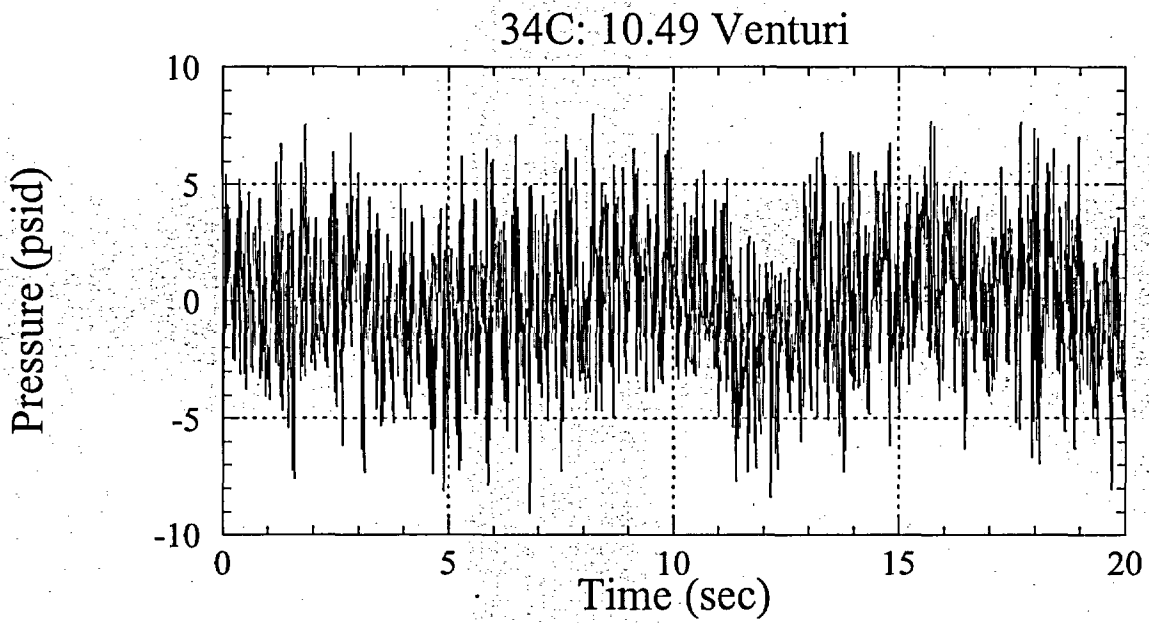


Figure 10-c.

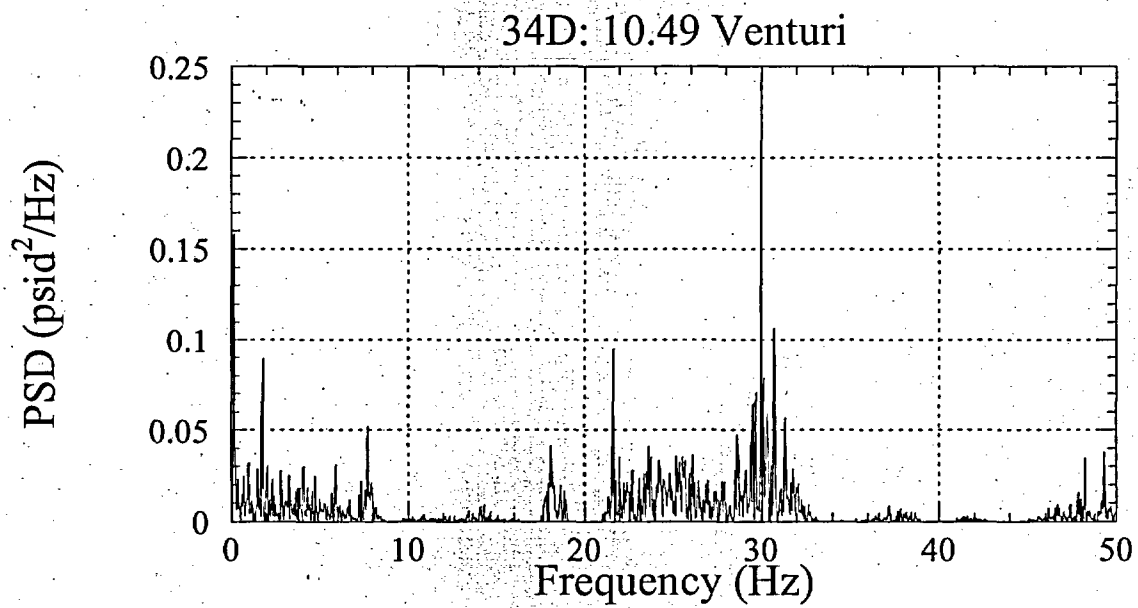
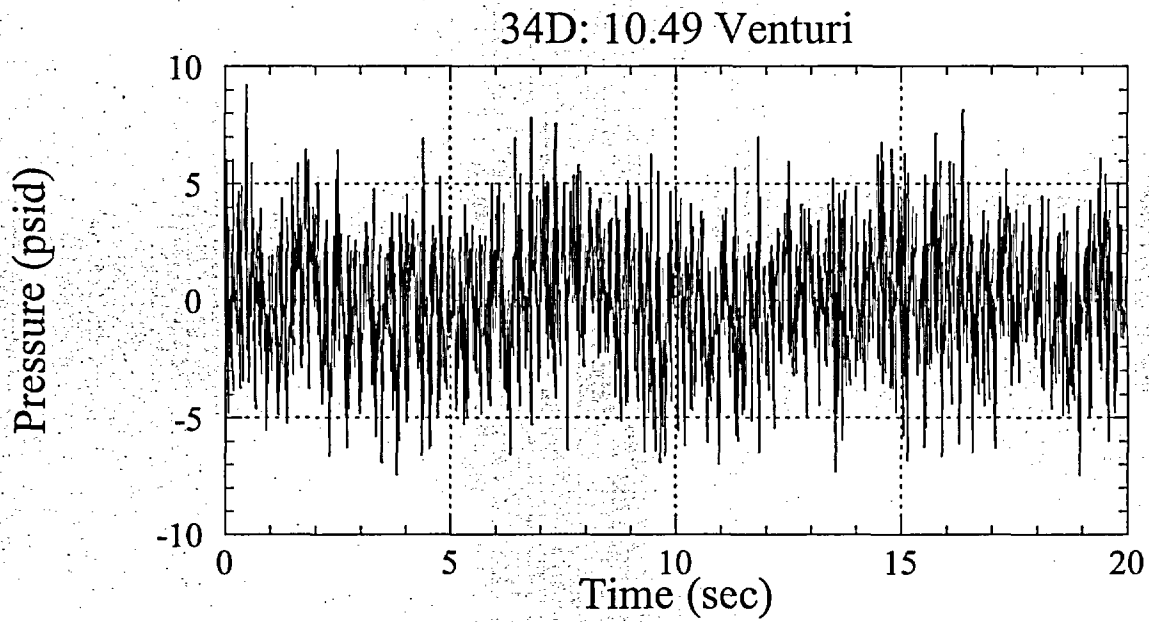


Figure 10-d.

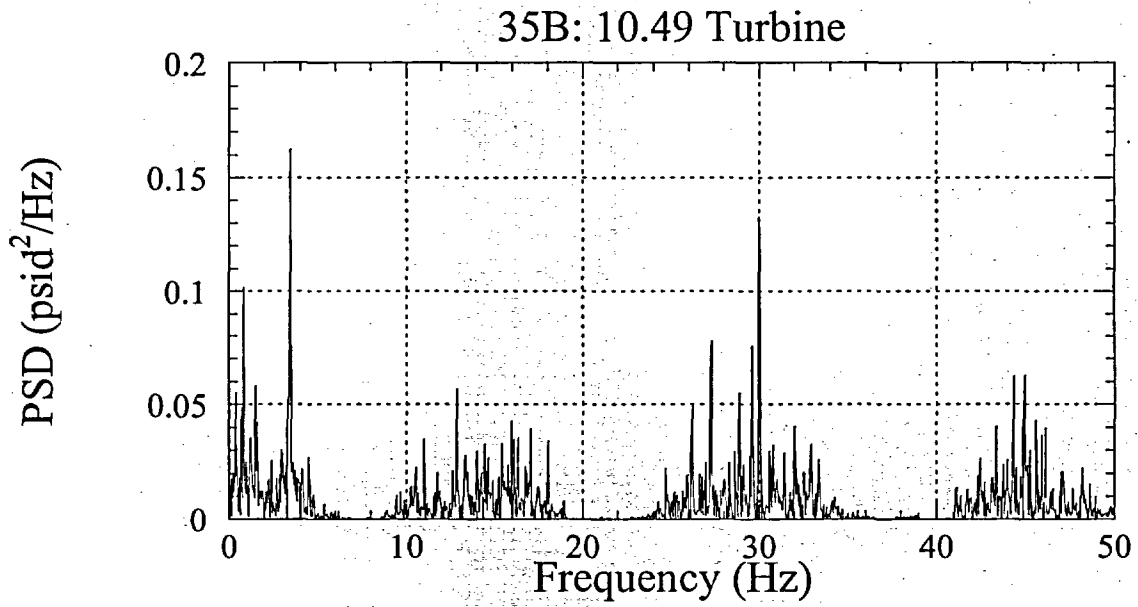
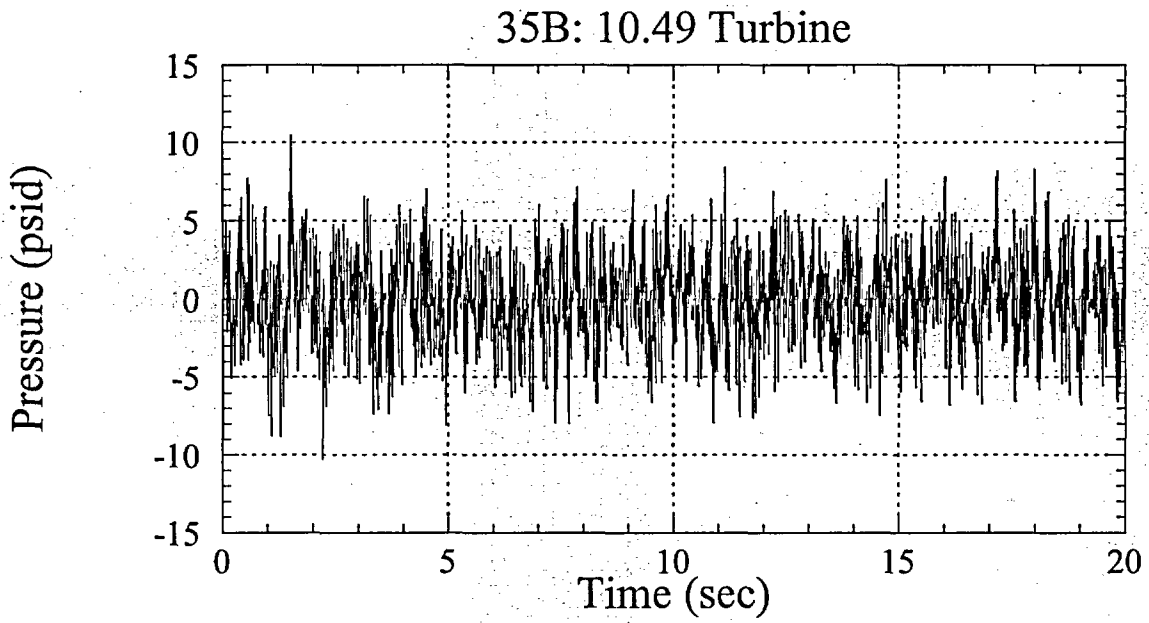


Figure 11-a.

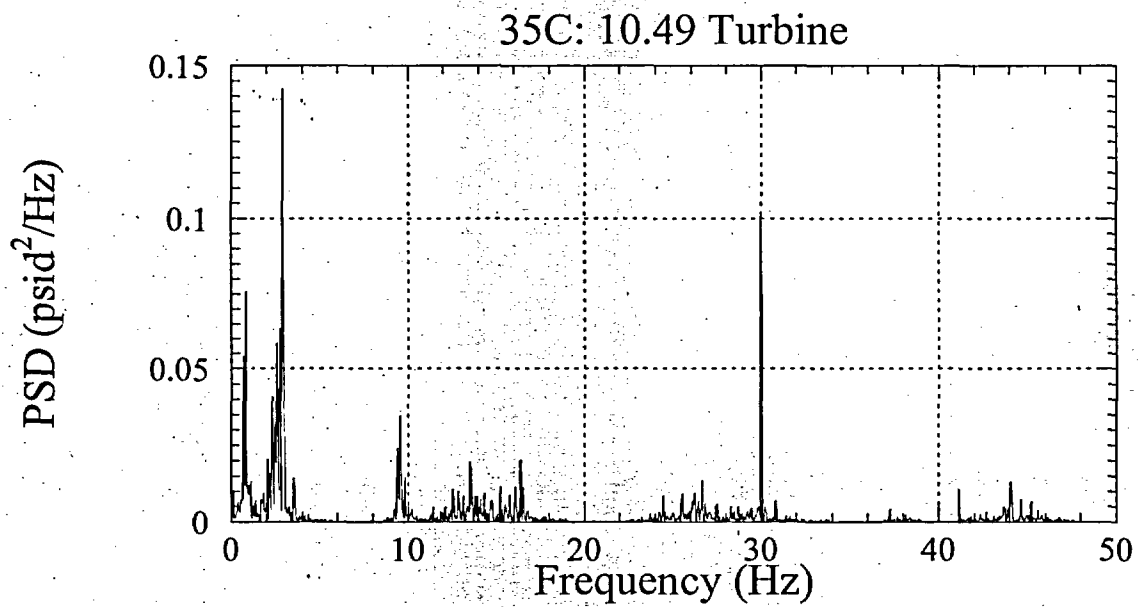
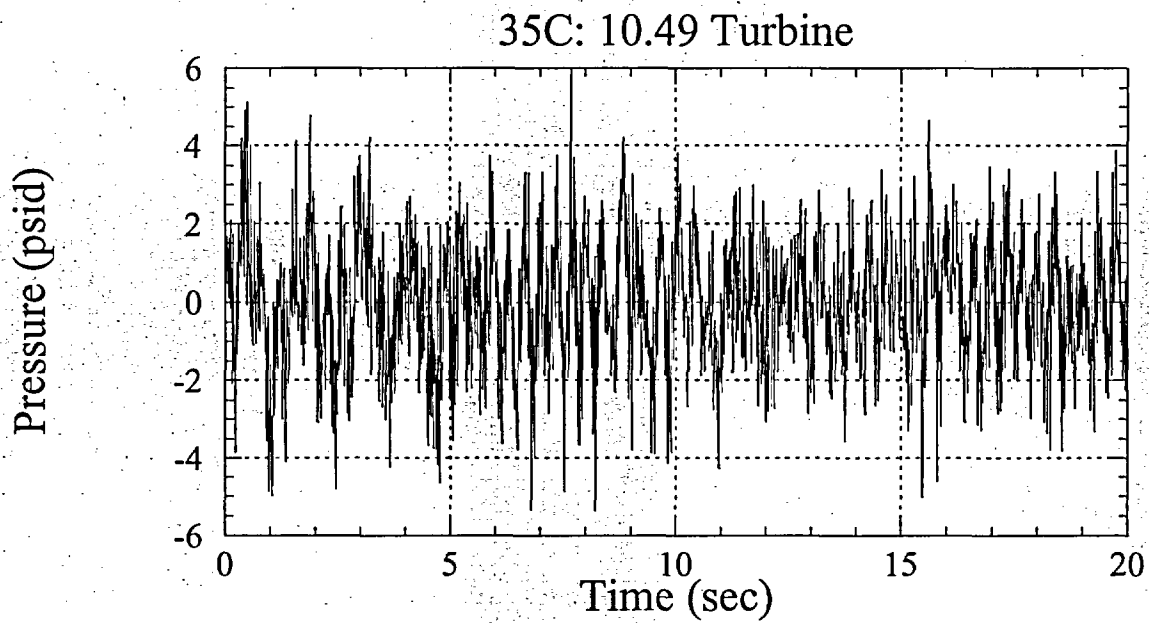


Figure 11-b.

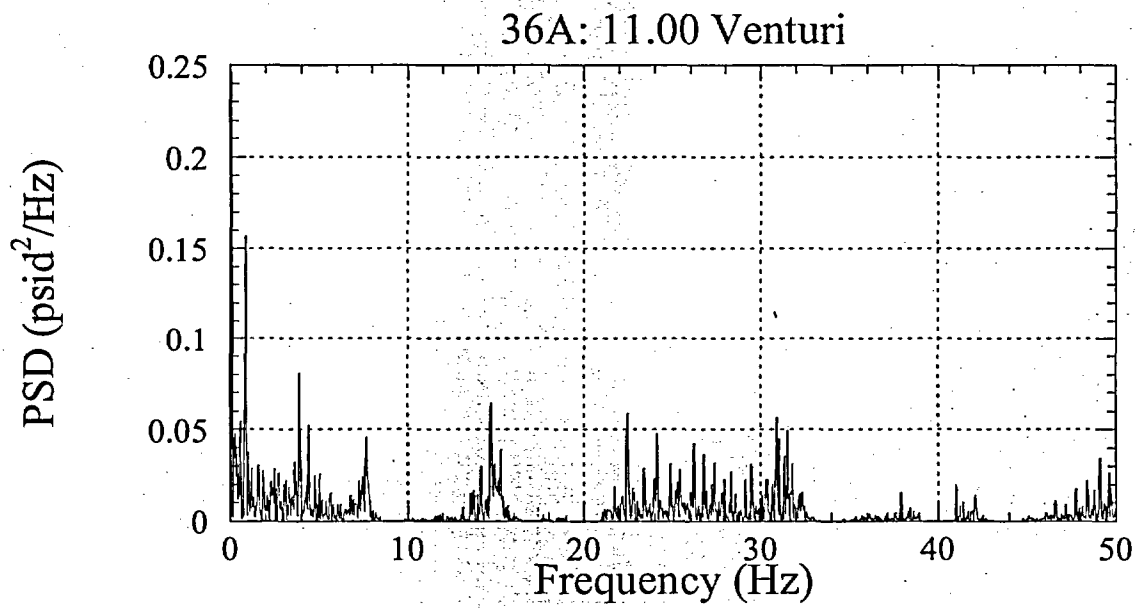
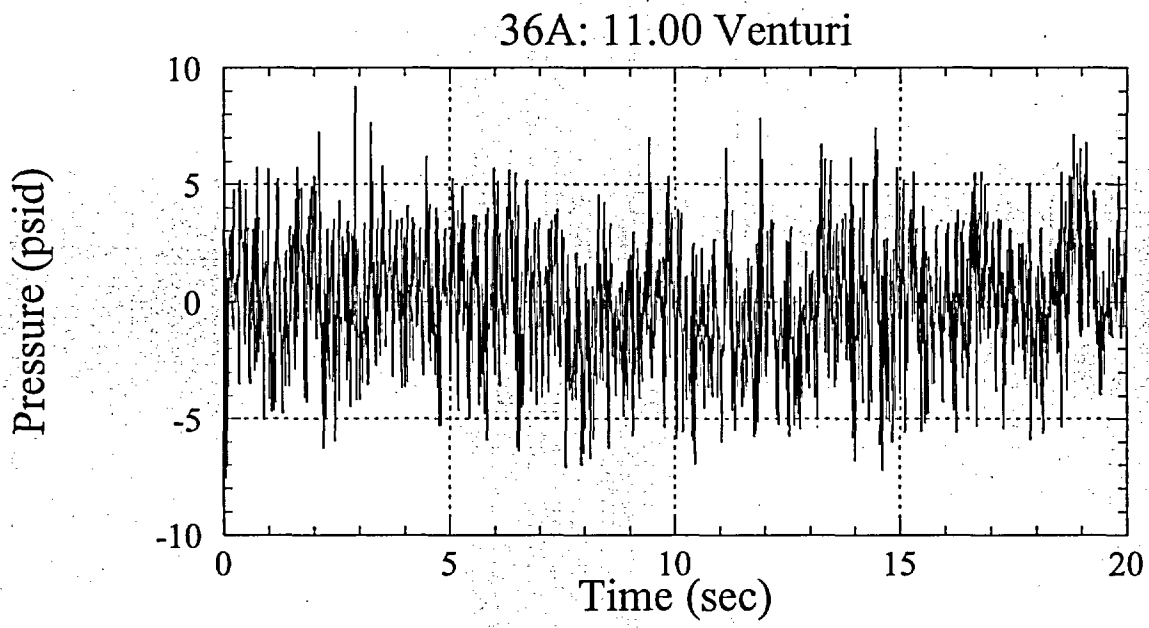


Figure 12-a.

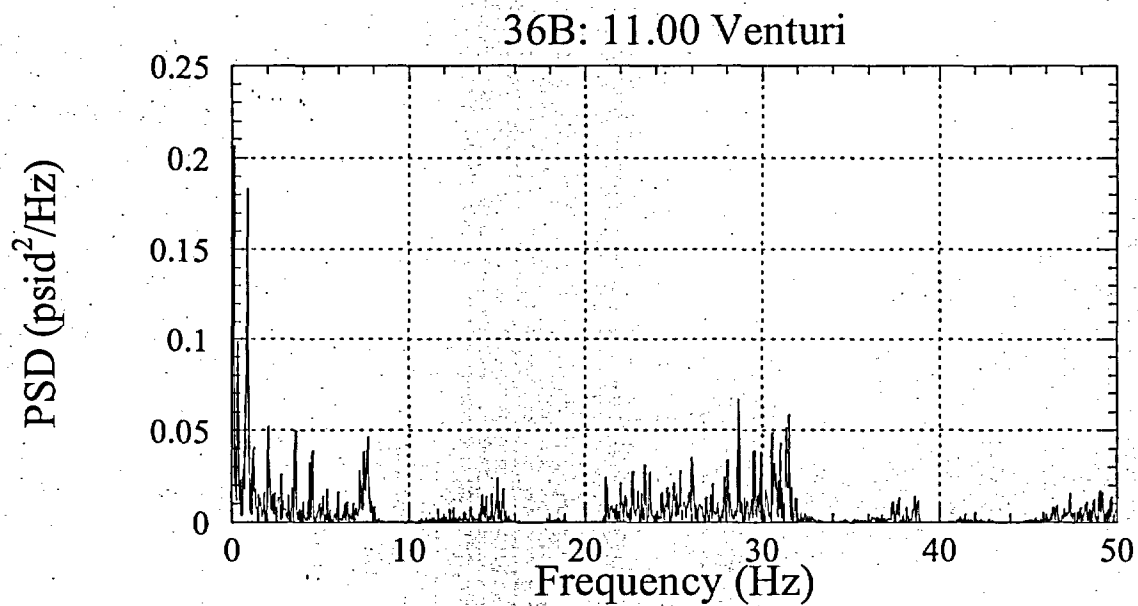
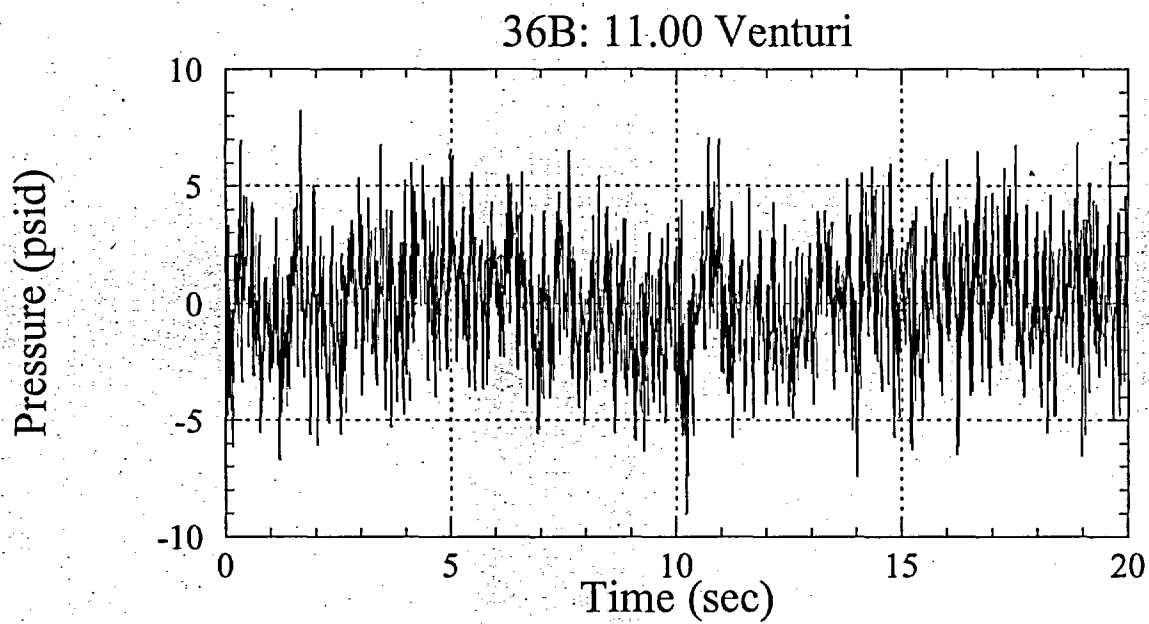


Figure 12-b.

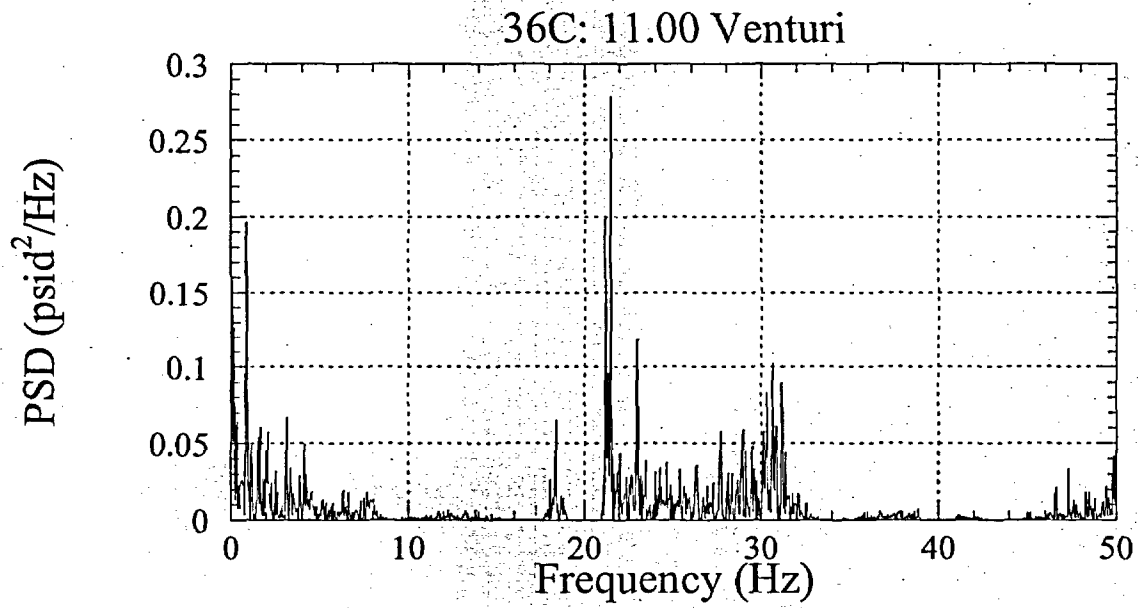
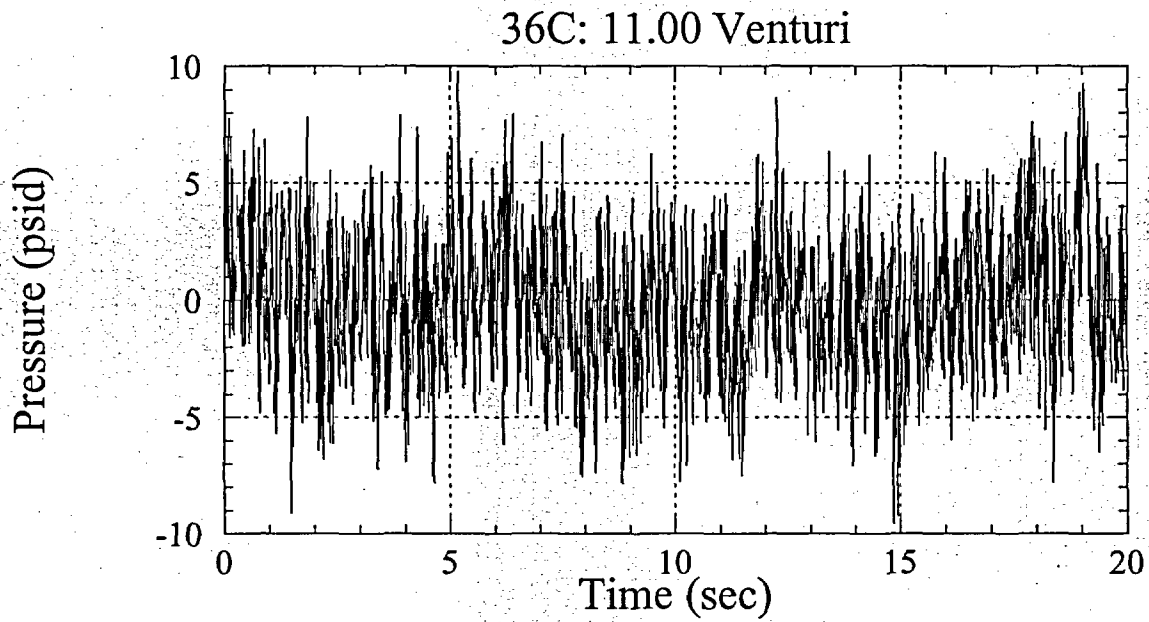


Figure 12-c.

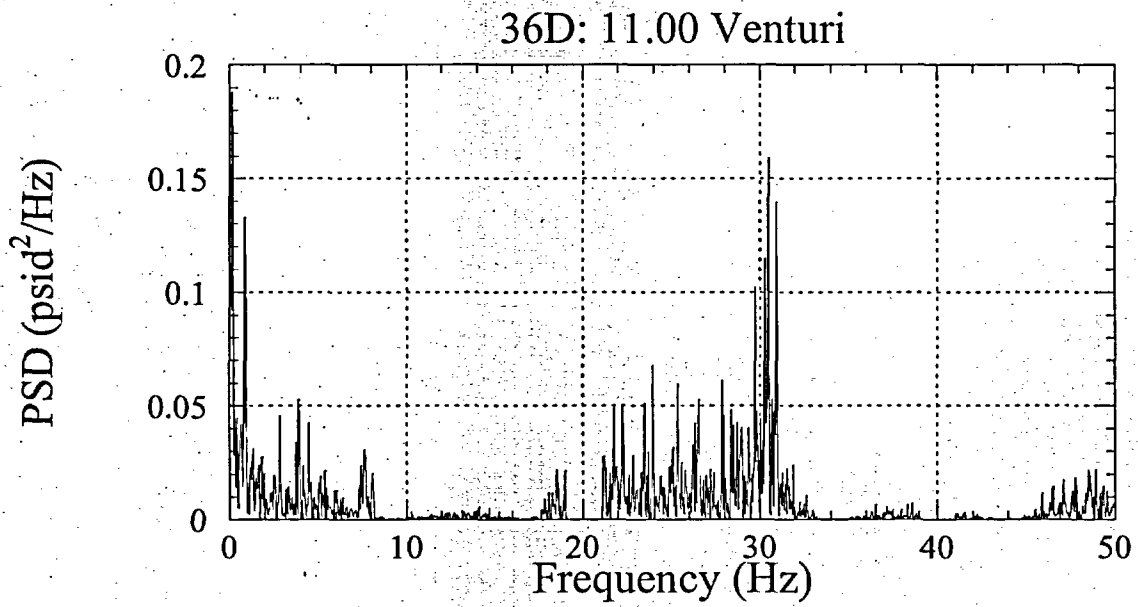
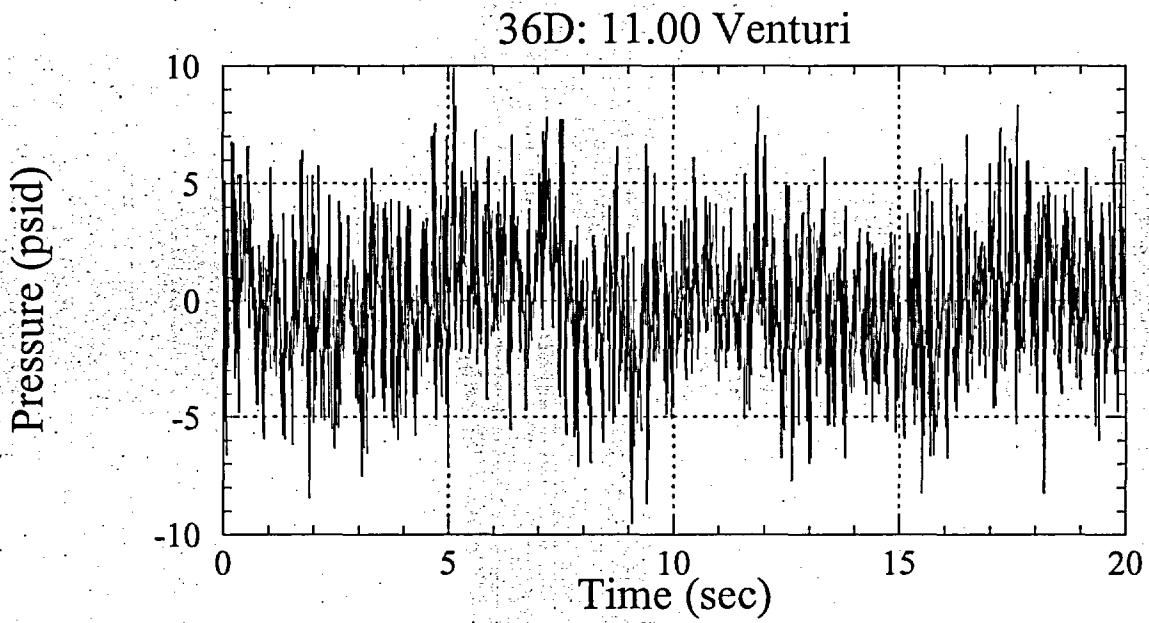


Figure 12-d.

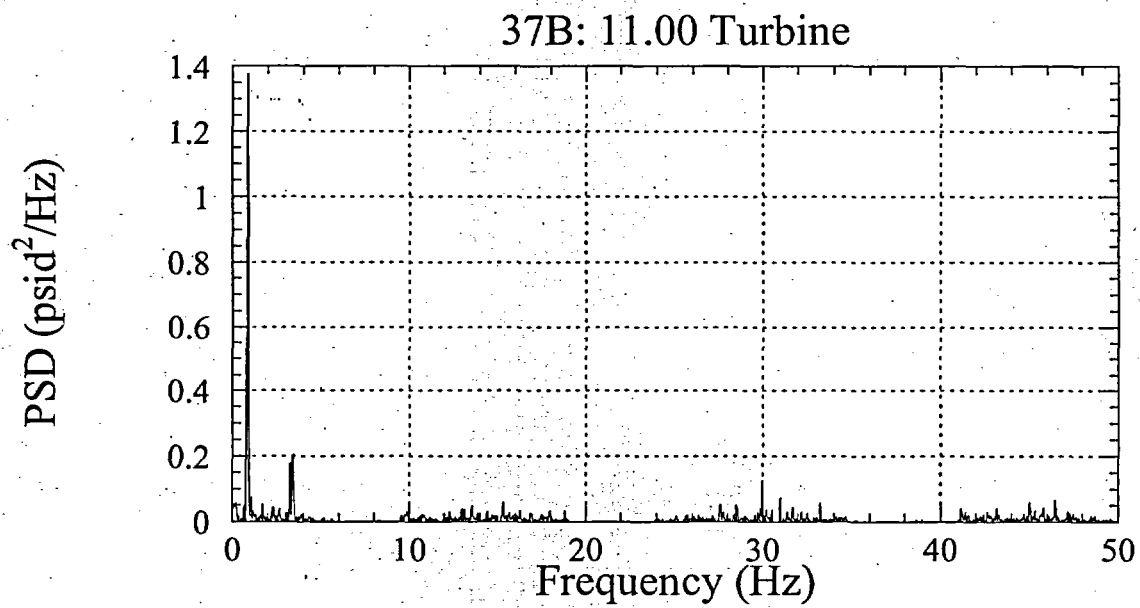
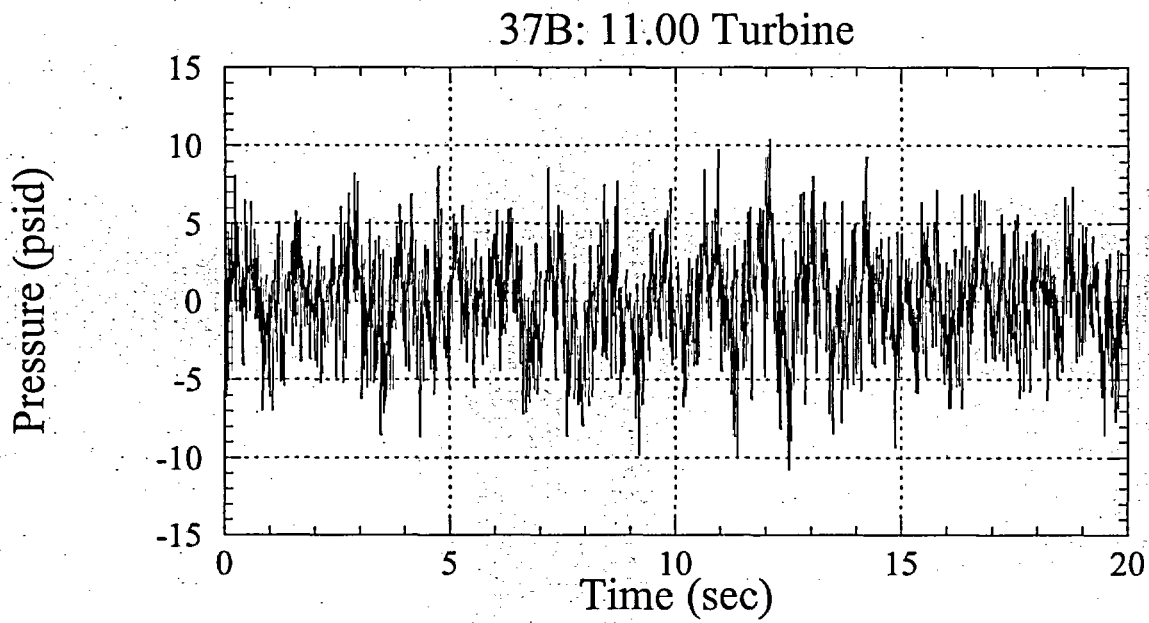


Figure 13-a.

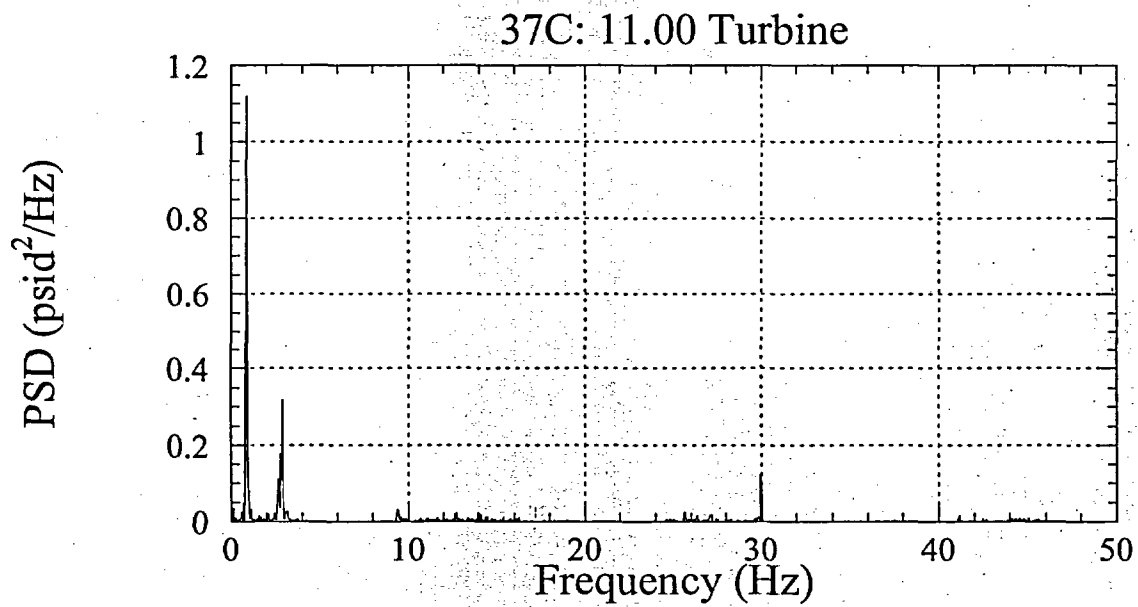
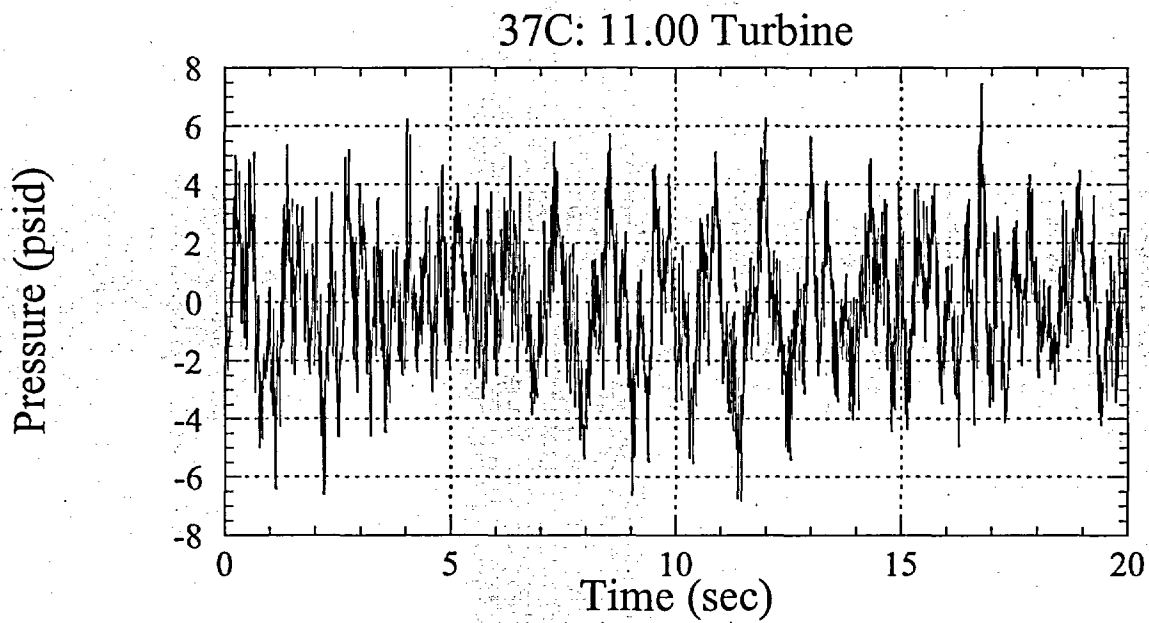


Figure 13-b.

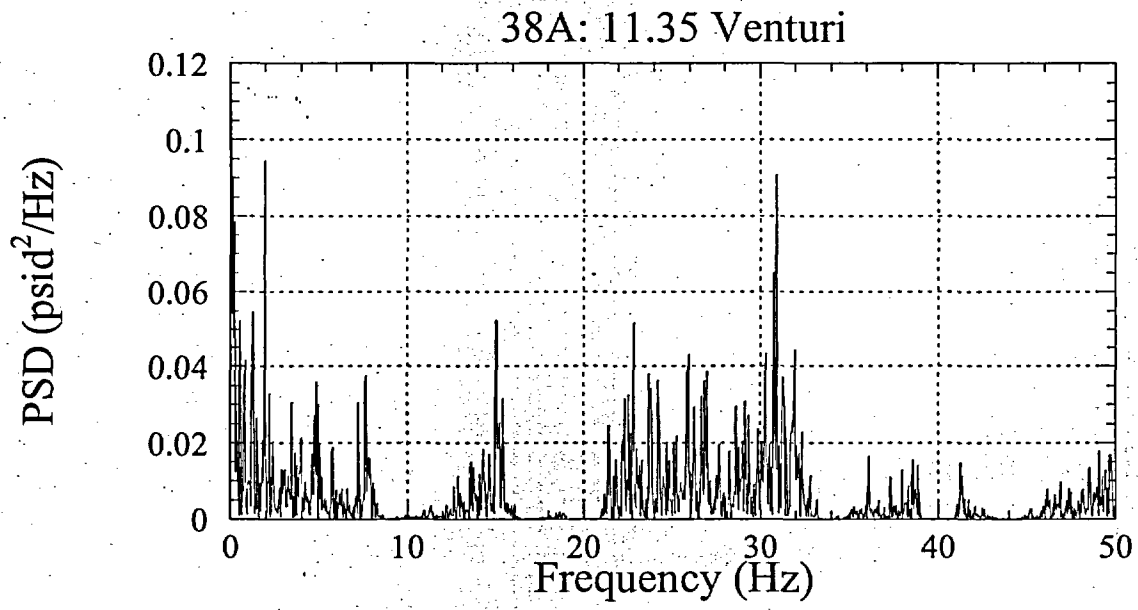
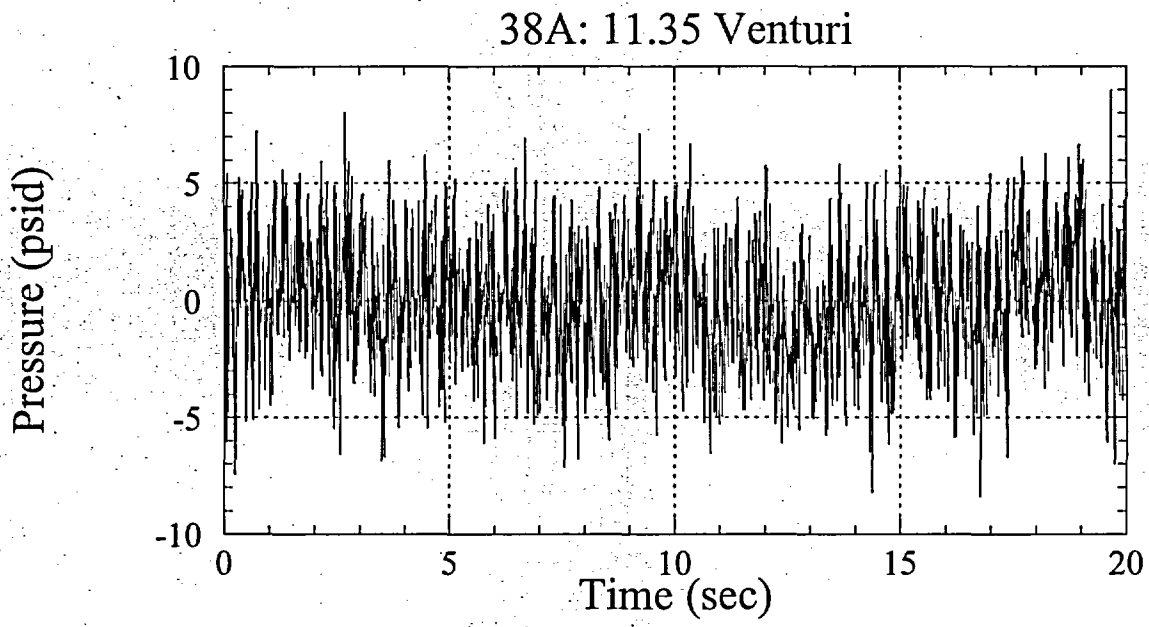


Figure 14-a.

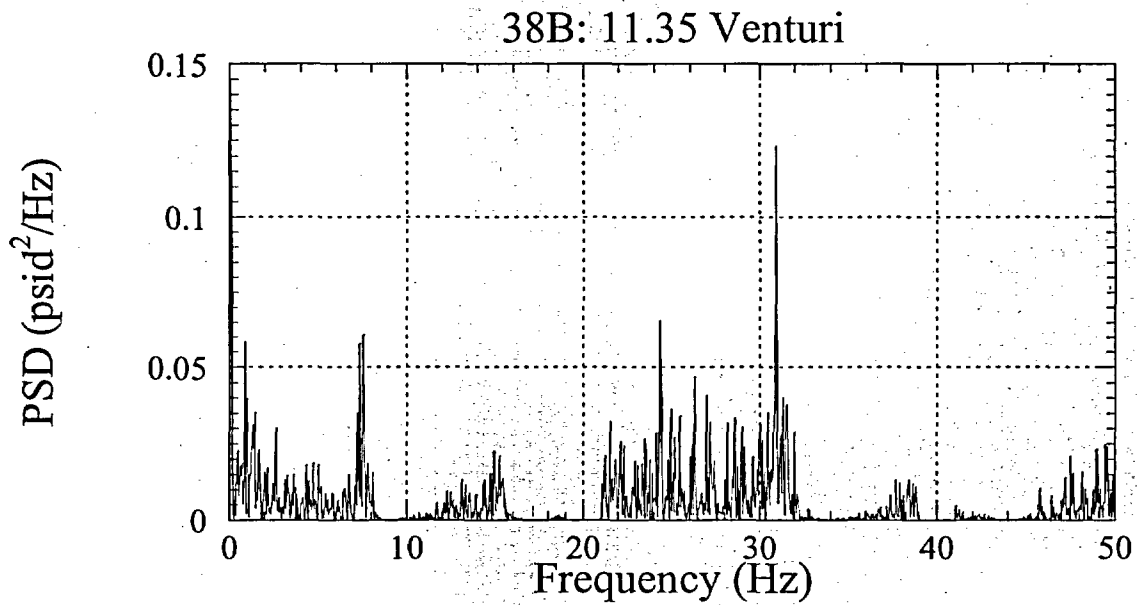
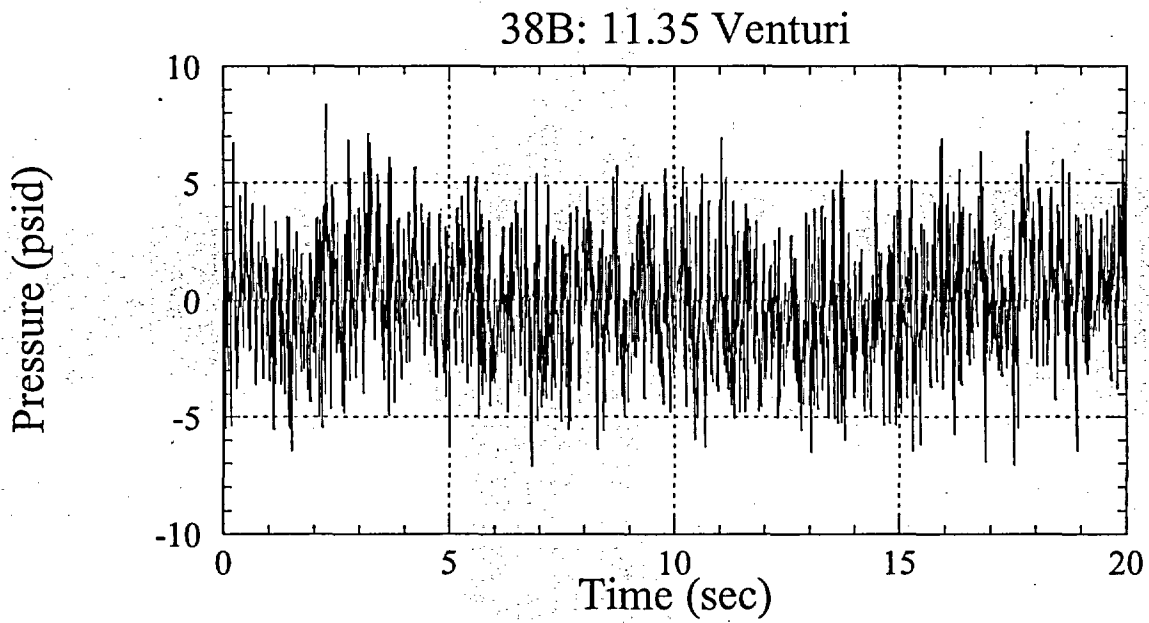


Figure 14-b.

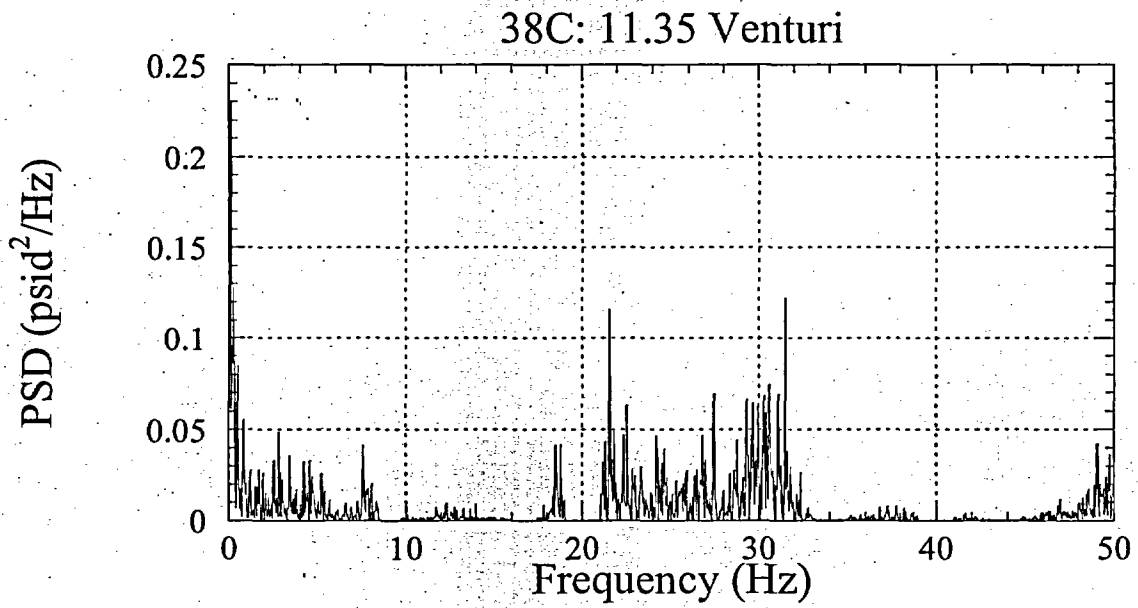
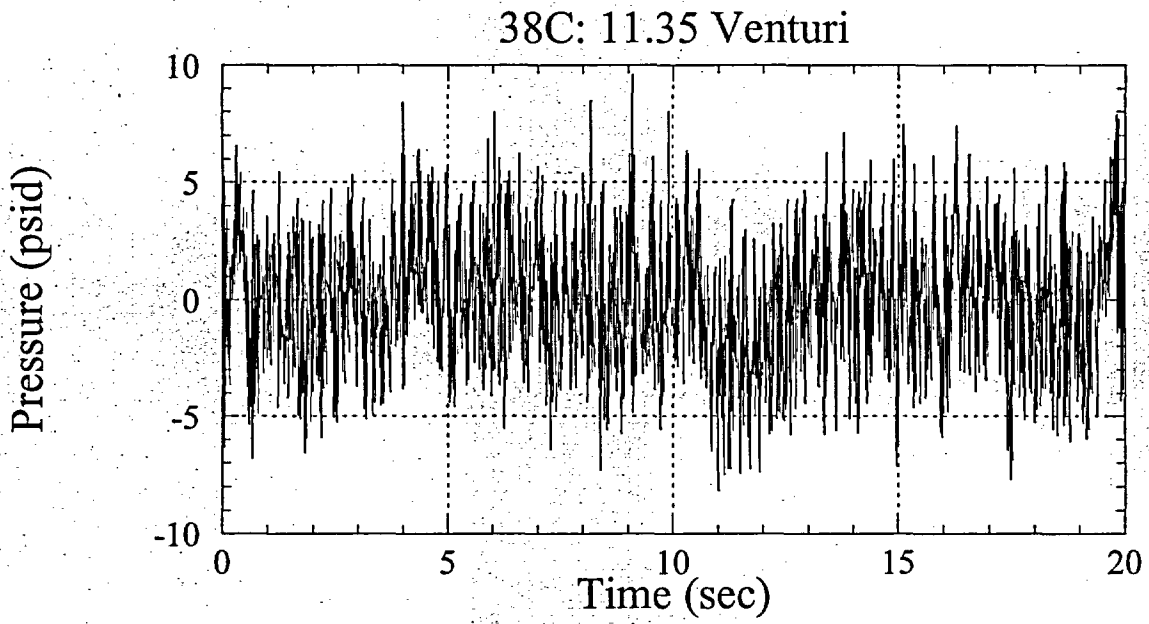


Figure 14-c.

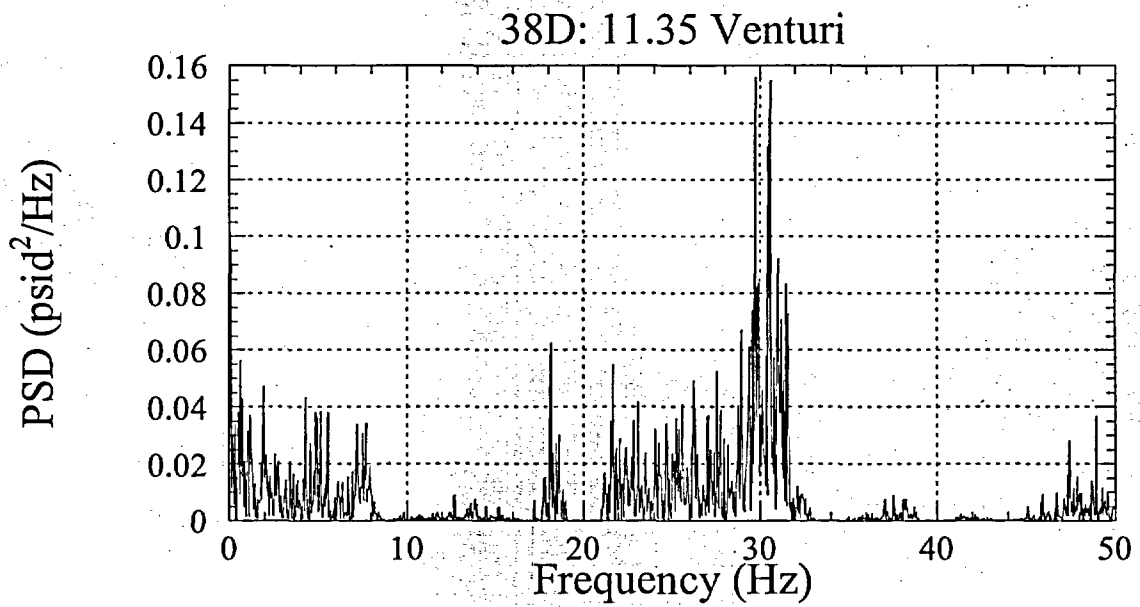
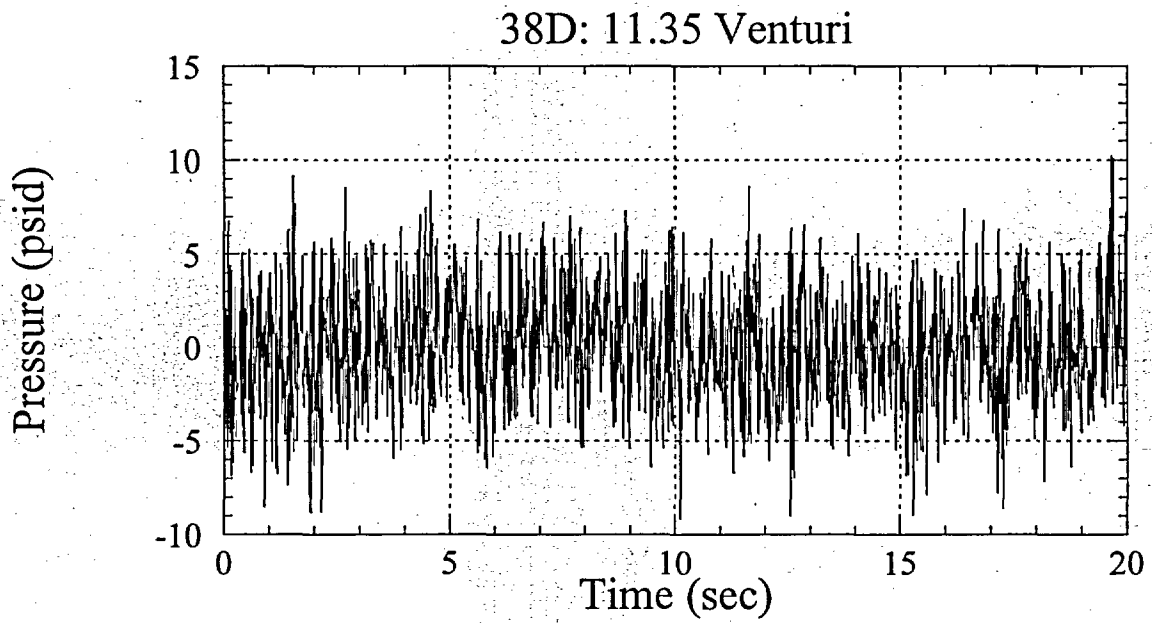


Figure 14-d.

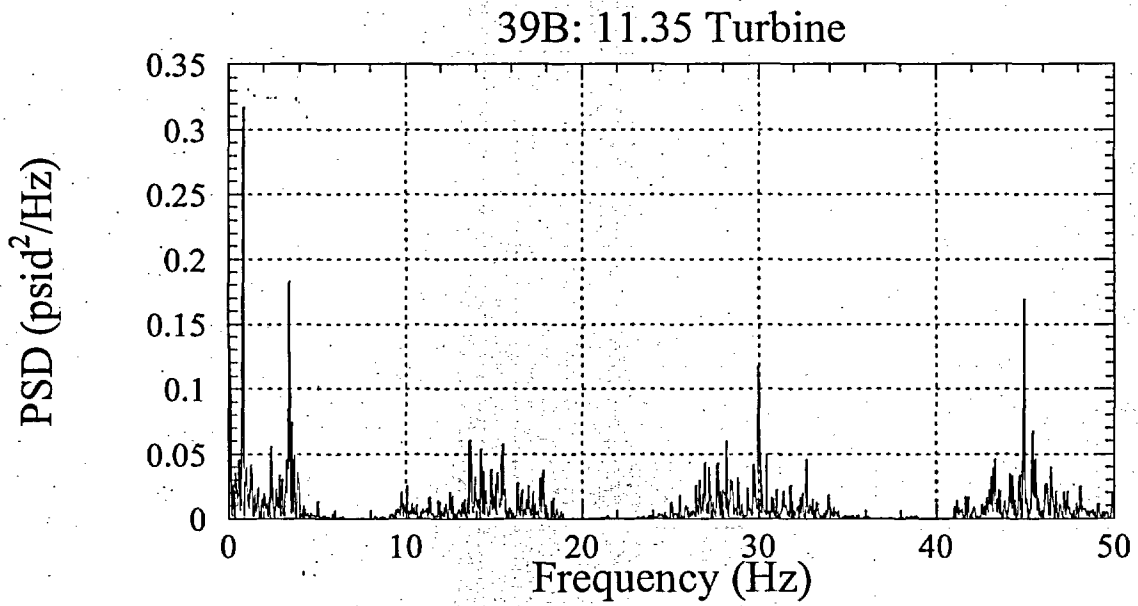
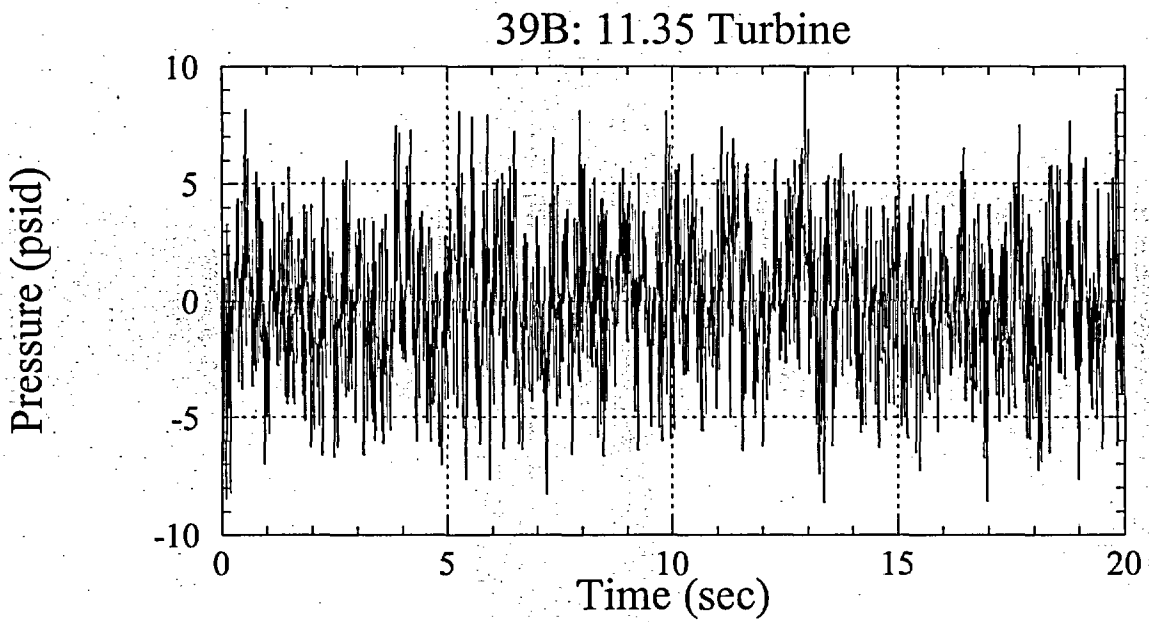


Figure 15-a.

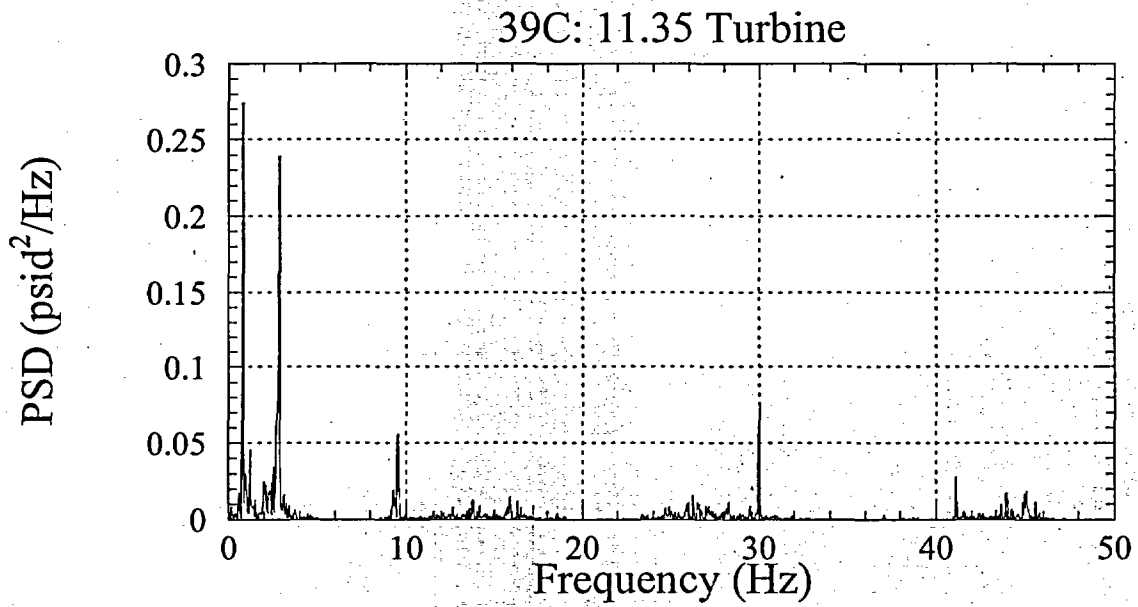
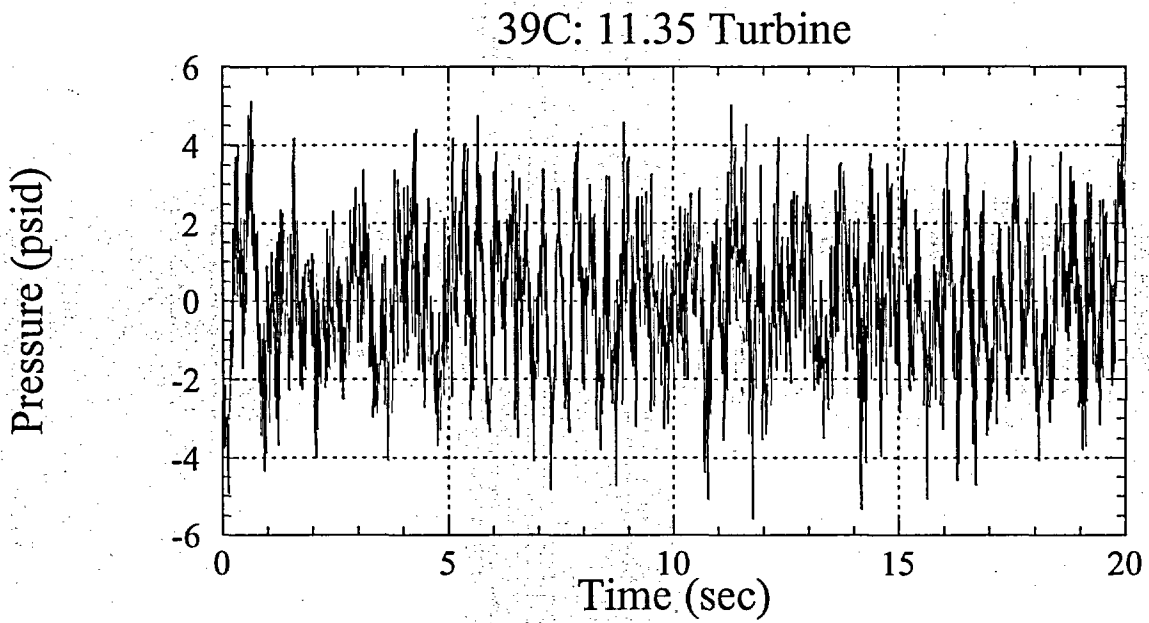


Figure 15-b.

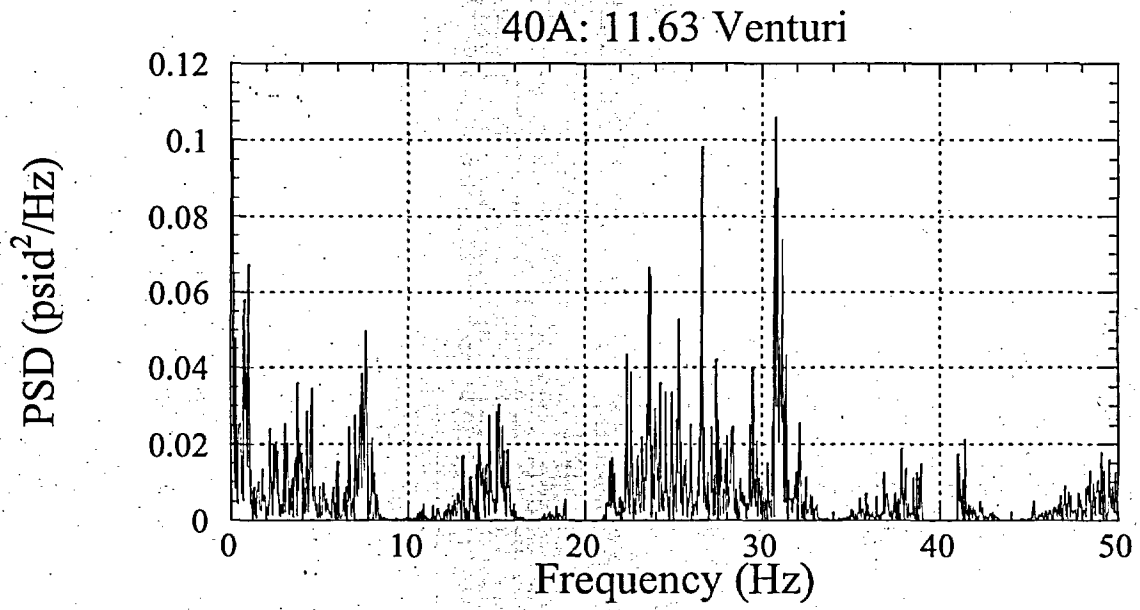
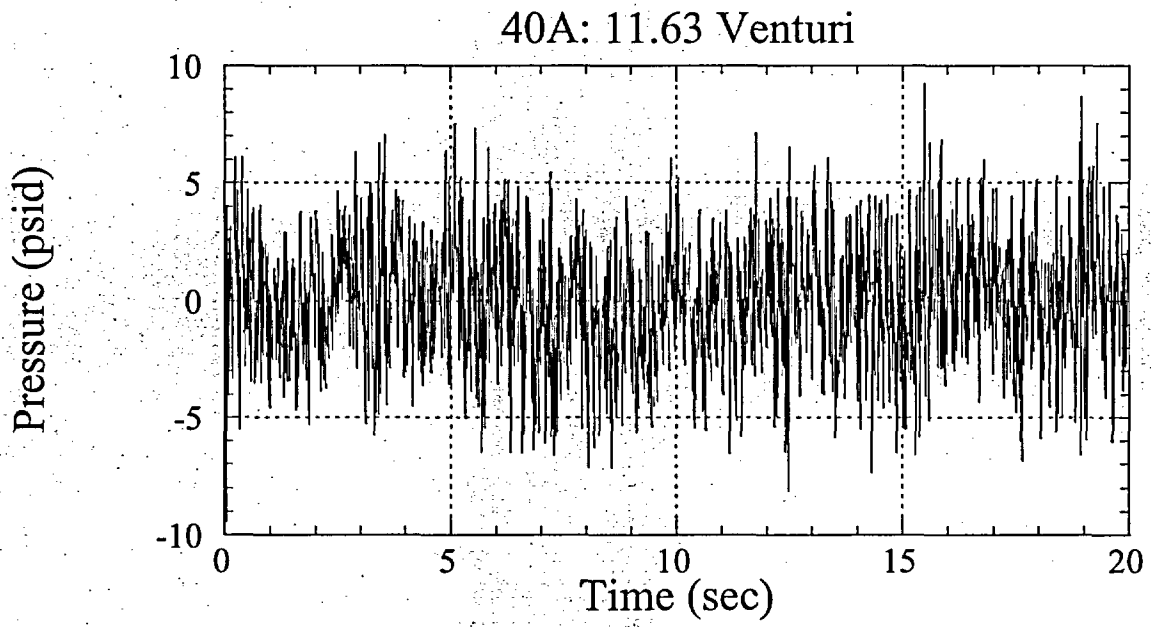


Figure 16-a.

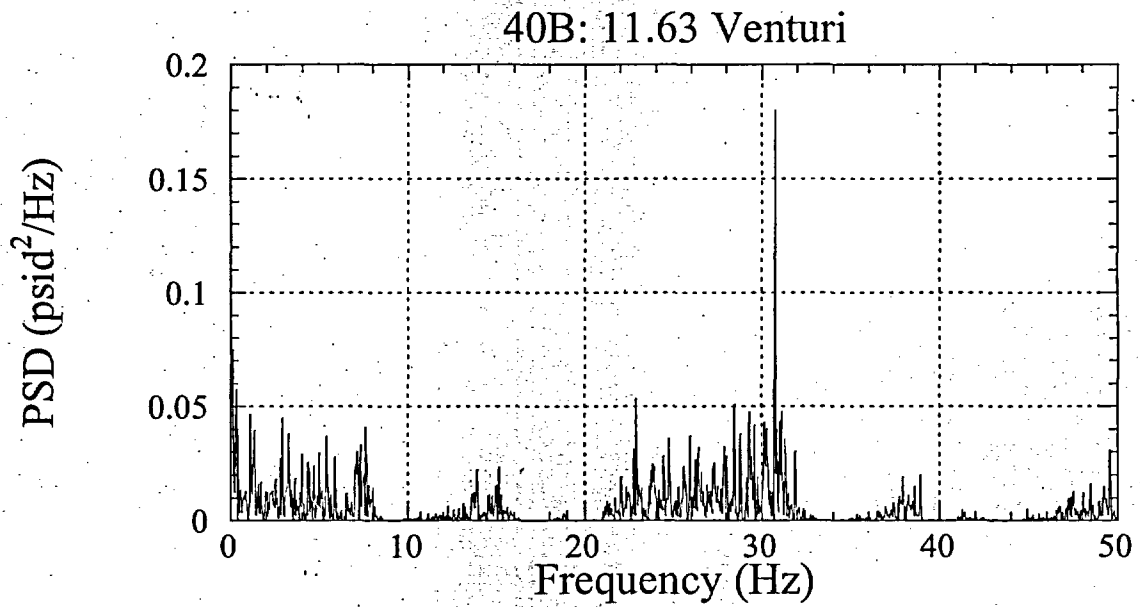
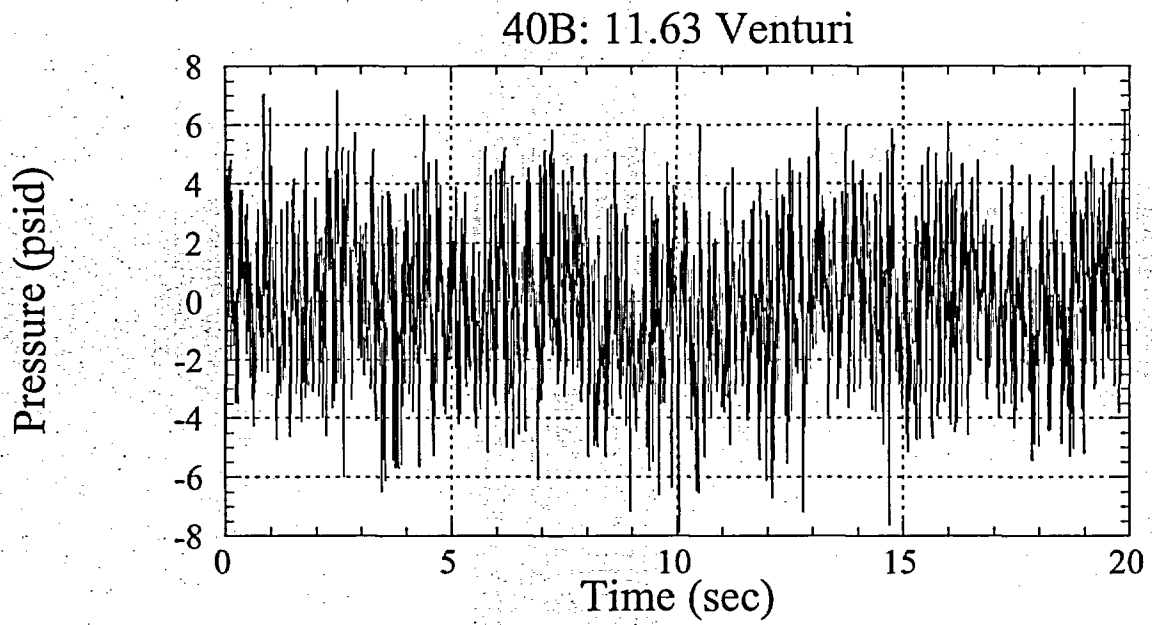


Figure 16-b.

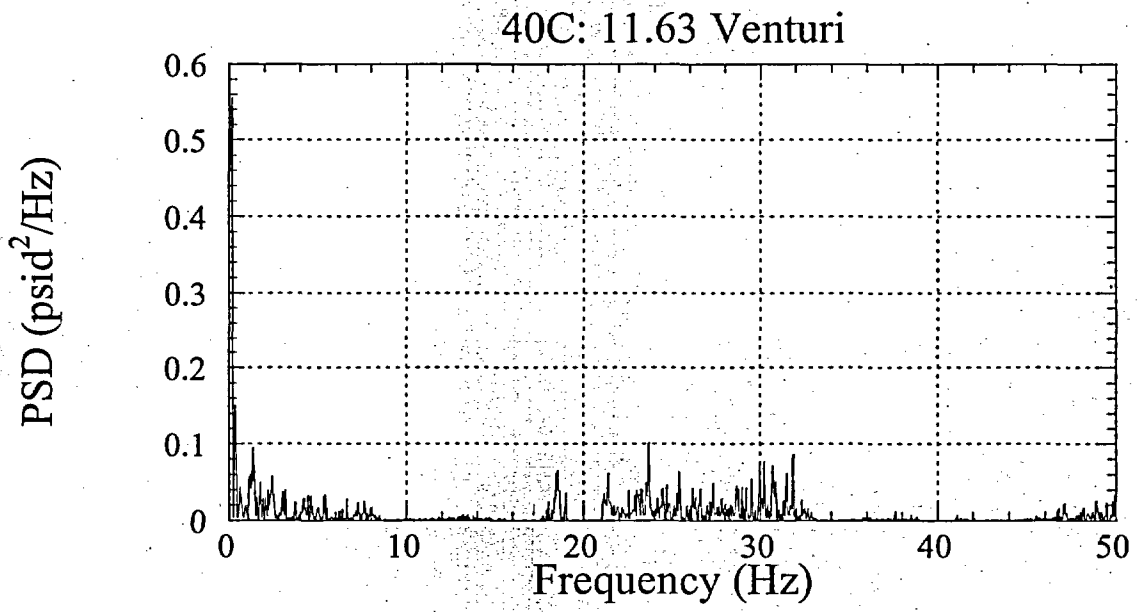
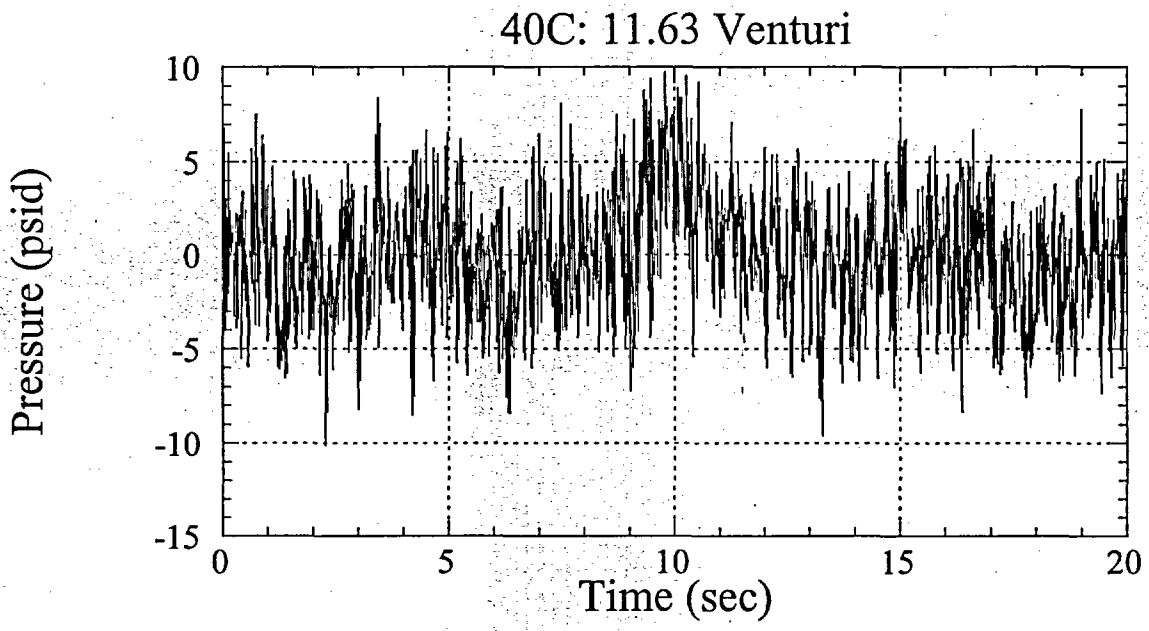


Figure 16-c.

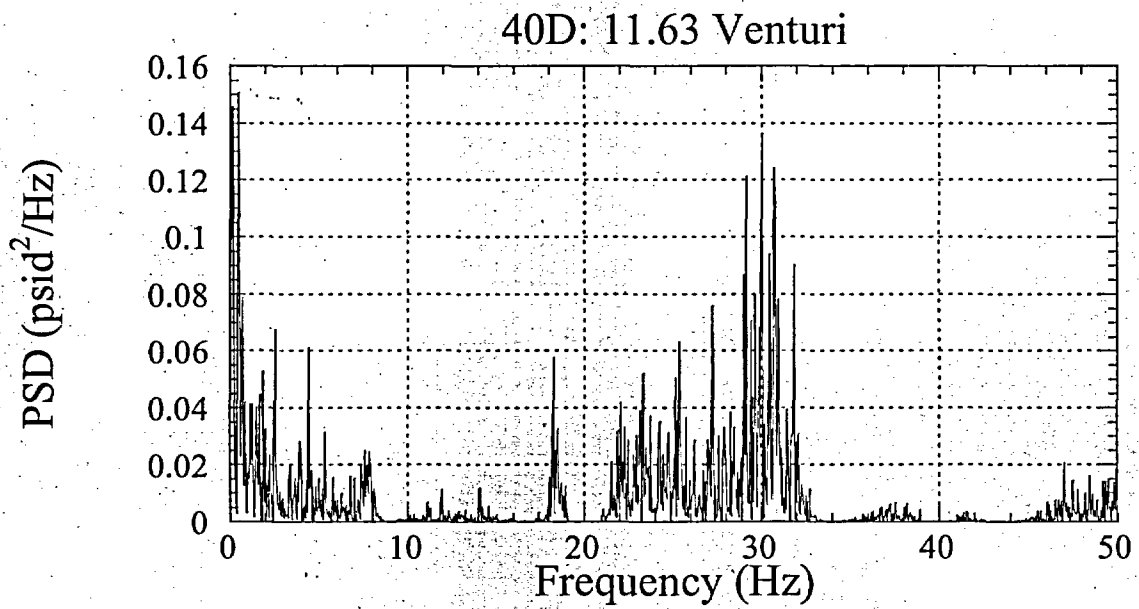
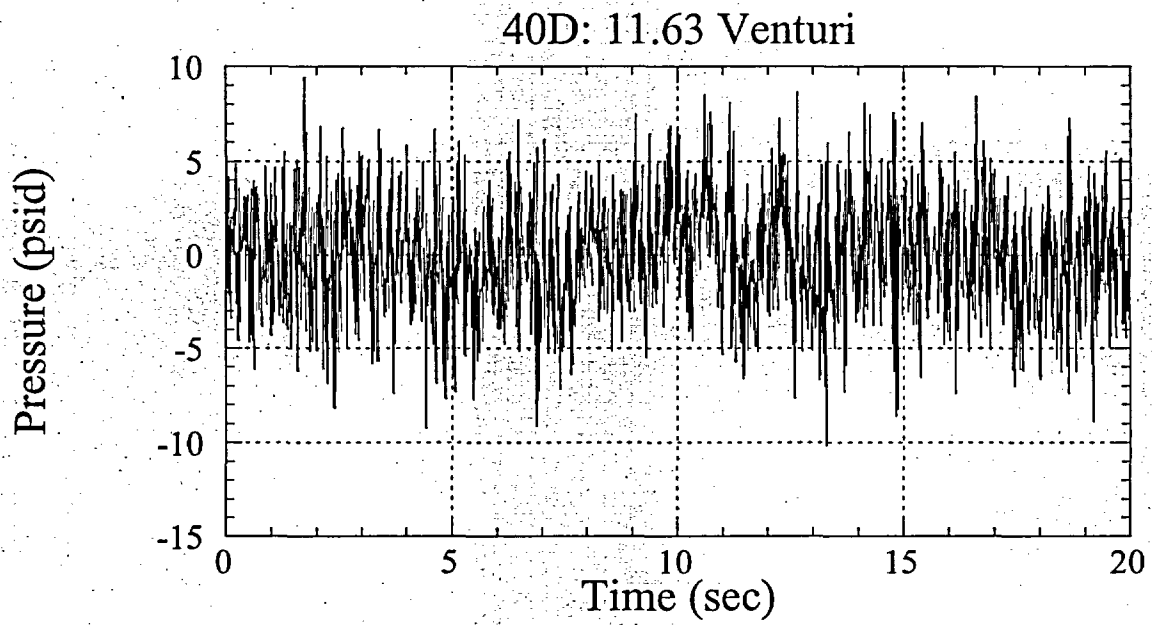


Figure 16-d.

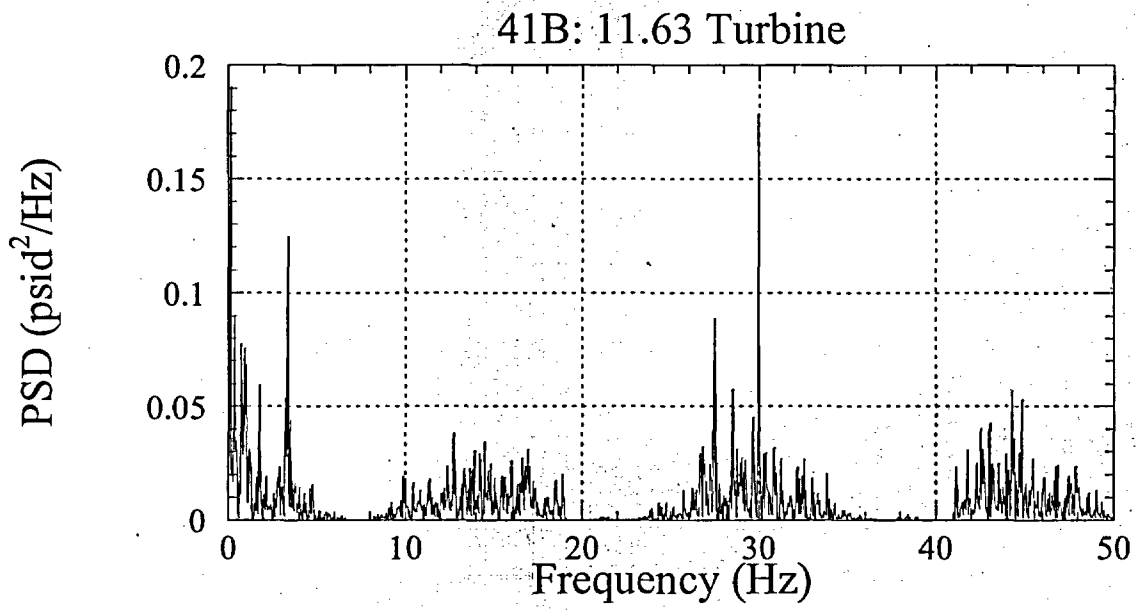
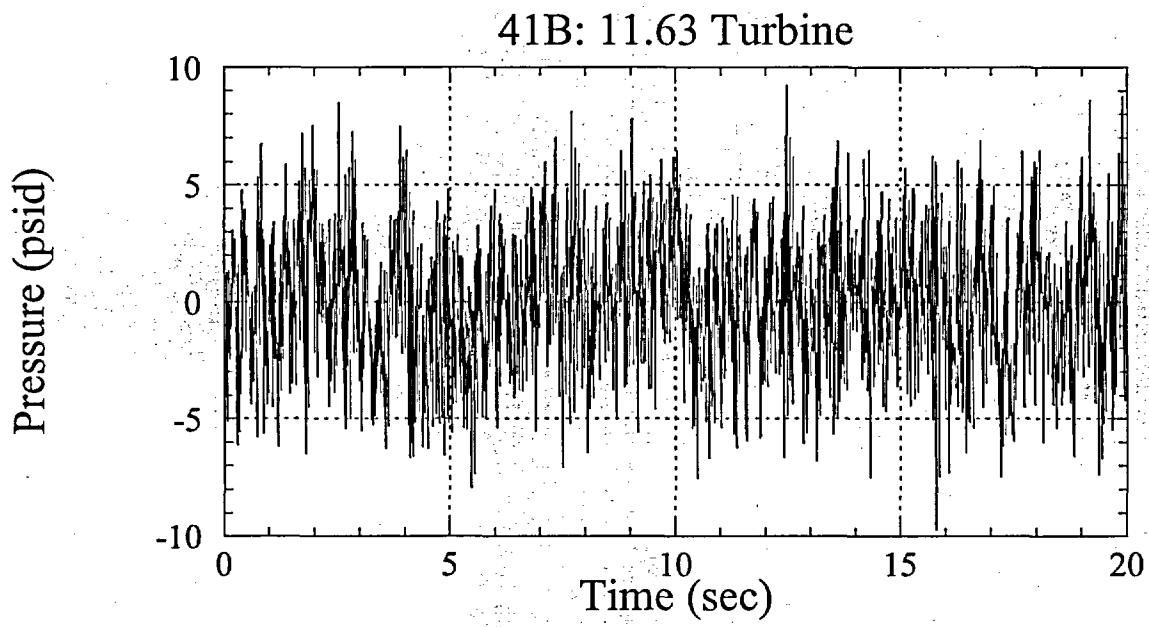


Figure 17-a.

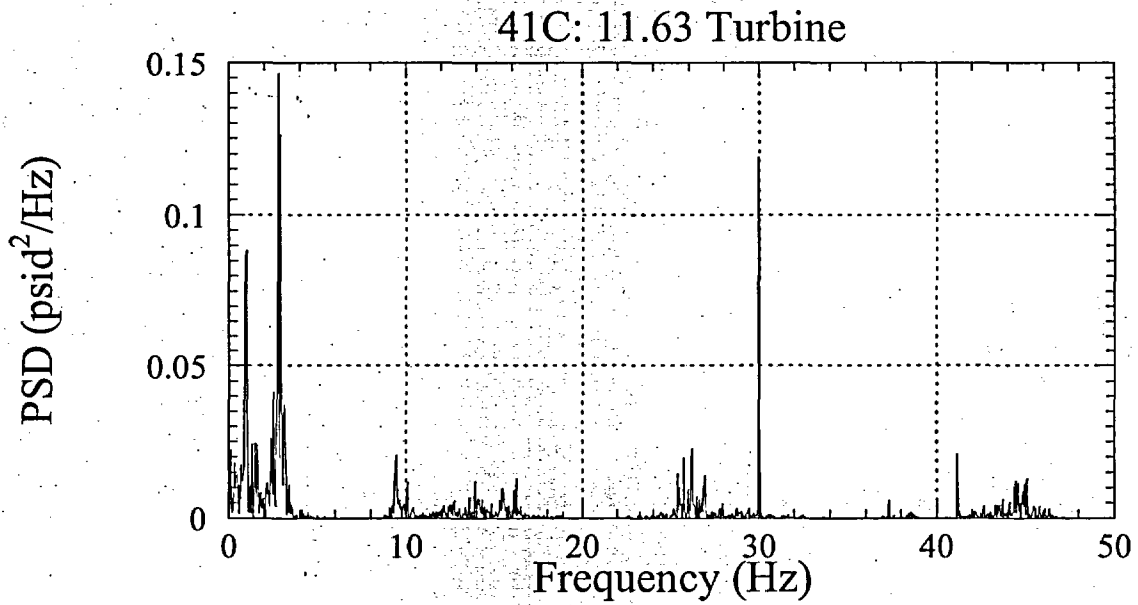
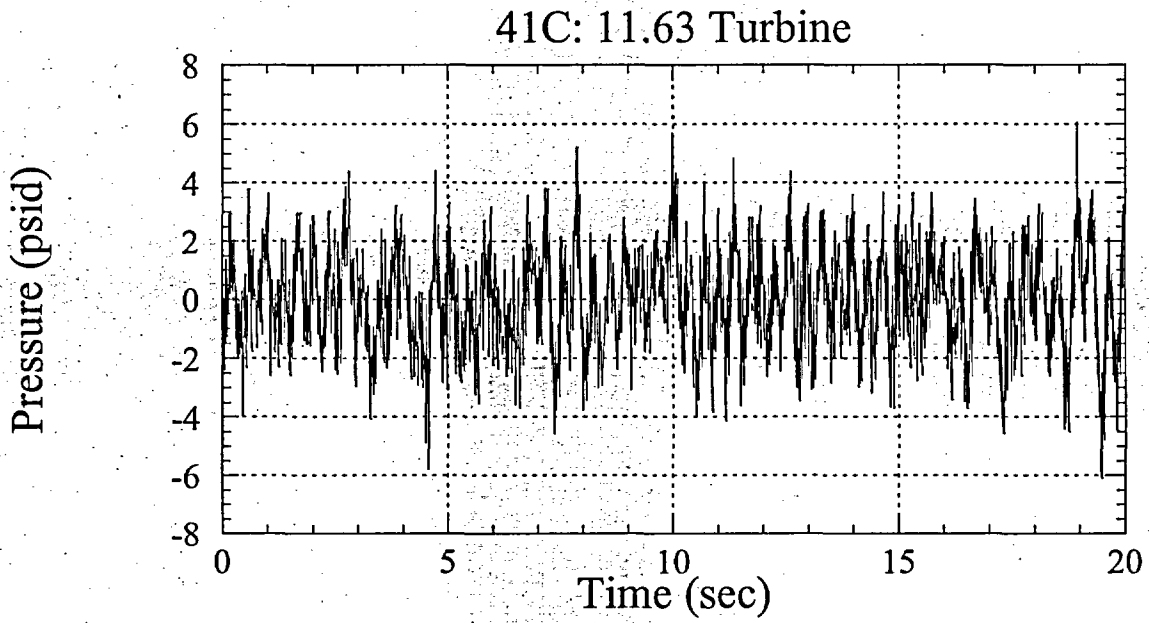


Figure 17-b.

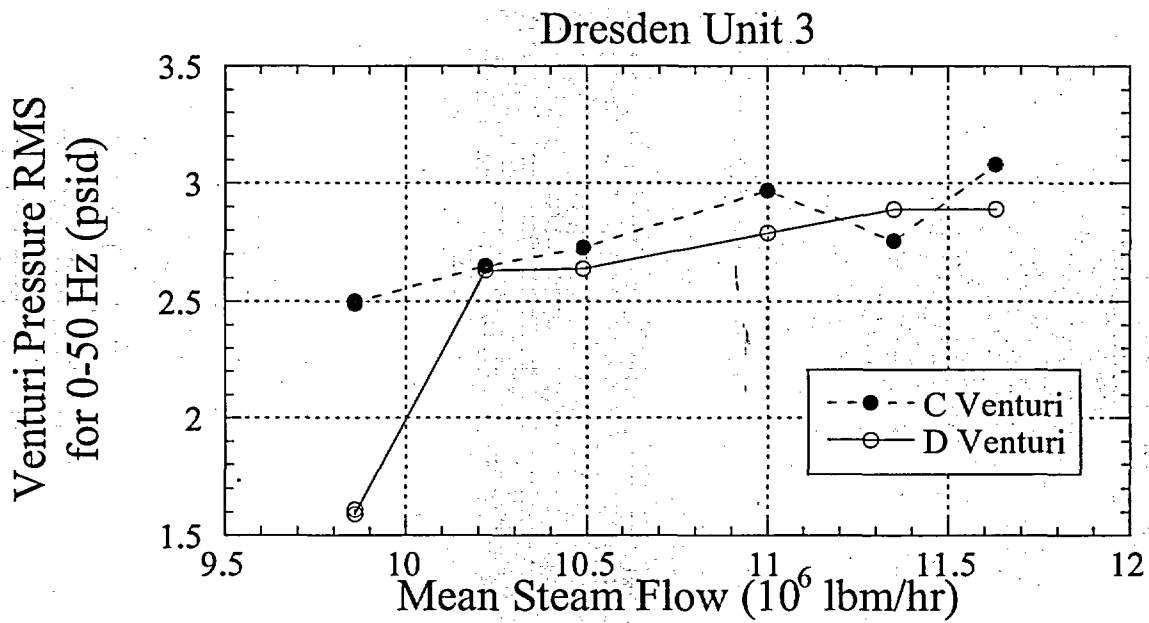


Figure 18. Comparison of RMS pressure data at the C and D venturi, corrected for instrument line length, for 0 to 50 Hz. Results for the mean steam flow rate of 11.63×10^6 lbm/hr are detailed in the following figures.

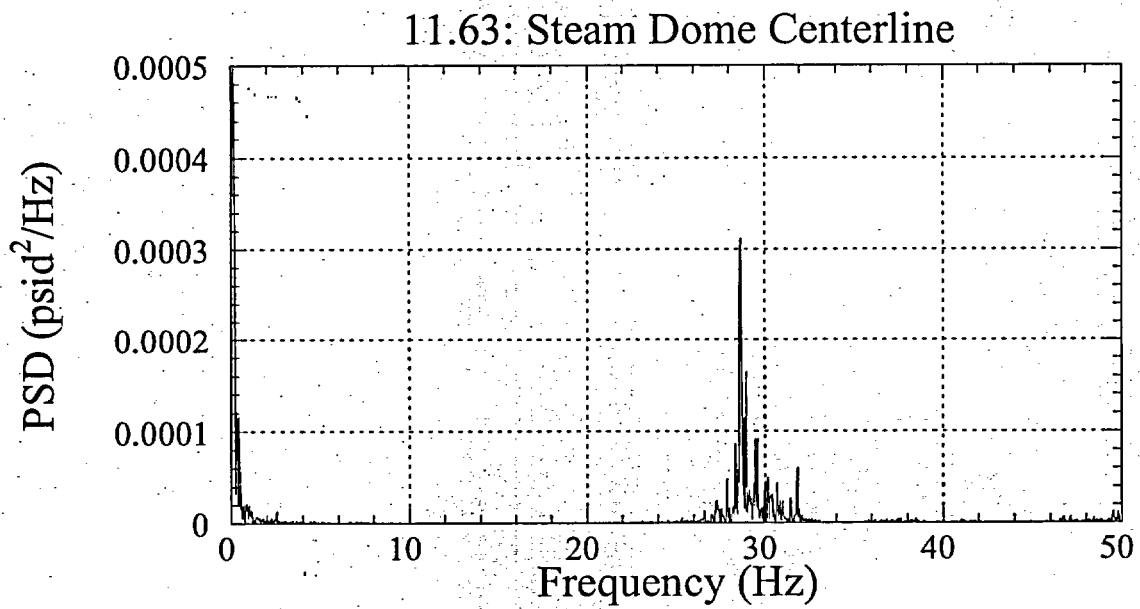
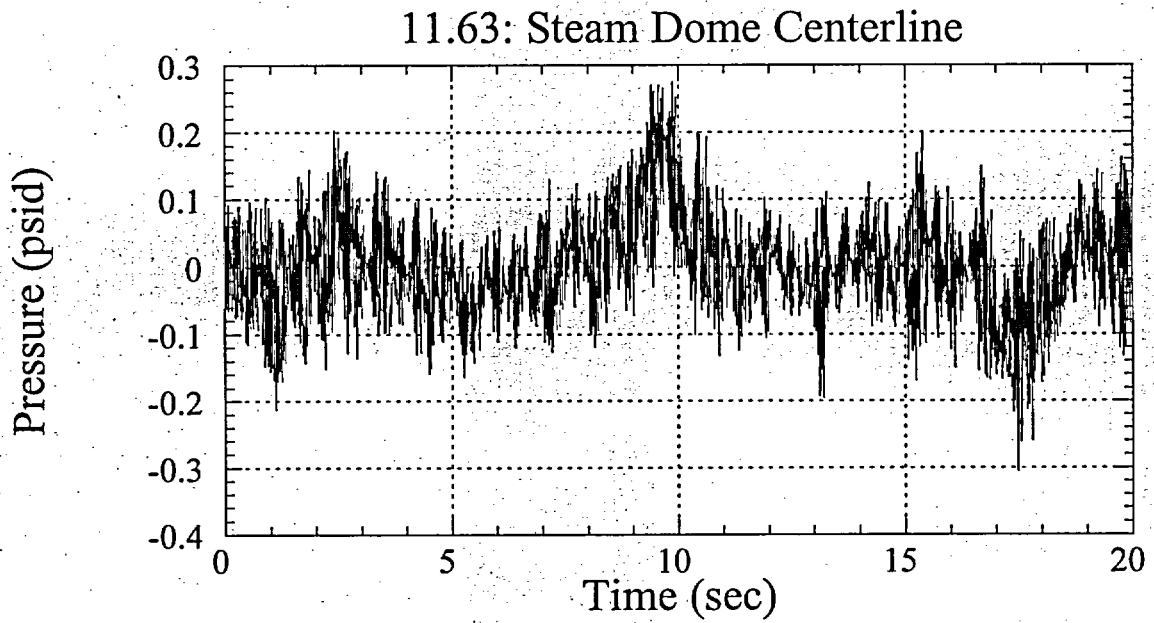


Figure 19. Predicted steam dome centerline pressures and associated PSD at a steam flow rate of 11.63×10^6 lbm/hr.

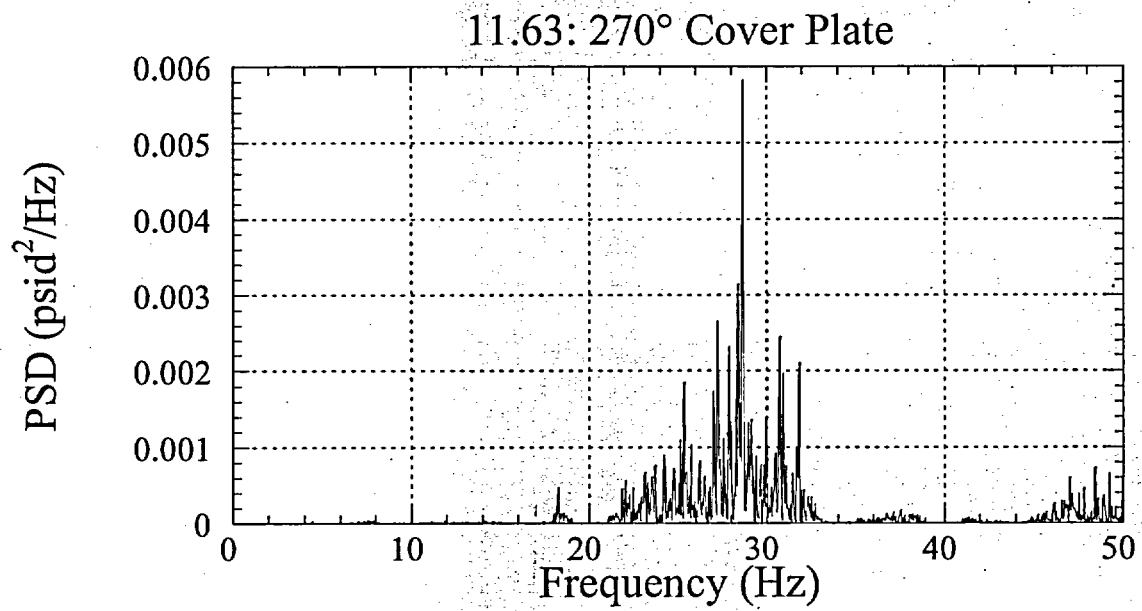
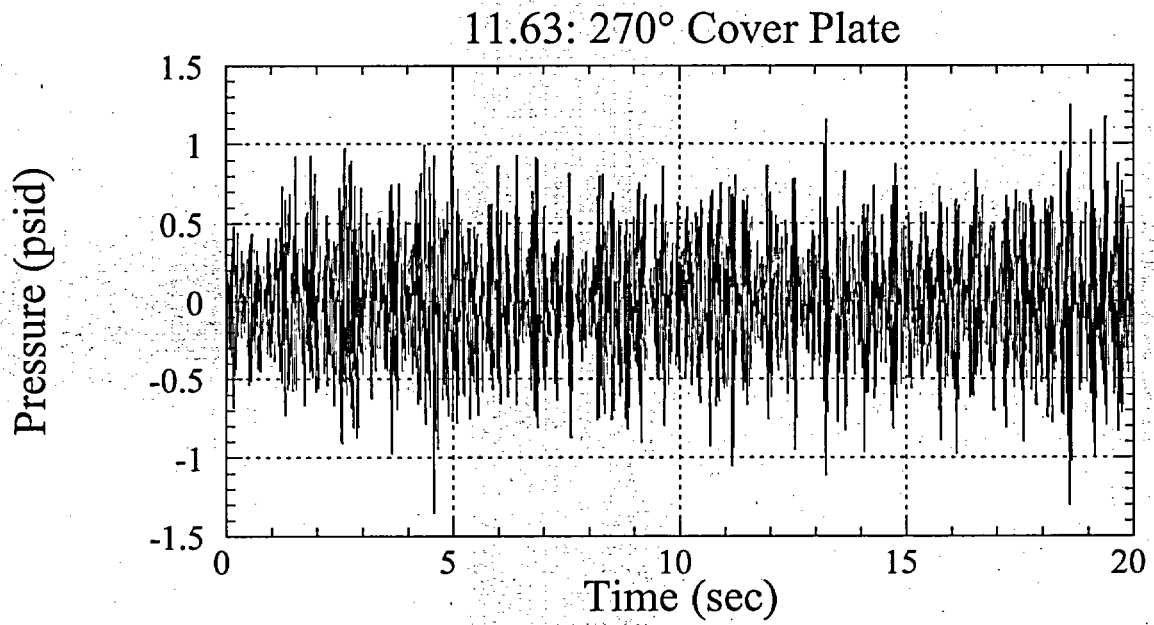


Figure 20. Maximum differential pressure load predicted across a dryer component.

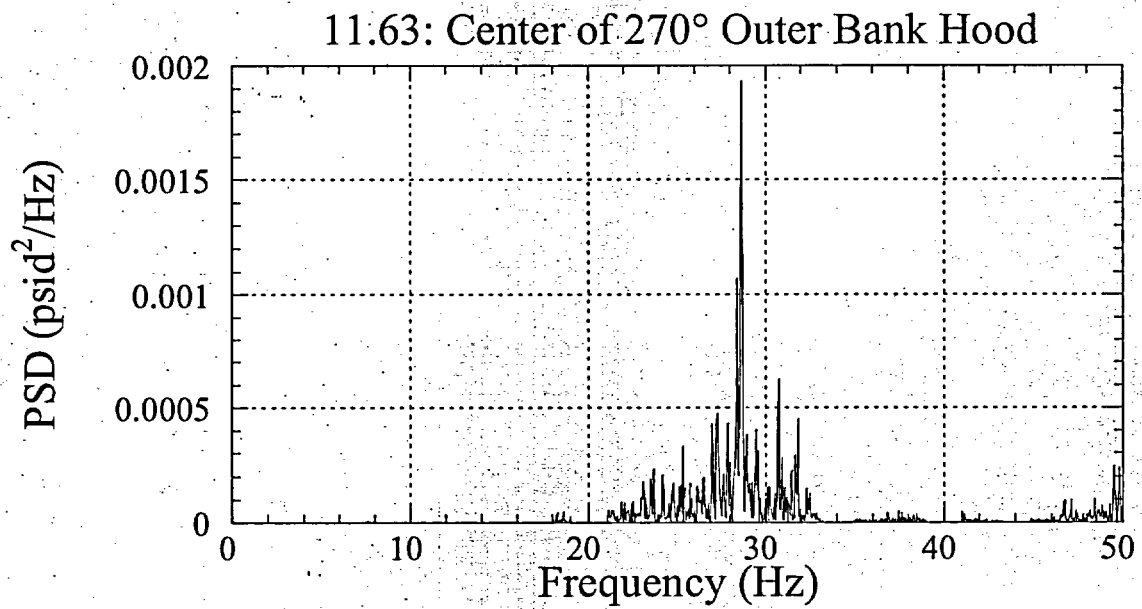
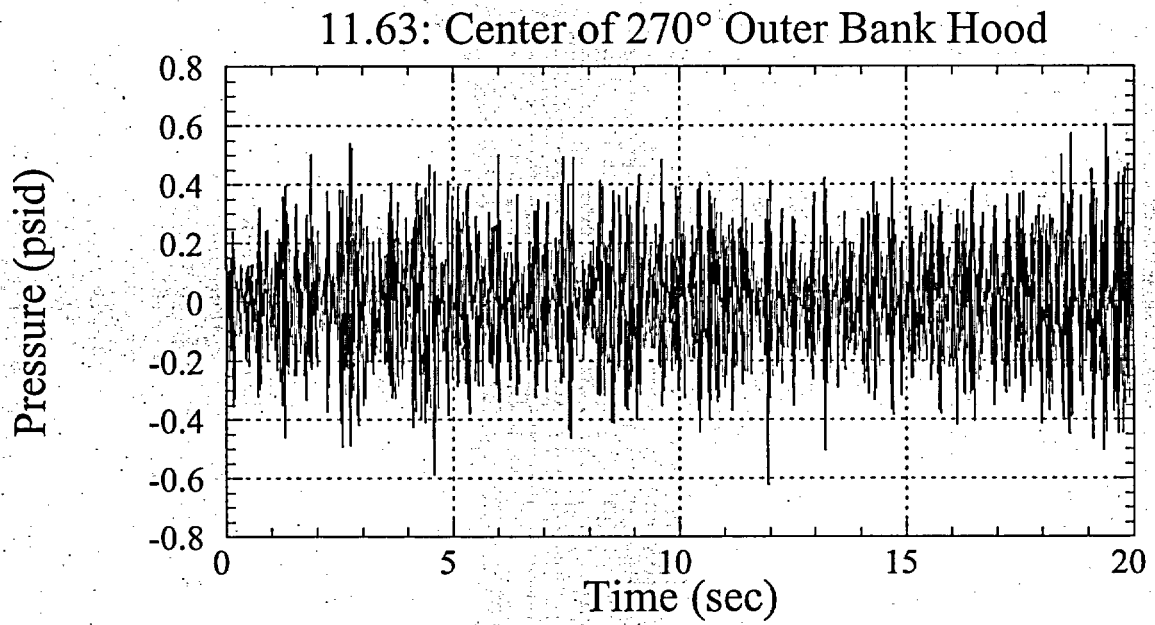


Figure 21.

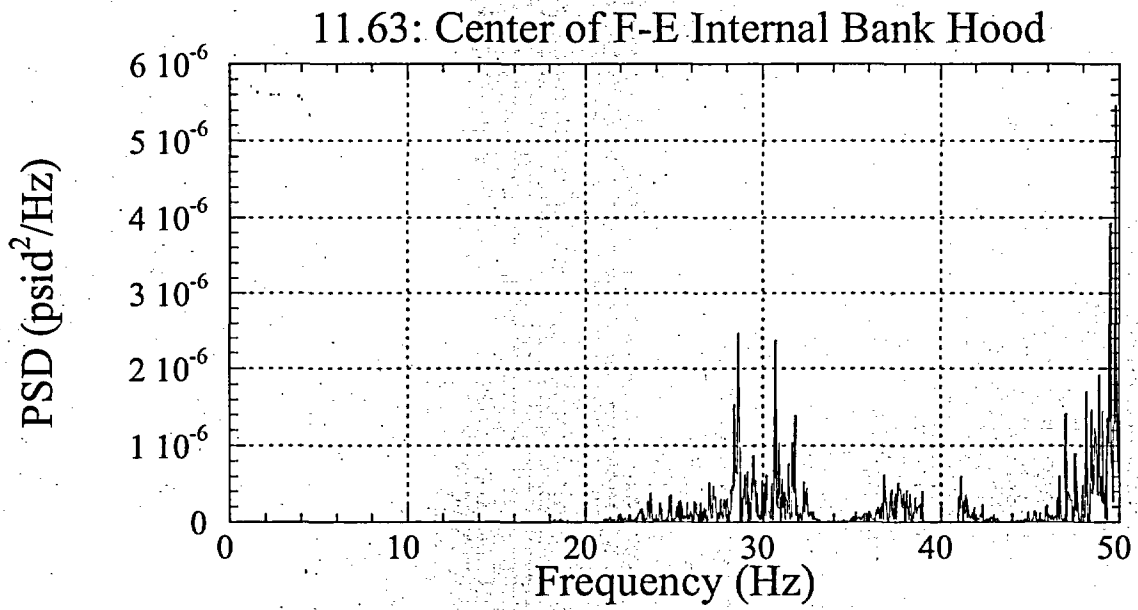
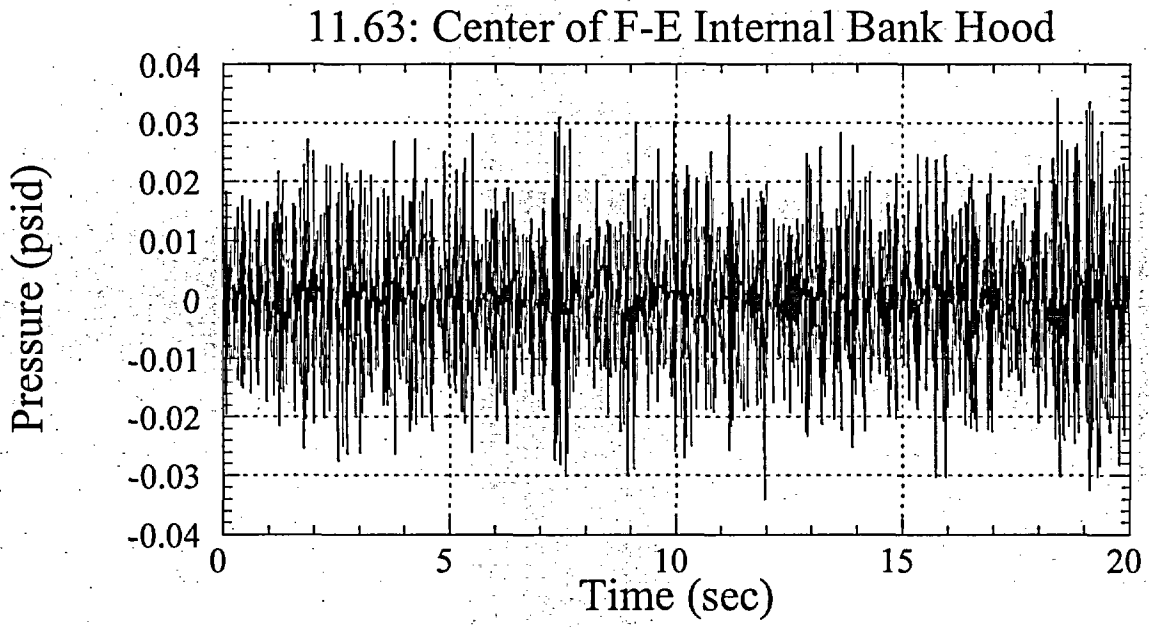


Figure 22.

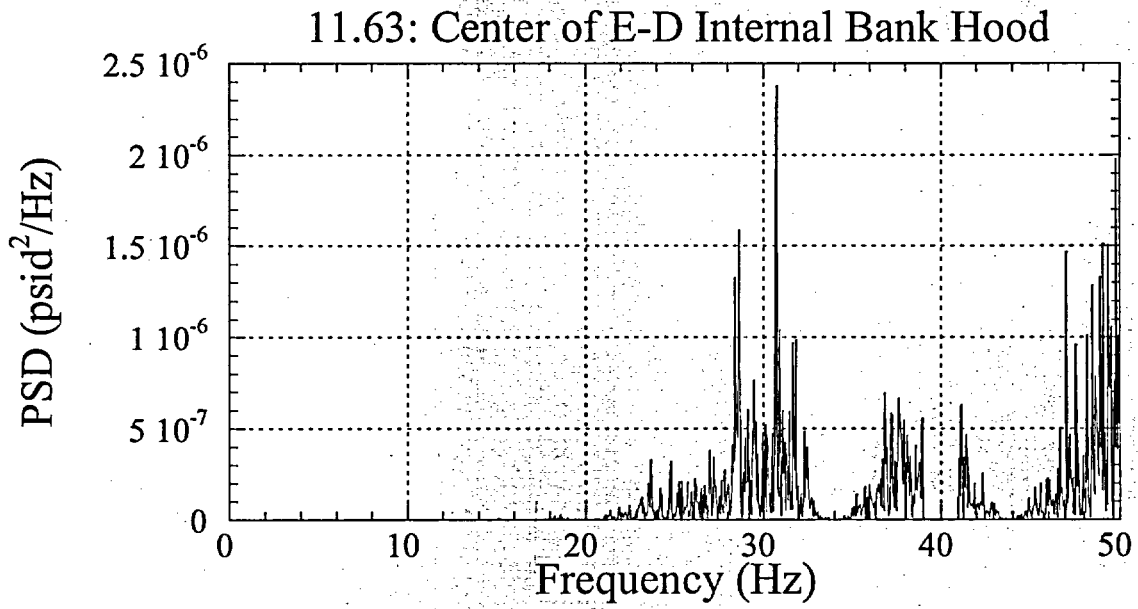
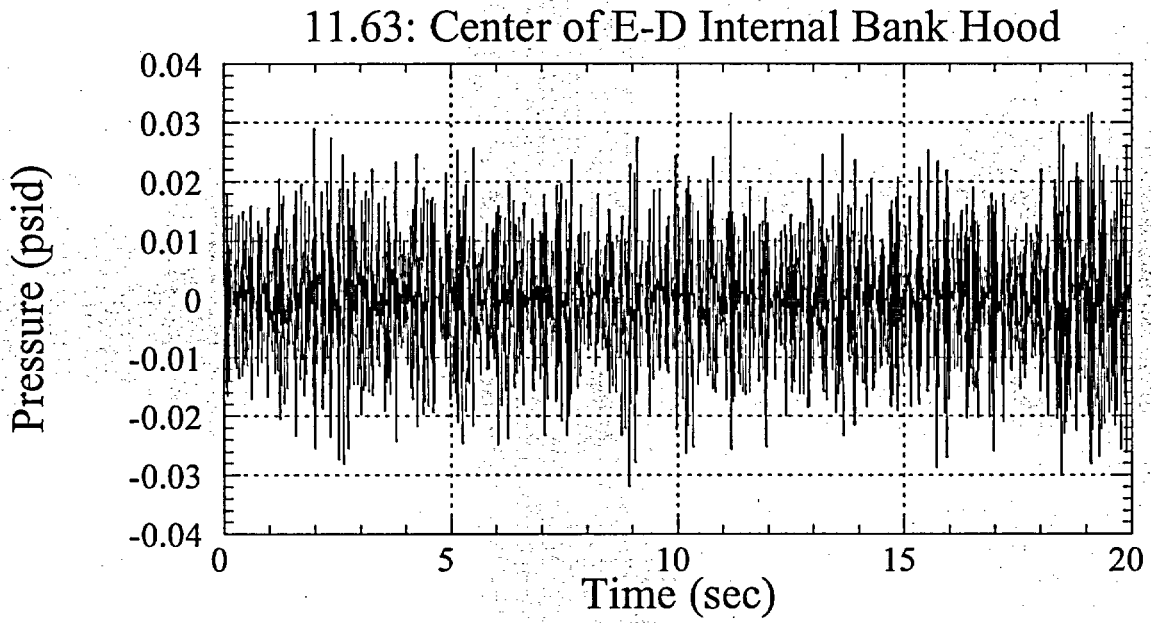


Figure 23.

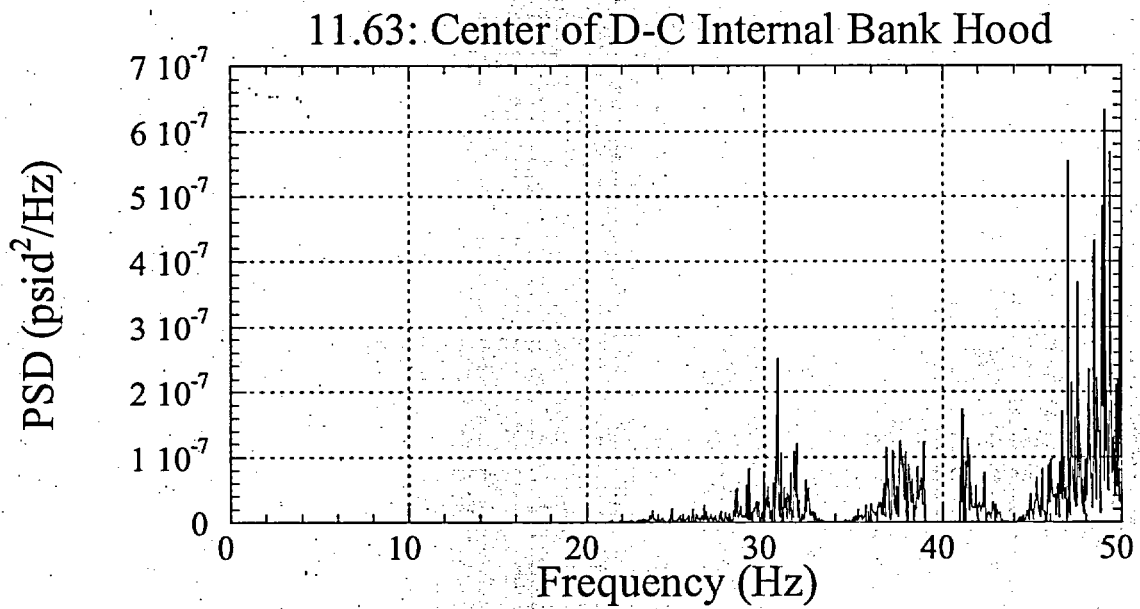
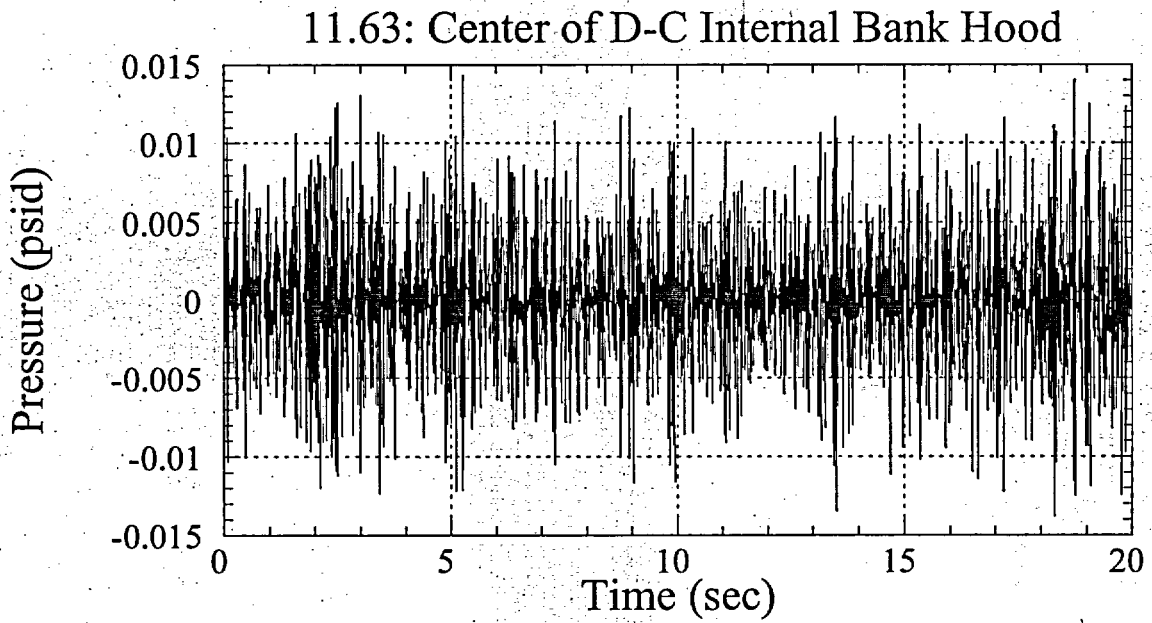


Figure 24.

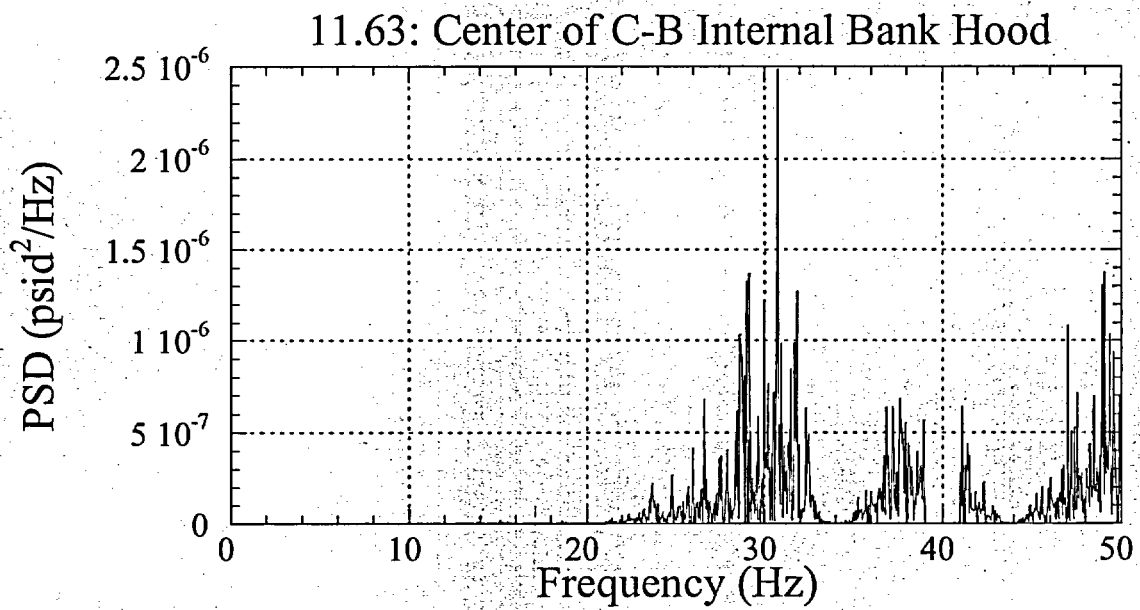
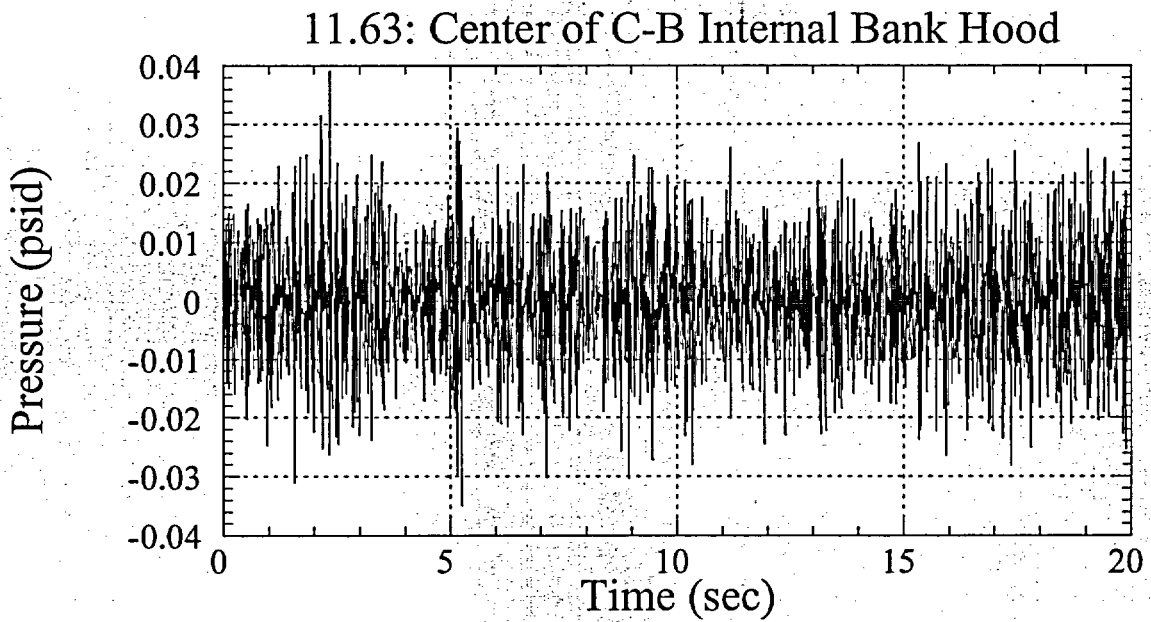


Figure 25.

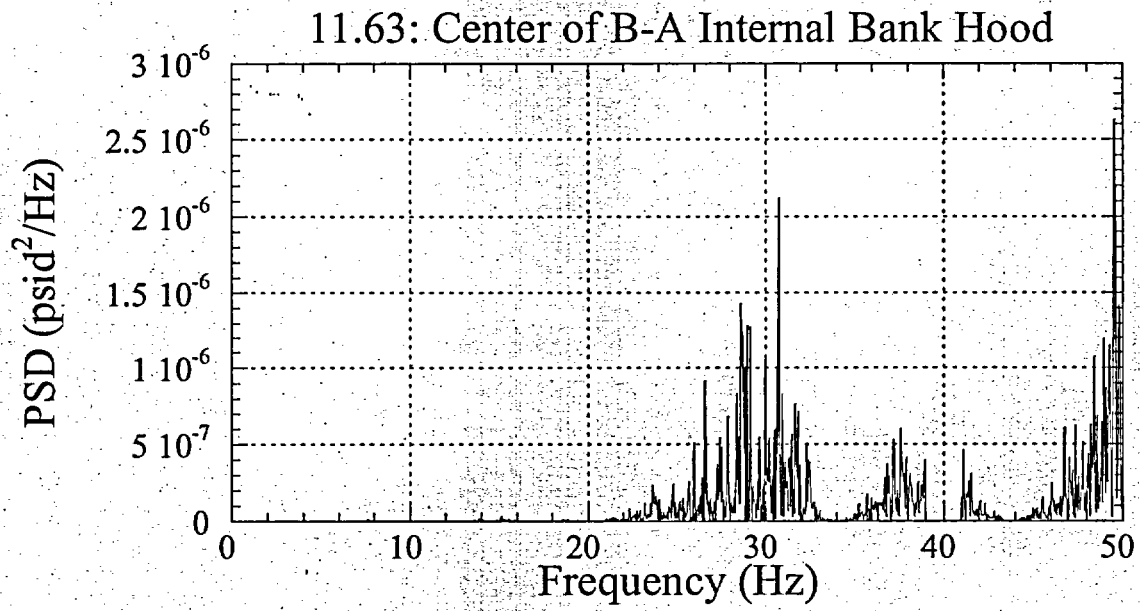
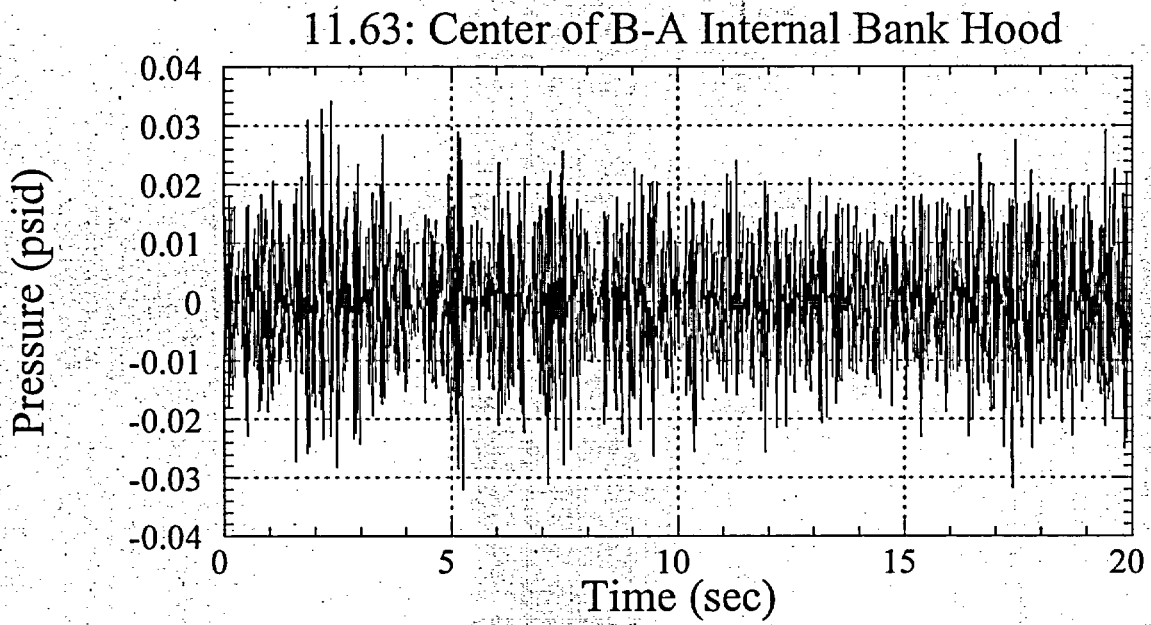


Figure 26.

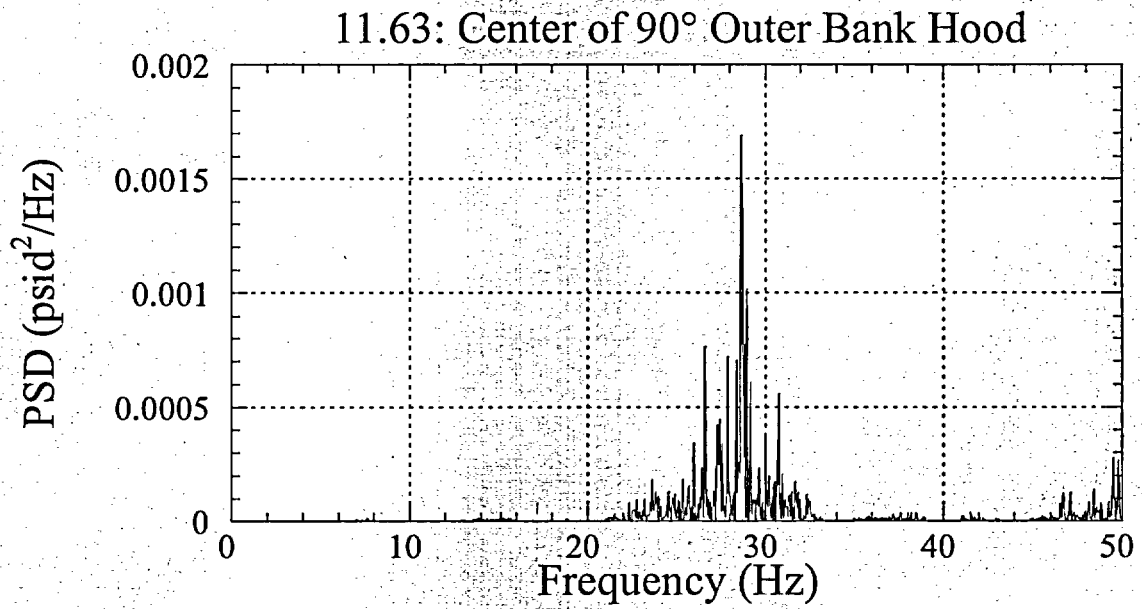
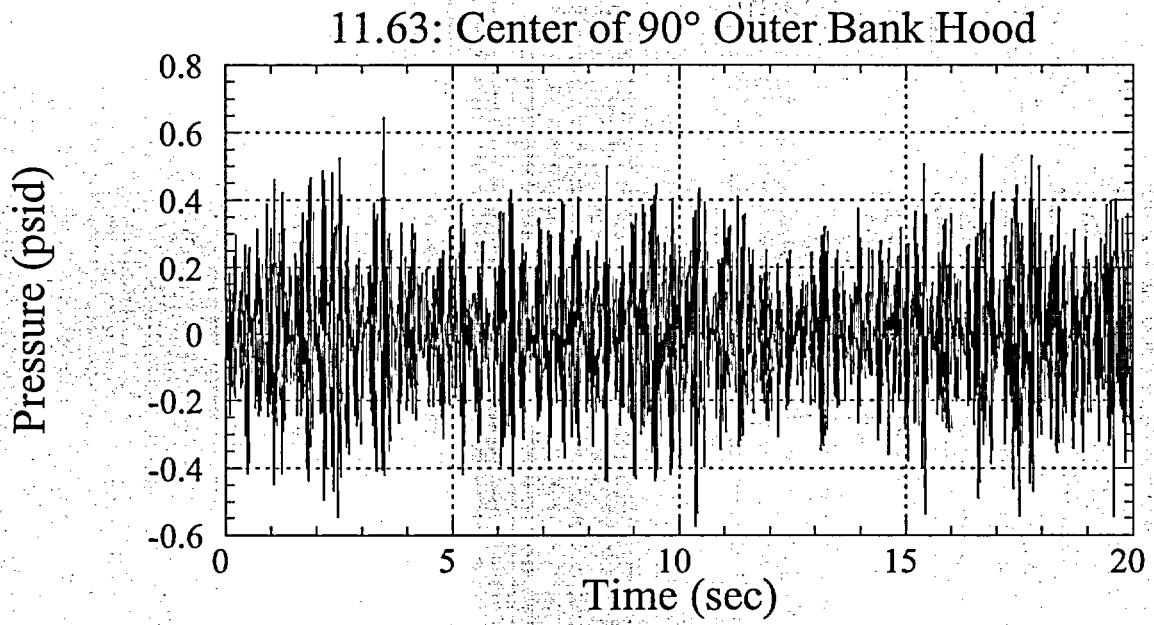


Figure 27.

ATTACHMENT 2
Summary of Commitments

The following tables identify commitments being made by Exelon Generation Company, LLC (EGC). Any other actions discussed in this letter represent intended or planned actions by EGC. They are described for the NRC's information and are not regulatory commitments.

	Commitment	Committed Date or Outage
1	EGC will limit operation on both Quad Cities Nuclear Power Station (QCNPS) units to 2511 MWt (i.e., the maximum original licensed power level prior to NRC approval of extended power uprate (EPU)), with the exception of one or more brief periods not to exceed a total of 72 hours for each QCNPS unit to allow collection of data as described in the Plan for Evaluation of Flow Effects. EGC will not resume long-term operation of the QCNPS units above the pre-EPU power level until NRC approval is obtained.	Effective April 2, 2004
2	EGC will modify the electromatic relief valves on QCNPS Unit 1 based on analysis of previous failures prior to briefly increasing power above 2511 MWt for collection of data as described in the Plan for Evaluation of Flow Effects.	Prior to commencing data collection above 2511 MWt in accordance with evaluation plan
3	<p>EGC will meet with the NRC technical staff to discuss the following topics:</p> <ul style="list-style-type: none"> a. Results of the reevaluation of previous assessments of the impact of flow-induced vibration under EPU conditions on reactor pressure vessel internals, steam and feedwater systems and components, including an evaluation of previous evaluation deficiencies; b. Description of how the data collected was used to assess the dynamic loading on plant components other than the steam dryer; c. Results of the review to identify potential EPU-related equipment vulnerabilities; and d. Plans for monitoring the performance of the steam dryer and other potentially affected components, including the criteria for prompt corrective action in response to performance degradation. 	Third quarter 2004
4	EGC will submit to the NRC the results of the analyses described in commitment 3 above.	Three weeks after completion of commitment 3
5	EGC will meet with NRC management to present the information submitted to the NRC in commitment 4. At the meeting, EGC will demonstrate that the remaining EPU vulnerabilities have been identified and action plans have been developed to resolve the vulnerabilities.	Three weeks after completion of commitment 4

**ATTACHMENT 2
Summary of Commitments**

	Commitment	Committed Date or Outage
6	EGC will conduct an inspection of the internal and external surfaces of the Dresden Nuclear Power Station (DNPS) Unit 3 steam dryer using "best effort" VT-1 and VT-3 methods including areas of the steam dryer previously inspected at QCNPS Unit 2. The acceptance criteria will be that no structurally significant cracking is identified that would limit operation.	Fall 2004 refueling outage for DNPS Unit 3
7	EGC will submit to the NRC the justification for those areas of the steam dryer not inspected as part of commitment 6.	August 27, 2004
8	Where lessons learned from evaluations or inspections conducted pursuant to commitments described in this letter indicate significant potential degradation of the steam dryer, or the reactor pressure vessel internals, steam or feedwater systems and components, EGC will take appropriate actions up to and including shutting down the applicable unit to conduct inspections or modifications on an expedited basis.	Spring 2006 refueling outage for QCNPS Unit 2
9	During the next scheduled refueling outage on each DNPS and QCNPS unit following completion of the EPU vulnerability team effort, EGC will perform a general visual inspection of the reactor pressure vessel internals, steam, and feedwater systems, including inspection and disassembly if needed of the most susceptible components, which include electromatic relief valves.	Fall 2004 refueling outage for DNPS Unit 3 Spring 2005 refueling outage for QCNPS Unit 1 Fall 2005 refueling outage for DNPS Unit 2 Spring 2006 refueling outage for QCNPS Unit 2